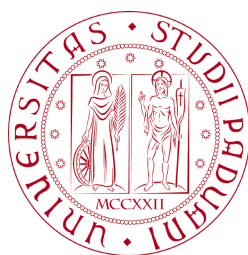


UNIVERSITÀ DEGLI STUDI DI PADOVA
FACOLTÀ DI INGEGNERIA



Finito di scrivere il giorno September 5, 2012 utilizzando L^AT_EX 2_ε

UNIVERSITÀ DEGLI STUDI DI PADOVA
FACOLTÀ DI INGEGNERIA

—
DIPARTIMENTO DI INGEGNERIA DELL' INFORMAZIONE

—
TESI DI LAUREA MAGISTRALE IN BIOINGEGNERIA

DEVELOPMENT AND EVALUATION
OF PID CONTROLLERS FOR
GLUCOSE CONTROL IN PEOPLE
WITH TYPE 1 DIABETES MELLITUS

RELATORE: CH.MO PROF. ING. CLAUDIO COBELLI

CORRELATORI: PROF. EYAL DASSAU,

PROF. DALE SEBORG,

PROF. FRANCIS J. DOYLE III

LAUREANDO: TAGLIAVINI ALESSIA

ANNO ACCADEMICO 2011-2012

Contents

Summary	XI
Introduction	XIII
1 The Artificial Pancreas System	1
1.1 Physiology of the Pancreas	1
1.2 Type 1 Diabetes Mellitus	3
1.3 Type 2 Diabetes Mellitus	4
1.4 Insulin Therapy	5
1.5 Artificial Pancreas System	6
1.5.1 Continuous Subcutaneous Insulin Infusion (CSII) Pump	9
1.5.2 Continuous Glucose Monitoring (CGM)	10
1.5.3 Control Algorithm	12
2 Control Algorithms and Models	15
2.1 Control Algorithms	15
2.1.1 Model Predictive Control	15
2.1.2 Continuous PID Control	17
2.1.3 Intuitive Description of PID Control Action	21
2.1.4 Controller Tuning Using The IMC method	22
2.2 Process Models	27
2.2.1 Control-relevant Models	29
2.2.2 Novel PID Control Approach Based on Personalized Model	31
3 Controller design and Implementation	33
3.1 Main Design Issues	33

3.2	Model Identification	34
3.3	Controller Design	36
3.3.1	Model Approximation	37
3.3.2	PID Controller Tuning	41
3.4	Simulator PID Implementation	41
3.4.1	Discrete PID Control	41
4	Controller With a Non-personalized Controller Gain	45
4.1	Effect of τ_c	45
4.1.1	Robustness Test	51
4.1.2	Discussion	61
4.2	Validation Test: Post-prandial Results	61
5	Controllers With a Personalized Controller Gain	65
5.1	Effect of τ_c	65
5.1.1	Robustness Test	73
5.1.2	Discussion	84
5.2	Validation Test: Post-prandial Results	84
6	Comparison of The Controllers Performance	89
6.1	Normal output	89
6.2	Controller output increased of the 50%	94
6.3	Validation test	98
	Conclusion	103
A	The UVA/Padova Metabolic Simulator	105
A.1	Model Development	105
A.2	Software	108
B	Step Response Test	111
C	Non-personalized Model Gain Results	115
C.1	Robustness Test Single results	119

D Personalized Model Gains Single Results	127
D.1 Robustness Test Single Results	132
Bibliography	145

Summary

The thesis was conducted during a period of six months at the University of Santa Barbara in collaboration with prof. Eyal Dassau¹², PhD, Francis J. Doyle III¹², PhD, Dale Seborg¹², PhD . An abstract of the thesis was submitted for the Diabetes Technology Meeting (DTM) Bethesda, Maryland 8th-10th November.

For people with type 1 diabetes mellitus, the pancreatic β -cell is completely unable to produce insulin, and thus they require an insulin therapy for all their life in order to survive. The common insulin therapy consists of multiple daily insulin injections. In the last forty years, a new approach to provide continuous insulin delivery has been introduced and it consists of three main elements: a continuous glucose monitoring sensor, an insulin pump and a control algorithm. This system is called Artificial Pancreas System (APS). The aim of this research is to develop and evaluate a novel, model-based *proportional-integral-derivative* (PID) control law for algorithmic insulin dosage computation.

The proposed PID design method is based on the Internal Model Control (IMC) approach and a simple dynamic model proposed by van Heusden et al. [1]. This third-order-plus-time-delay linear model has a single adjustable parameter that is personalized based on the subject's TDI value. Thus, the model is developed using readily available clinical information and does not require time-consuming experimental tests. The resulting model is then approximated by a second-order-plus time model which allows the controller settings to be calculated using the IMC design method. This design method has a single adjustable

¹Department of Chemical Engineering, University of California, Santa Barbara, CA, USA

²Sansum Diabetes Research Institute, Santa Barbara, CA, USA

parameter that allows the controller to be tuned to be more, or less, aggressively. As a consequence, the three PID degrees of freedom are reduced to two: model gain (K) and controller aggressiveness (τ_c).

The proposed controller design method is evaluated *in silico* study using the FDA-approved UVA/Padova metabolic simulator. Ten simulated subjects are used to determine a conservative value of the IMC design parameter, both in the case of fixed model gain and in the case of personalized gains, with a single announced meal. Then the same subjects are used to evaluate the performance considering changes of $\pm 50\%$ in the insulin sensitivity. Subsequently, a different population of ten subject is used to perform a validation test with three unannounced meals. The personalized PID controllers perform better than controllers based on a fixed model. Neither approach result in hypoglycemia for any of the 20 subjects.

Simulation studies have demonstrated that the proposed controller design method is practical (no special tests required) and superior to controllers based on non-personalized models.

Introduction

The term diabetes mellitus (DM) covers a group of common metabolic disorders that cause an increase in blood glucose concentration, called hyperglycemia. In the medical field, distinct types of DM exist, and are caused by a complex interaction between genetic, environmental and behavioral factors. The causes that lead to hyperglycemia are different, such as decrease of insulin secretion, decrease of glucose use, and increase of glucose production [2]. Consequences for people who suffer from this disorder are serious and dangerous, since DM compromises the correct function of other metabolic pathways and causes haemodynamic changes, leading to the damage of the eyes, kidney, and nerves [2]. In the USA, DM is the main cause of renal failure, non-traumatic amputation of the lower limb and blindness in adults. Even though all the kinds of DM are characterized by hyperglycemia, there are many different types depending on the causes. Classification of DM is based on the pathogenesis processes that lead to hyperglycemia [2, 3].

Currently, there are two main categories of DM: type 1 and type 2. Type 1 diabetes mellitus (T1DM) is caused by the destruction of the insulin-producing β -cells in the pancreas which leads to an insulin deficit. It can be further divided into subcategories. First, insulin-dependent type 1 is defined by the damage immune-mediated of the β -cells. Second, type 1 idiopathic is characterized by a deficient secretion of insulin by the pancreas, but without any proof of autoimmune destruction of β -cells [3].

Type 2 DM (T2DM), once known as not insulin-dependent, is characterized by insulin resistance either by relative or absolute deficit of insulin, causing a heterogeneous set of diseases with the common factors of insulin-dependence at different levels, alteration in insulin secretion, and increased production of glucose

[3].

During the last two decades, the presence of DM has significantly increased. In the occidental world the number of diabetes cases of a specific population over a certain period exceeds 3% of the general population. Between 1976 and 1994 the spread of DM among adults in the USA increased from 8.9% to 12.3%. Furthermore, the number of patients affected by DM increased with the population age, differing from an incidence of 1.5% in individuals between 20 and 39 years to 20% in individuals over 75 years old. In the same way, alteration in postprandial glycemia increased from 6.5% to 9.7% [3].

Numerous epidemiological studies highlight that the number of type 1 and 2 DM patients dramatically depends on geographic location, and revealing the influence of different genetic and environmental factors. Furthermore, recent studies assert that the prevalence of T2DM is 10 times greater than T1DM in the European population and even more in Asia and Pacific countries. Additionally, type 2 DM is likely to rapidly increase in the future because of the growing rate of obesity and the decrease of physical activity, mostly in the industrialized countries [3].

With regards to T1DM, it was found that the disease affects subjects with a particular genetic susceptibility. The prevalence of type 1 DM is higher in northern countries: indeed Scandinavia shows the highest prevalence of type 1 DM and Finland shows an incidence of 35 cases per 100,000. On the other hand, countries bordering the Pacific have the lowest incidence, reaching incidence of 1-3 case per 100,000 in Japan and China. North Europe and USA shared the same incidence of 8-17 cases per 100,000 [2].

T1DM generally starts in an infant-juvenile age, and it requires insulin administration for the entire life of the patient, since the destruction of the β -cells causes an absolute hormone deficiency. Because of the complete lack of insulin secretion, T1DM can be considered to be the most critical type of diabetes and this is why many studies are focused on it.

The most common therapy is insulin delivery by daily insulin injections, but this approach does not reproduce the real dynamics of insulin secretion. In fact, continuous insulin secretion is provided by the pancreas and is called basal insulin.

In addition, another dose of insulin is delivered after meal ingestion according to the glucose concentration in the blood. Because of this biphasic behavior of insulin secretion, new approaches that are able to mimic it are desired [3]. A novel technique has been developed in the last four decades consisting of the use of an insulin pump that provides continuous insulin administration.

The most critical part of this new approach lies in the development of a feasible, robust and safe algorithm for insulin delivery which, along with the pump and a glucose sensor, form the artificial pancreas system. The main aim of this system is to improve patients' lives by avoiding the dangerous situations of hypo- and hyperglycemia [4].

Chapter 1

The Artificial Pancreas System

In this chapter brief physiological overview of the insulin production and the characteristics of the diabetes mellitus are provided. Furthermore, the artificial pancreas system is presented along with a description of its elements.

1.1 Physiology of the Pancreas

The Pancreas is an organ located in the abdomen with two different functions: exocrine and endocrine. The exocrine function is the production and secretion of digestive enzymes; the cells of the pancreas which have this purpose are known as pancreatic acini. The endocrine function is the production of several important hormones such as insulin and glucagon, and cells involved in this secretion are called isles of Langerhans or pancreatic islets. Each distinct type of islet cell is involved in the production of a different hormone: the β -cells (or B cells) secrete insulin, whereas α -cells (or A cells) provide glucagon. Another molecule that is secreted by the islet cells is somatostatin which is produced by δ -cells (D cells). This hormone has the capability of inhibiting the secretion of both insulin and glucagon [5].

Insulin is a protein hormone composed of two chains: A and B, with 21 and 30 amino acids, respectively. Insulin's task is to control organic metabolism since it induces glucose to enter from the extracellular fluid into cells. The insulin effect is felt by the target cells, which are insulin-dependent. These target cells are

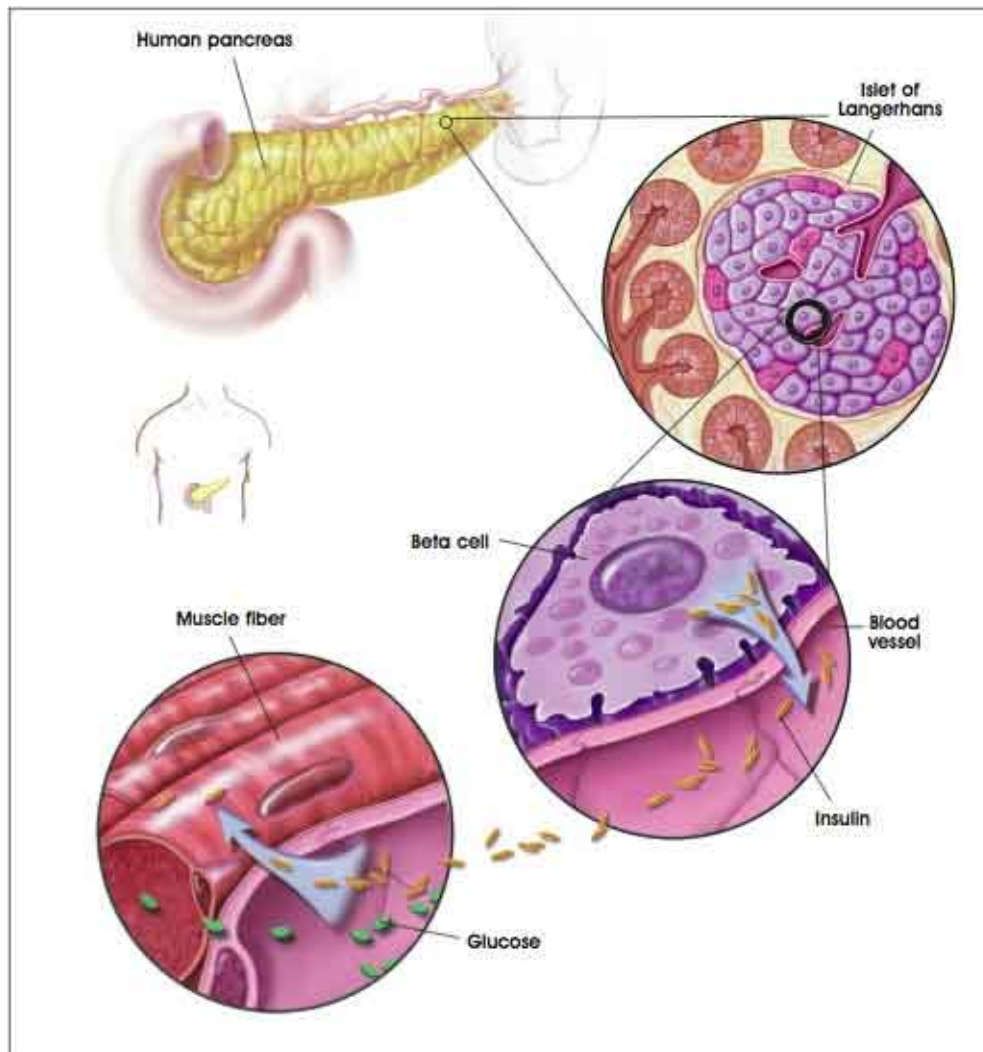


Figure 1.1: Insulin secretion by pancreatic islets and insulin path throughout the blood before reaching the target cells [6].

mainly muscle cells (both cardiac and skeletal), adipose tissue cells and liver cells. When insulin is secreted, it circulates throughout the blood and reaches the insulin receptors of the cells as shown in Figure 1.1. Once the insulin hormone binds to the cell receptors, they stimulate cytoplasmic vesicles containing the glucose transporter, inducing them to reach the plasma membrane and then merge with it. An increase in the number of glucose transporters in the plasma membrane facilitates the glucose movement from the extracellular fluid into the cells by facilitated diffusion. Plasma glucose concentration plays the most important role in

controlling the insulin secretion. Stimulation and activation of pancreatic β -cells depends on changes in plasma glucose concentration. If plasma glucose concentration increases, e.g after a meal, the β -cells are activated and the secretion of insulin begins. On the other hand, a decrease in plasma glucose concentration leads to removal of the insulin secretion stimulus [5].

Figure 1.2 provides a schematic representation of the glucose-insulin mechanism. An increase in plasma glucose concentration causes a rapid stimulation of insulin secretion and consequently an increase in plasma insulin concentration. Afterwards, plasma insulin passes to the liver which degrades half of it, avoiding liver glucose output since insulin inhibits conversion of the glycogen into glucose. The other half of plasma insulin induces cells of the insulin-dependent tissues to uptake glucose. As a result of the two different actions of the insulin, one over the cells and the other over the liver, the plasma glucose concentration is returned to normal, around 80-140 mg/dl [5].

The antagonist of insulin is glucagon which has the function of reducing the insulin concentration in the plasma, and therefore stops the insulin action and in this way prevents hypoglycemia.

1.2 Type 1 Diabetes Mellitus

T1DM is an autoimmune disorder characterized by destruction of insulin-producing β -cells in the pancreas. The consequence of this damage is the loss of endogenous secretion of insulin that is essential to maintain euglycemia, causing life-threatening hyperglycemia and keto-acidosis. As written above, the lack of insulin secretion causes a loss in the ability to regulate glycemic levels in people affected by T1DM, thus making them suffer from long periods of hyperglycemia without proper insulin management [3, 7].

This process usually develops in a few years, and hyperglycemia rises when 10% of the beta cells are still working. At that point, functional β -cells still exist, but they are not able to supply a minimum level of insulin needed to maintain euglycemia. Nevertheless, during this phase, glycemic control can be reached with modest insulin administration. Unfortunately, this is a temporary phase and it

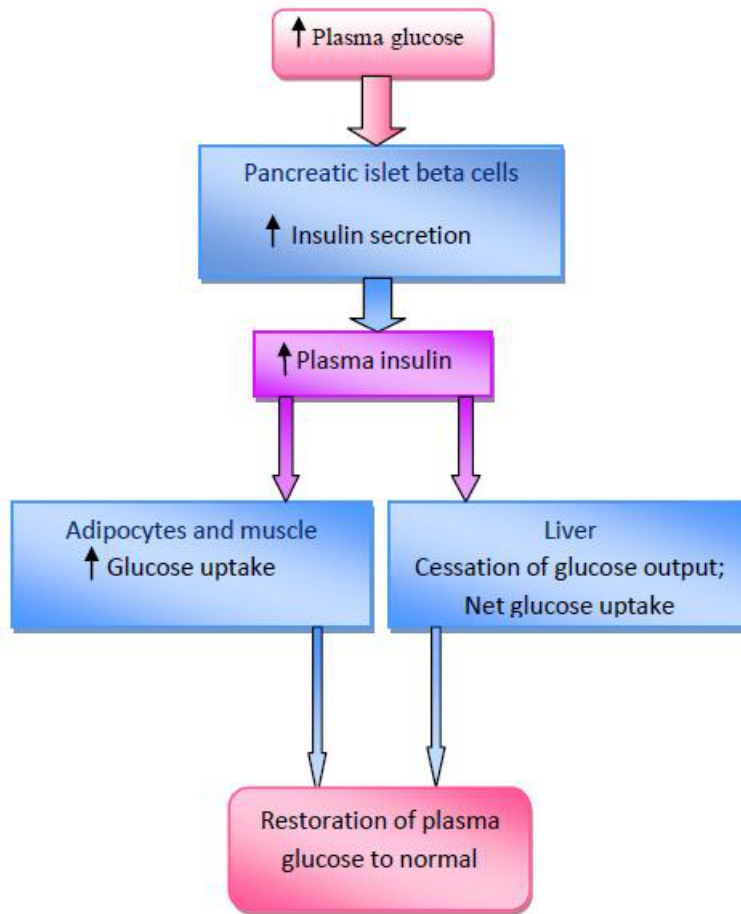


Figure 1.2: Effect of plasma glucose concentration over insulin secretion [5].

ends when all β -cells are completely destroyed by the autoimmune process [3, 2].

1.3 Type 2 Diabetes Mellitus

Type 2 Diabetes Mellitus is a disorder characterized by insulin resistance and partial or absolute deficit of insulin which is caused by progressive β -cell deterioration. Most of the causes of this disease are genetic, it usually appears later in life and it is associated with cardiovascular risk factors such as obesity. Indeed, the majority of T2DM patients are obese with a high prevalence of fat in the intra-abdominal area [3].

Typically, in T2DM there is a progressive reduction of β -cell secretion. Since

frequently T2DM patients show also a lack of willingness to follow dietetic and behavioral therapy, it is often necessary to have more complex therapy scheme before the insulin. Since the recourse to insulin therapy is often the final stage for T2DM and the disease typically emerges in older age, insulin therapy is mostly focused on T1DM patients [3].

1.4 Insulin Therapy

The insulin hormone is synthesized by pancreatic β -cells and once in the blood, it flows throughout the hematic system and reaches the target organs: liver, muscles and adipose tissue. In the target organs, insulin has the role of keeping suitable glycemic levels either in the fasting phase (80 and 100 mg/dl), both nightly and between meals, or in the pre-and postprandial phase (less than 140 mg/dl), after the meal intake. As a result of the complete lack of insulin in T1DM, the liver overproduces glucose and prevents food glucose from being completely used. The possibility to produce artificial insulin was discovered in 1920s and as a result, a fatal disease turned into a treatable condition requiring life-long insulin-replacement therapy [8]. It should be emphasized that the therapy goal is not only survival, but also the prevention of chronic complications associated with diabetes. Hypoglycemia can lead to a coma, and even death while hyperglycemia can bring on several chronic diseases.

Insulin, like all proteins, cannot be taken orally because it would be degraded by digestive enzymes, T1DM treatment consists of providing insulin either with daily insulin injections or continuous insulin infusion (CII). Both therapy approaches require intravenous capillary glucose measurement in order to determine the daily insulin dose for euglycemia [7].

With daily insulin injections, the insulin administration is provided in a subcutaneous way by either syringe or pen. Injection must be given in the subcutaneous tissue where specific enzymes lie and where there are capillaries which are suitable for carrying insulin. If the insulin is injected too deeply, an intramuscular administration would occur and the time of absorption would be modified causing unpredictability of the absorption process [3].

The CII therapy was introduced about twenty-five years ago and consists of the use of a pump in order to provide continuous insulin administration. The use of CII, along with continuous glucose sensing and a control strategy necessary to bring a person with diabetes as close as possible to euglycemia, gives rise to a closed-loop system known as the Artificial Pancreas (AP) [4].

1.5 Artificial Pancreas System

The history of the Artificial Pancreas (AP) dates back to four decades ago when closed-loop control was used to regulate blood glucose in individuals with T1DM [7]. In general, the AP is a system that, on the basis of measurements of the level of blood glucose, delivers the needed quantity of insulin with the use of an insulin pump based on an algorithm. There are two main approaches for the implementation of the AP System (APS). The first approach is the use of subcutaneous-subcutaneous (sc-sc) in which an sc route for both glucose monitoring and insulin delivery is adopted. On the other hand, an intravenous-intraperitoneal method exists in which glucose monitoring is achieved by intravenous measurements and intraperitoneal insulin is delivered [9].

In this paper an sc-sc body interface will be considered. The three main elements of the APS are a subcutaneous glucose monitor (CGM), a continuous subcutaneous insulin infusion (CSII) pump and the control algorithm which controls the insulin dose. A schematic overview of this closed-loop system is shown in Figure 1.3 [4].

Besides these three elements, other features are enclosed in APS such as a safety algorithm, modeling, communication and interfaces. Hence, the APS is often described as a puzzle and the primary piece of this puzzle regards safe communication and data transfer between the three main elements listed above. Naturally, the system provides a clear human interface in order to give all the information needed to physicians and patients as well as a safety system using interlocks, checklists and alarms [4].

In order to provide the right amount of insulin, it is sensible to understand and take into account the dynamics of insulin delivery of an healthy pancreas. The

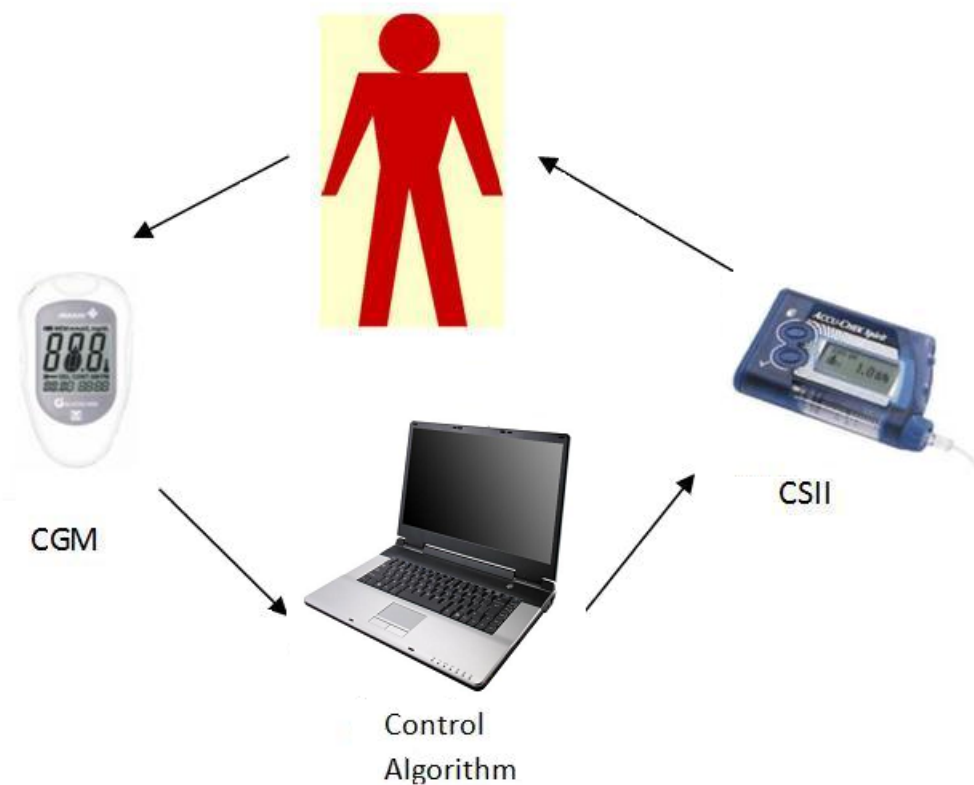


Figure 1.3: APS: blood glucose concentration is detected by the CGM sensor and on the basis of this information the control algorithm can calculate the amount of insulin necessary to achieve the final goal that is blood euglycemia. The calculated insulin amount is delivered by the CSII [4].

pancreas of healthy subject continually produces a small basal amount of insulin in order to keep glucose hematic levels stable. Furthermore, after each meal, an insulin amount (bolus) is added to this basal insulin caused by the blood glucose growth in the postprandial phase [3, 10]. As a result, in a healthy pancreas, the response to a glucose clamp will show a biphasic behavior[11]. In the same way, a subcutaneous pump should be able to provide the physiologic delivery of insulin described above, releasing insulin in two ways:

- continuous for 24 hours through basal infusion, in order to hold glucose blood value stable

- intermittent during a postprandial phase using an insulin bolus in order to control glucose blood after carbohydrate intake in a meal.

The insulin boluses and the basal insulin rate are based on an insulin-to-carbohydrate ratio (I:C) and a correction factor (CF). These two parameters are calculated through the use of measurements of the blood glucose concentration. The I:C rate expresses the unit of insulin necessary to compensate for the amount of carbohydrate (CHO), whereas the CF gives the unit of insulin necessary to reduce the blood glucose concentration. The way in which the previous value is obtained empirically is tailored to specific individuals. The combination of the two values allows the calculation of the amount of insulin required in order to control the blood glycemia at each given moment as a function of blood glucose level and CHO intake [12].

However, control of glycemia is a rather complicated process which in healthy subjects concerns various neural and hormonal inputs from the brain, gut, liver, and pancreas; thus, the two values mentioned previously might not be sufficient to achieve a good insulin administration. Moreover, the process is affected by various situations such as meal type, stress levels and exercise. As a consequence, insulin requirements differ throughout the day and from day to day; therefore, the initial setting needs to be fine-tuned to prevent insulin overdosing or under-dosing [7, 4].

Currently, this biphasic behavior can be achieved with the use of only the insulin pump, which provides bolus and basal insulin delivery. The new insulin pumps can provide four different ways to supply the bolus [10]:

- a) only one infusion with the total amount of the insulin bolus
- b) two infusions with half of the total amount of the insulin bolus for each
- c) two infusions, one with half of the total amount of the insulin bolus delivered in the usual way, and the other delivered over a prolonged period of time
- d) one infusion of the total amount of insulin in the form of a basal rate.

1.5.1 Continuous Subcutaneous Insulin Infusion (CSII) Pump



Figure 1.4: Insulin Pump.[13]

The CSII pump is an electric-powered syringe pump which delivers rapid action insulin. The rapid-acting human insulin, or an analog, is mainly used for the CSII pump since their pharmacodynamic and pharmacokinetic behavior mimics physiological insulin behavior. Moreover, this kind of insulin minimizes the formation of crystals inside the plastic tubes of the pump, thus reducing the possibility of obstructions. The syringe is linked to the subcutaneous abdomen tissue by an infusion set in whose end a metal or Teflon needle is placed. The abdomen tissue is the ideal place for insulin infusion since the uptake is more rapid and constant in that region [10].

Technological progress in coming years will further improve instrument performance, leading to a reduction in weight and size (new models measure $5 \times 8.6 \times 2$ cm and weight about 100 g). Over the years, the metal needle of the infusion set has been replaced by a Teflon catheter which is introduced into the body by a metal runner, immediately removed after the catheter insertion.

A schematic figure of the main parts of the pump is provided in Figure 1.5. It consists of the main device which encloses a disposable reservoir of insulin (300 units), a mechanism for the delivery of insulin at different rates, and a microcomputer which executes the program using batteries [10].

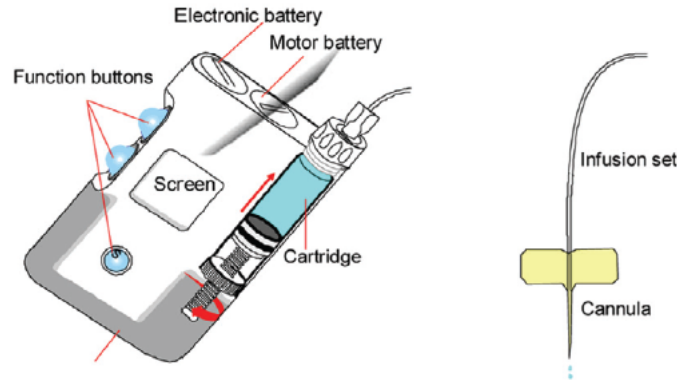


Figure 1.5: Insulin pump components [10].

It is important to emphasize that the main issue in the use of a CSII pump is the delay in action since the subcutaneous insulin absorption needs time. In particular, after the injection of a regular subcutaneous bolus, insulin takes up to 120 min to be absorbed and able to have peak glucose. From a safety point of view, this slow insulin absorption may cause insulin under-delivery which, if not controlled, can lead to ketoacidosis [14].

Another limit of the CSII therapy is the need for training patient. This therapy has best results with well-trained patients who are motivated in learning and self-monitoring [5]. On the other hand, patients with a low willingness might impair the required management of pump treatment. Moreover, an external pump can be uncomfortable for the patient, and therefore the quality of life may worsen because of this choice of therapy [3].

1.5.2 Continuous Glucose Monitoring (CGM)

Continuous glucose monitoring techniques were first introduced about ten years ago in order to provide a retrospective analysis of glucose profiles. Afterwards, real-time device were developed that gave on-line readings of blood glucose concentration [14]. The first commercially available continuous glucose monitoring device was the *MiniMed*[®] continuous glucose monitoring system (CGMS; MiniMed Inc., Sylmar, CA). It was composed of a sterile, disposable subcutaneous glucose sensor which collected measurements of glucose concentration in the in-



Figure 1.6: A CGM device [15].

terstitial fluid. The sensor was connected via external electrical cable to a small monitor and information was sent to the control algorithm usually via a wireless system. The glucose concentration was measured every 10 s and an average value was stored and provided to the controller every five minutes for a total of 288 measurements each day [15].

Since CGM information is the basis of the control algorithm of the AP system, a good knowledge of CGM limitations and issues is essential. First, it should be taken into account that the glucose concentration that is detected is interstitial and significantly different from the actual blood glucose when conditions change quickly. In order to reduce this difference, a device calibration is required with several daily blood glucose samples. Studies indicate that relevant improvements in CGM accuracy can be achieved by calibrating the sensor during periods of relative glucose stability [14]. A second issue which influences the CGM accuracy is the time lag due to the blood-to-interstitial glucose transportation and the sensor processing time.

Moreover, errors from transient loss of sensitivity and random noise complicate issues further. Obviously, the main aim is to avoid all these complications since

accurate readings of the CGM are fundamental for the closed-loop controller. To this end, filtering, denoising and artifact rejection in CGM data should be performed. Even though these issues may influence CGM accuracy, the device provides frequent sampled data, e.g every 5-10 min, allowing for the successful development of the APS [14].

1.5.3 Control Algorithm

The control algorithm plays a fundamental role in the artificial pancreas. Because of its great importance, many studies have been conducted over the years developing various algorithms. However, two main types of algorithms have been identified as the most attractive: proportional-integral-derivative (PID) control [16, 17, 18] and model predictive control (MPC)[7, 1].

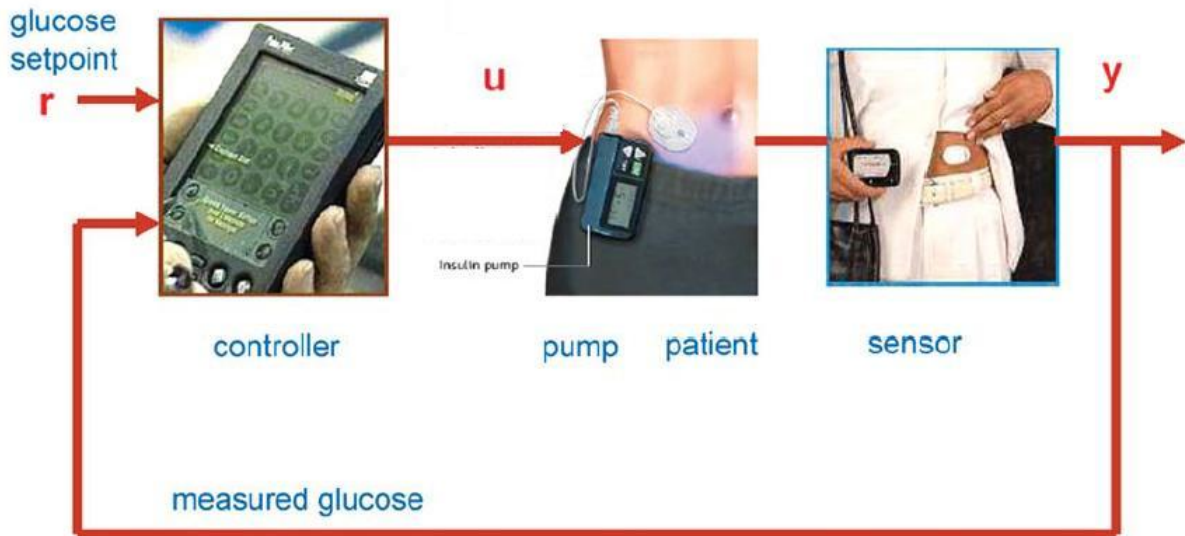


Figure 1.7: Closed-loop of the APS [11].

PID algorithms use three components in order to administrate insulin: the deviations from a target glucose level (the proportional component), the area under the curve between the measured and the target glucose level (the integral component) and the rate of change in the measured glucose levels (the derivative component). The PID controller is merely reactive since it responds to changes

in glucose concentration after their occurrence. As a result, the inherent delays and inaccuracies in both glucose sensing and insulin delivery may lead to an unstable system if the controller is too aggressive. In general, a good controller design should account for time delay in measurements and insulin delivery. However, if the controller response is too slow, postprandial glucose peaks cannot be appropriately reduced [8]. On the other hand, MPC algorithms, compute the insulin delivery by minimizing the difference between predicted glucose concentrations and the target glucose levels over a prediction horizon of 1.5 to 3 hours, or longer. Prediction of the current and future insulin infusion rates, and thus the corresponding predicted glucose amount, is based on a model of the patient metabolic system. Since the MPC algorithm predicts the level of glucose in the blood due to the effect of the insulin administered and the disturbances, e.g; meals and physical activity, it is called proactive. This controller design is well-suited to compensate for time delay due to subcutaneous insulin delivery and subcutaneous glucose measurements [14, 8].

Despite the remarkable advantages that MPC algorithms show, glucose clamp studies illustrate a biphasic insulin response and in the same manner PID can also provide this type of response. This observation suggests that the β -cells' behavior can be replaced with a PID controller. It is important to underline that any controller with integral action will respond in a biphasic way. For this reason, new methods of control algorithms have been introduced, e.g; Internal Model Control (IMC). This type of controller is related to the PID controller since it can be rearranged to be equivalent to a PID controller, but with less tuning parameters, this is why it can be considered as a conventional tuning methods for the PID controller [19].

However, with for IMC approach the model chosen to represent the insulin-glucose dynamics is very important since the controller performance depends on it.

Chapter 2

Control Algorithms and Models

In this chapter a brief theoretical introduction to the PID controllers and the IMC method is provided. Furthermore, an overview of the most common model for the glucose/insulin dynamic are presented, focusing on the control-relevant models which are the type used for the controller implementation.

2.1 Control Algorithms

The two main controller algorithms utilized in the Artificial Pancreas design are considered with a particular attention paid to the PID controller, since it is the controller that is evaluated in this work.

2.1.1 Model Predictive Control

The MPC is basically composed of three main elements: the model, the cost function and the constraints. The model allows the prediction of future states of the outputs with information about the current state, future values of the manipulated variables and future values of the measurable or predictable disturbances. The performance of the closed-loop control is calculated by minimizing the cost

function [20, 11]. The cost function is usually a weighted quadratic form [20]:

$$J(k) = \sum_{i=0}^N (q(y_{sp}(k+i) - y(k+i))^2 + (u_0(k+i) - u(k+i))^2) \quad (2.1)$$

y : glucose concentration

u : insulin infusion rate

q : weight

(2.2)

which penalize future deviations of the output (y_m) from the set point (y_{sp}) and it can also include also a quadratic penalty on future control actions which can be either the difference between u and a reference u_0 or the incremental changes, $\Delta u(k) = u(k) - u(k-1)$ [20]. Constraints are applied over the variables, e.g over the insulin administration rates by the pump and over the glycemia which has to be in an admissible rates.

$$u(k)_{min} \leq u(k) \leq u(k)_{max} \quad (2.3)$$

$$\Delta u(k)_{min} \leq \Delta u(k) \leq \Delta u(k)_{max} \quad (2.4)$$

$$y(k)_{min} \leq y(k) \leq y(k)_{max} \quad (2.5)$$

In Figure 2.1 a schematic overview of the basic idea about MPC is provided. The two sub-figures are divided into past and future. The top sub-figure shows the history of both glucose (y) and insulin (u) before the current time t_k . At each time value of t_k the sequence of current and future insulin delivery rates is computed by optimizing the object function subjects to the constraints over a future horizon of P time steps. Than, only the first control move out of M steps is actually implemented, resulting in a new glucose value $y(k+1)$ at the next step $t(k+1)$. The next step, at the time t_k shown in the bottom sub-figure, consists of the translation of the predictions, the control horizons and, repetition of the same procedure, always implementing only the first control move [20, 11]. An advantage of this optimization-based approach is that the control objective can be weighted on the basis of the glucose hyperglycemia or hypoglycemia conditions [11].

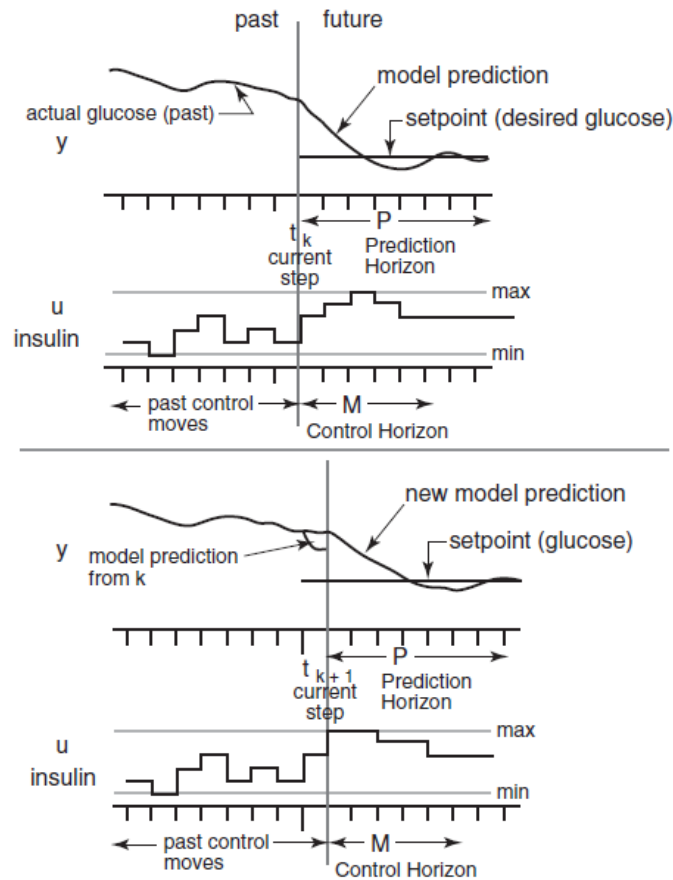


Figure 2.1: MPC prediction scheme. The top portion shows the MPC algorithm at time t_k and the future model prediction both of the glucose and the insulin. The bottom portion shows the results of glucose and insulin after the first move of the previous prediction has been implemented and the new model prediction computed at the time t_{k+1} . [11]

2.1.2 Continuous PID Control

The proportional-integral-derivative (PID) controller is the predominant feedback control algorithm in the process industries [19]. In general, the feedback control algorithm aims to minimize the difference between the desired output value (setpoint) and the actual output measured. This difference is called the error and it will be equal to zero only in the case in which the actual output, that is the measured level of glucose, is exactly equal to the set point. In this case, the system

will be perfectly controlled [19].

$$e(t) = y_{sp}(t) - y_m(t) \quad (2.6)$$

- $e(t)$: error signal
 $y_{sp}(t)$: set point
 $y_m(t)$: measured value of the controlled variable (glucose concentration)

As the name suggests, PID controller is composed of combination of three control modes, and each of them operates a specific action over the error in order to compute the control variable.

Proportional Control

The first contribution is proportional to the error; therefore it is called proportional control mode.

$$u(t) = \bar{u} + K_c e(t) \quad (2.7)$$

- $u(t)$: controller output (insulin infusion rate)
 \bar{u} : bias (steady-state) value
 K_c : controller gain

The proportional controller has two advantages:

1. By tuning the controller gain, it is possible to make the controller more or less aggressive.
2. The sign of K_c determines whether the controller output increases or decreases when $e(t)$ increases.

The value of \bar{u} is set so that the controller output is equal to its nominal steady-state when the error is zero. For the artificial pancreas control applications, the K_c dimension is (pmol/min/mg/dl) since u is the insulin amount and \bar{u} is the

basal insulin I_b . The basal insulin brings the subject to their glucose steady state which can be different from the set point. A disadvantage of a controller with only the proportional mode is the presence of the steady-state error called (offset) after changing in the set point or a prolonged disturbance. However, this offset can be eliminated by the introduction of the integral mode [19].

Integral Control

The integral control contribution is proportional to the integral of the error over time:

$$u(t) = \bar{u} + \frac{1}{\tau_I} \int_0^t e(t^*) dt^* \quad (2.8)$$

τ_I : integral time

Its most important advantage is elimination of the offset. u changes as far as the $e(t^*)$ is different to zero, bringing the steady-state error equal to zero.

When a set point change or a significant disturbance perturbs the system, it is possible that the controller output reaches an upper or lower limit. In this case, even though the error is not equal to zero, the controller action cannot increase. This situation is called controller saturation.

Furthermore, at saturation, the error usually can still be not equal to zero, and the integral term continues to increase without producing any effect on the output variable. This phenomenon is referred to as reset windup on integral windup [19]. In the APS, the CSII pump plays the role of the control action actuator and it is subject to a maximum delivery constraint; thus this actuator bound should be considered while implementing an integral controller.

Derivative Control

The derivative control contribution has the aim to anticipate the error signal variations by taking into account its rate of change. The ideal derivative action

is:

$$u(t) = \bar{u} + \tau_D \frac{de(t)}{dt} \quad (2.9)$$

τ_D : derivative time

Since the control output will be equal to the nominal value only with a constant error, derivative control is never used alone [19].

Proportional-Integral-Derivative Control

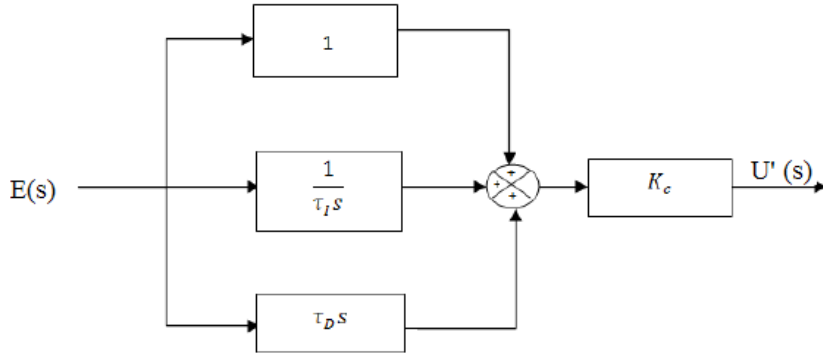


Figure 2.2: Block diagram of the parallel form of PID control [19].

The combination of the three components described above gives rise to the popular PID controller. The control law of the PID parallel form is given by[19]:

$$u(t) = \bar{u} + K_c \left[e(t) + \frac{1}{\tau_I} \int_0^t e(t^*) dt^* + \tau_D \frac{de(t)}{dt} \right] \quad (2.10)$$

$$u'(t) = u(t) - \bar{u} \quad (2.11)$$

And the corresponding controller transfer function is:

$$\frac{U'(s)}{E(s)} = K_c \left[1 + \frac{1}{\tau_I s} + \tau_D s \right] \quad (2.12)$$

$U'(s)$: $u'(t)$ Laplace transform

$E(s)$: $e(t)$ Laplace transform

A PID control disadvantage is the so-called derivative kick. It is a momentary large value of the derivative term due to a fast change in the set point and thus in the error change rate. The undesirable spike can be avoided by setting $y_{sp}=0$ in the derivative terms [19].

2.1.3 Intuitive Description of PID Control Action

Considering the three PID components from a physical point of view, it is possible to understand the role that each component plays in determining the insulin infusion rate.

The proportional element provides a contribute only when the glucose concentration is above or below the set point value. When the glucose is at the set point, the proportional contribution does not affect the output [21].

The integral term changes value when either the glucose concentration is above or below the set point. Since the integral contribute is always active unless $e(t) = 0$, it ensures that target is always achieved when the system is at the steady-state [21].

The derivative component increases when glucose rate of change is rising and decreases when it is falling. As a results, each detection of glucose rate of change leads to a change in insulin delivery independent of the current glucose level [21].

Figure 2.3 shows the response of the three PID modes of Steil et al. [21] to a hyperglycemic clamp.[21] The blue area shows the proportional contribution ($P(n)$), the green area represents the integral action ($I(n)$) and the pink area shows the derivative component ($D(n)$).

Stability

It is essential that the closed-loop system is stable which means that the output response is bounded for all bounded inputs [19].

Fortunately, the desired control system behavior can be achieved changing specific control settings. This kind of setting regulation is referred to as controller tuning [19]. Different PID controller tuning techniques exist, and they all aim to

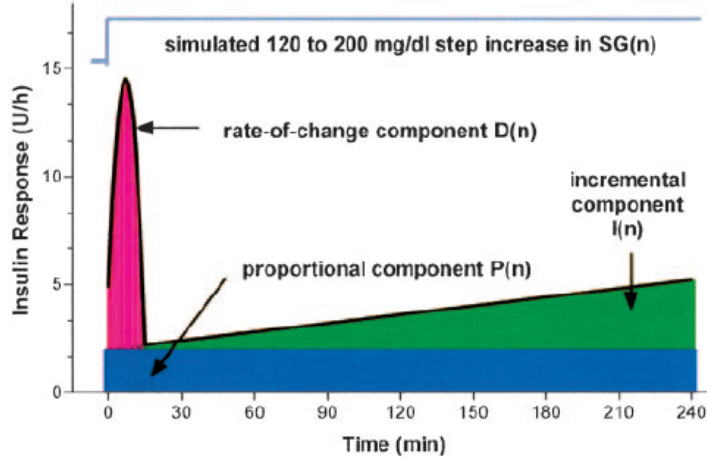


Figure 2.3: PID control contribution during an hyperglycemic clamp [21].

provide a good initial setting that can be later improved on-line. A method widely used for the PID controller design for the artificial pancreas system is Internal Model Control.

Since it is a model-based method, this technique provides the best performance when a reasonable accurate dynamic model is available [19].

2.1.4 Controller Tuning Using The IMC method

The basic idea of the IMC method is the controller should include a model of the controlled process. Ideally, if the process model is perfect and there are no disturbances identified, the control will be perfect. The structures of both IMC and the classical feedback control are shown in Figure 2.4 and Figure 2.5. The two structures are related by an algebraic transformation. Once IMC controller G_c^* is designed it can be implemented as the corresponding classical PID controller G_c [19]:

$$G_c = \frac{G_c^*}{1 - \tilde{Y}G_c^*} \quad (2.13)$$

$$G_c^* = \frac{G_c}{1 + \tilde{Y}G_c} \quad (2.14)$$

The relation of input to output for the IMC block diagram is:

$$Y = \frac{G_c^*G}{1 + G_c^*(G - \tilde{G})} Y_s P + \frac{1 - G_c^*\tilde{G}}{1 + G_c^*(G - \tilde{G})} D \quad (2.15)$$

where D is an external disturbance.

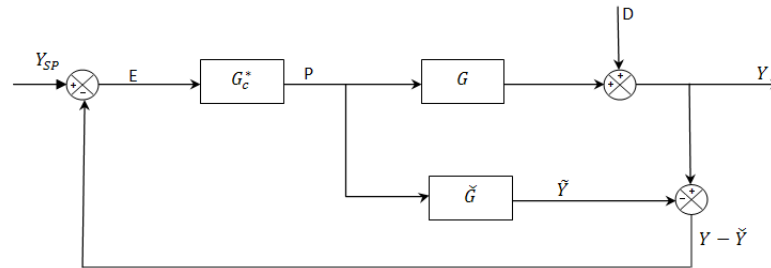


Figure 2.4: Internal Model Control blocks diagram scheme [19].

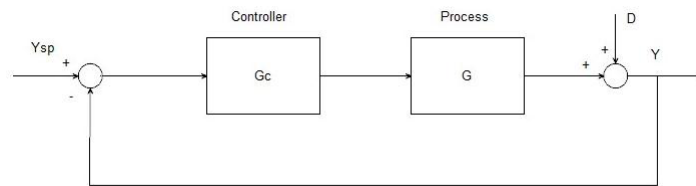


Figure 2.5: Classical feedback blocks diagram scheme [19].

This G_c^* controller is designed in two main steps [22]:

1. Obtain a simple transfer function model (e.g, first/second order model plus time delay) from the original process model (model approximation)
2. Calculate PID settings from simple model (PID Tuning).

Step 1: Model Approximation

This step consists of approximate an original transfer function model $G_0(s)$ form which can be approximated either theoretically or empirically [22].

FOPTD model:

$$\tilde{G}(s) = \frac{K}{(\tau s + 1)} e^{-\theta s} \quad (2.16)$$

SOPTD model:

$$\tilde{G}(s) = \frac{K}{(\tau_1 s + 1)(\tau_2 s + 1)} e^{-\theta s} \quad (2.17)$$

Consequently, the approximate model is determined by following model parameters:

- a) model gain K
- b) lag time constant (τ or τ_1 and τ_2)
- c) time delay θ

In order to compute the model parameters from the higher order model, Skogestad's Half Rule [22] can be applied.

Skogestad's Half Rule (JPC 2002)

The model approximation of the model is mainly based on two Taylor approximations of the time delay transfer function:

$$e^{-\theta s} \approx 1 - \theta s \quad (2.18)$$

or

$$e^{-\theta s} = \frac{1}{e^{\theta s}} \approx \frac{1}{1 + \theta s} \quad (2.19)$$

Using the first the first approximation in (2.18), a negative numerator term (a right half plane zero) can be approximated as a time delay:

$$(-T_0 s + 1) \approx e^{-T_0 s} \quad (2.20)$$

where $T_0 > 0$, in the same way, a small time constant τ_0 can be approximated as a time delay using Eq. (2.19):

$$\frac{1}{\tau_0 s + 1} \approx e^{-\theta_0 s} \quad (2.21)$$

Consequently, considering either approximation Eq. (2.20) and approximation Eq. (2.21), the effect delay is the sum of the original delay and the approximated terms as demonstrated in [22]:

$$\frac{-T_0 s + 1}{\tau_0 s + 1} e^{-\theta_0 s} \approx e^{-\theta_0 s} e^{-T_0 s} e^{-\tau_0 s} = e^{-(\theta_0 + T_0 + \tau_0)s} = e^{-\theta s} \quad (2.22)$$

Consider an original model in the form:

$$\tilde{G}(s) = \frac{\prod_j (-T_{j0} + 1)}{\prod_i (\tau_{i0} + 1)} e^{-\theta_0 s} \quad (2.23)$$

lags τ_{i0} are in descending order and $T_{j0} > 0$.

The two approximated models are:

FOPTD model:

$$\tau_1 = \tau_{10} + \frac{\tau_{20}}{2} \quad (2.24)$$

$$\theta = \frac{\tau_{20}}{2} + \tau_{20} + \theta_0 + 3T_0 + \frac{T_s}{2} \quad (2.25)$$

SOPTD model:

$$\tau_1 = \tau_{10} \quad (2.26)$$

$$\tau_2 = \tau_{20} + \frac{\tau_{20}}{2} \quad (2.27)$$

$$\theta = \frac{\tau_{20}}{2} + \theta_0 + 3T_0 + \frac{T_s}{2} \quad (2.28)$$

where T_s is the sampling time for the digital implementation of a PID controller [22].

Step 2: PID tuning

In the IMC design PID tuning is a two step procedure.

1. The process model obtained with the half rule is factored as:

$$\tilde{G}(s) = \tilde{G}_+(s)\tilde{G}_-(s) \quad (2.29)$$

where $\tilde{G}_+(s)$ contains time delays and any right-half plane zeros, and therefore it is the non-invertible component. In contrast, $\tilde{G}_-(s)$ is the invertible term.

FOPTD model In this case the time delay term is approximated with a Padé approximation :

$$e^{-\theta s} = \frac{1 - \frac{\theta}{2}s}{1 + \frac{\theta}{2}s} \quad (2.30)$$

Therefore, the factorization of the process model becomes:

$$\tilde{G}_+(s) = 1 - \frac{\theta}{2}s \quad (2.31)$$

$$\tilde{G}_-(s) = \frac{K}{(\tau s + 1)(\frac{\theta}{2}s + 1)} \quad (2.32)$$

SOPTD model Factorization of the process model with the Taylor series approximation:

$$\tilde{G}_+(s) = 1 - \theta s \quad (2.33)$$

$$\tilde{G}_-(s) = \frac{K}{(\tau_1 s + 1)(\tau_2 s + 1)} \quad (2.34)$$

2. In this step, the IMC controller includes a filter f with a steady-state gain of one with the common form:

$$G_c^* = \frac{1}{\tilde{G}_-(s)} f f = \frac{1}{(\tau_c s + 1)} \quad (2.35)$$

τ_c is an adjustable parameter which determines the speed-of-response. In particular, if it increases, the speed of response decreases and vice versa. In order to compensate the mismatch between the process model and the actual process, τ_c can be adjusted and a higher value of τ_c will determine a robust control system [19]. The final IMC controller will be:

$$G_c^* = \frac{1}{\tilde{G}_-(s)} \frac{1}{(\tau_c s + 1)} \quad (2.36)$$

Once the IMC controller with the two steps is designed, it can be easily brought back to a PID controller with the relationship in (2.13):

Leading to the PID tuning for FOPTD model [19]:

$$K_c = \frac{1}{K} \frac{\tau + \frac{\theta}{2}}{\tau_c + \frac{\theta}{2}} \quad (2.37)$$

$$\tau_I = \tau + \frac{\theta}{2} \quad (2.38)$$

$$\tau_D = \frac{\tau\theta}{2\tau + \theta} \quad (2.39)$$

For the SOPTD model

$$K_c = \frac{\tau_1 + \tau_2}{K(\tau_c + \theta)} \quad (2.40)$$

$$\tau_I = \tau_1 + \tau_2 \quad (2.41)$$

$$\tau_D = \frac{\tau_1\tau_2}{\tau_1 + \tau_2} \quad (2.42)$$

2.2 Process Models

In light of the relevant role that models play for a glucose controller development, it is quite understandable that the lack of accurate models for individual subjects is a key problem in the development of reliable closed-loop control system. A patient-model mismatch could cause hypoglycemia and the controller performance would be reduced. In particular, it can be argued that the needs which a model should satisfy may change in the different phases, e.g; design, tune and validation. Indeed, models for the controller design are generally compact in order to capture the system dynamic behaviors. On the other hand, the controller tuning and validation stages should make use of more detailed simulations which mimic the real system dynamics in a faithful way [20].

Over the years, different types of models which describe the insulin/glucose dynamic (also called "glucose kinetics models" [16]) have been proposed and an exhaustive overview can be found in the literature citeBequette2005, Steil2005, Cobelli2009.

Some models consist of ordinary or partial differential equations, artificial neural networks (ANNs), fuzzy logic or expert systems. In the physiological environment, compartmental models are often employed and they are based on ordinary differential equations. The most widely used model is the so-called "minimal model" of Bergman et al. Figure 2.6 [23]. The aim of this model is to provide a description of the insulin/glucose dynamic in as simple a way as possible, i.e with a minimum number of known or assumed parameters [11, 16, 24].

The model is described by the following differential equations:

$$\frac{dG(t)}{dt} = (p_1 - X(t))G(t) - p_1G_b \quad (2.43)$$

$$\frac{dX(t)}{dt} = p_2X(t) + p_3I(t) \quad (2.44)$$

$$dI(t)/dt = E(t) - n(I(t)) \quad (2.45)$$

The dependent variables are $G(t)$, $I(t)$ and $X(t)$ indicate the plasma glucose the plasma insulin and the insulin concentration in a remote compartment, respec-

tively. Insulin is assumed to be delivered only through exogenous means $E(t)$ and the parameters p_i and n are characterized by the individual patient. G_b is the basal glucose concentration. In recent studies, it was found that this model overestimates the ability of glucose to facilitate its own uptake and underestimates the contribution of elevated insulin levels [24]. Moreover, in this model, a description of how the system behaves after a meal disturbance, and of the insulin kinetics response to a subcutaneous insulin delivery, is not included. Other examples of well-known models are the AIDA model and Sorensen's model [16].

Alternatively, empirical models can be obtained from data. An effort to identify models retrieved from patient data can be found in [25] where various different data-based modeling approaches to diabetes mellitus are analyzed. On the basis of a patient's daily glucose monitoring, data-base models were developed. The glucose-insulin system was simplified and reduced at three main parts because of the modeling goal: the Glucose Sub-Model(GSM), the Insulin-Sub-Model (ISM) and the Glucose-Insulin-Interaction-Model (GIIM). The three parts are modeled separately using mainly compartment models and black-box models. In particular, the GSM describes the glucose absorption from meal, the ISM describes the absorption of insulin from insulin injection and the GIIM the interaction of glucose and insulin in the blood systems and organs. The results of this modeling approach based on the patient data show that they are often inaccurate for several reasons. One relevant cause of the accuracy problems is that clinical data in T1DM lacks sufficient excitation for model identification.

Autoregressive models (AR) have also been investigated for the blood glucose value prediction in order to address the identifiability issues, but they are not suitable for control applications because they do not contain an exogenous input [1]. In order to overcome the exogenous input limit, the autoregressive exogenous input (ARX) model have been demonstrated as a valid choice for control [4].

Fuzzy logic is also applied to the model identification aim. In a process in which a particular change in the input variable may result in three different magnitudes of changes in the output, the fuzzy logic provides a way to indicate that the output might be a mix of two of the magnitudes, for example. Expert systems are based on the knowledge of an "expert" that has a good understanding of the

system. For examples, this kind of model can be used as protocols for insulin delivery in critical care. In this case, clinicians would introduce specific rules such as the required units of insulin for a given blood glucose amount. This kind of approach can also be implemented in a fuzzy logic-based framework [11].

The ANNs models derived by physiological description of the function of neurons and neural networks in animals. An ANN model is normally used to provide a nonlinear relationship between inputs and outputs. The procedure consists of two steps: training and verification. In the first step, an ANN model is trained with a known input and output data, and it finds the best data fit with an optimization of the ANN parameters. Then, a verification with different input-output data from the one used for the training is conducted [11].

2.2.1 Control-relevant Models

All the models listed above are suitable both for a control purpose and for the prediction of the patient behavior. However, some of them are more appropriate for prediction rather than a control purpose. An important class of models for control system design is called control-relevant models. The main idea behind this type of model is that they are developed for the specific control goal rather than for the optimization of the prediction of future glucose value [1].

In order to achieve an accurate prediction of the patient's behavior, detailed models are more suitable, containing large number of parameters and differential equations along with nonlinearities which are typical for biological process [24]. However, when the purpose is different from prediction, the control-relevance issues must be addressed. An example of a model with a high level of complexity can be the detailed compartment model of glucose-insulin interaction [26], which contains 19 total differential equations, Figure 2.7, rather than the 3 differential equations in the Bergman 'Minimal Model'.

As mentioned above, the performance of a model-based control, e.g IMC-PID, is directly related to the model accuracy. In spite of the need for refined and accurate models, a good control performance can be achieved with approximate models whose requirements for control are based on frequency-domain arguments. Hence, an approximate model needs to be accurate at frequencies around the

closed-loop bandwidth in order to achieve a robust control performance which is a prerequisite in the artificial pancreas design. Indeed, if the correct frequency range is captured, a large amount of mismatch in an open-loop simulations response can be tolerated without leading to a decrease in the closed loop performance [1].

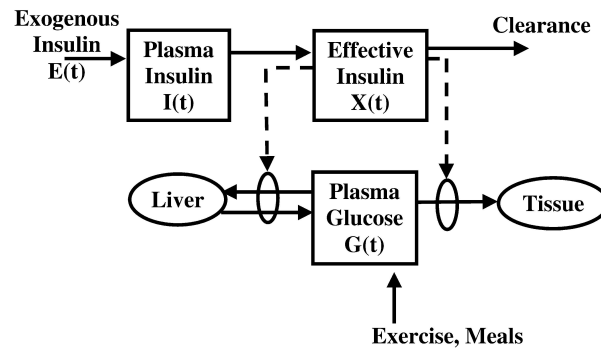


Figure 2.6: Schematic overview of the 'Minimal Model' of Bergman et al. [24].

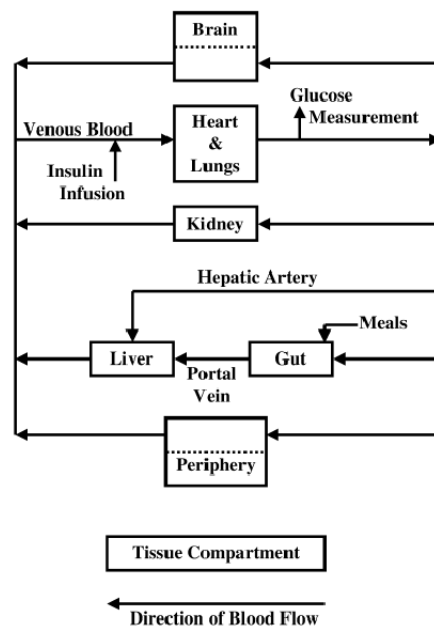


Figure 2.7: Detailed scheme for the insulin-glucose interactions [24].

Another key issue in finding proper models for control is the necessity of a personalization of the control algorithm. The artificial pancreas should ideally

perform safely and satisfactorily for all the patients. Unfortunately, the intra-individual and the inter-individual variability among the subjects make it difficult to achieve the controller robustness and if model and/or controller personalization is not implemented. On the other hand, identification of accurate individual models is very difficult. A solution to this problem has been proposed by van Hausden et al. [1], where parametric models are first identified to provide a model structure that captures the the dynamic around the expected closed-loop bandwidth. Then, a fixed model is defined which underestimates the robustness margins. Finally, a personalization of the model is achieved by modifying the model gain of the model for each subject on the basis of the *a priori* patient characteristics such as the total daily insulin (TDI).

2.2.2 Novel PID Control Approach Based on Personalized Model

The PID control algorithm for automated closed-loop insulin delivery system has been widely applied. In [16] PID control algorithm was used in order to demonstrate the feasibility of a closed-loop insulin delivery system based on subcutaneous insulin delivery and subcutaneous glucose sensing. In [18] the PID algorithm was used to evaluate the effect of controller gain on the insulin response to a meal. In both cases the controller gain was calculated taking into account the subject's TDI value. In [17] a combination of insulin boluses and PID control with switching criteria has been evaluated.

The novel approach proposed in this thesis consists in the use of a control-relevant model in order to design the PID controller, reducing the three tuning terms (proportional, derivative and integral terms) to two tuning variables that affect the controller gain: the model gain (K) and the speed of response to the meal (τ_c) as showed in Eq. (2.40). Furthermore, the model gain, and consequently the controller gain, are personalized based on the subjects' TDI value.

The detailed of the model, personalization of the gain and controller implementation will be presented in the next chapter

Chapter 3

Controller design and Implementation

In this chapter the details of the controller design and its implementation are presented. In particular, the main design issues are analyzed, and a brief description of the process model identification is provide, as well. Then, each implementation step is reported.

3.1 Main Design Issues

Even though the APS is supposed to improve glycemia control and thus avoiding high glucose blood values, it is important to emphasize the risks it may introduce. The main risk is hypoglycemia that occurs when the blood glucose concentration is below 60 mg/dl. This undesirable situation usually occurs after a meal intake, when the corresponding insulin bolus is too large. The increasing concentration of blood glucose after a meal may cause an over-delivery by the controller which will not be detected immediately, and it is too late to turn off the insulin delivery [1]. For this reason, avoiding postprandial hypoglycemia turned to be the most difficult challenge in developing an artificial pancreas controller. The main cause of a controller failure in regulating blood glucose and avoid hypoglycemia events is the inter-subject and intra-subject variability, leading to a patient-model mismatch. As a results of this mismatch, the controller can be either too aggressive

or too conservative. With a conservative controller, the meal response will be too slow to overcome hyperglycemia, on the other hand, an aggressive controller will provide more insulin than is desired, leading to low glycemic blood values.

The model identification is the first step in designing a robust controller algorithm which minimize the risk of hypoglycemia. Then, the tuning parameters can be optimized by using a personalized model, and thus a personalized control algorithm.

3.2 Model Identification

The aim of this research is to use simple control-relevant models in order to develop a PID-IMC controller for the Artificial Pancreas System, designing including the process model dynamics. Over the years, many models have been developed and used in order to design different controllers as described in Chapter 2. However, the main characteristic of this new type of control-relevant model is that it is more focused on achieving the desired control performance rather than providing an optimum prediction of the glucose blood concentration. Since the main aim in developing a controller for the artificial pancreas system should always be the safety of the patient, a valid control algorithm should either prevent risk situations of hypoglycemia and at the same time meet the performance specifications.

The personalized control-relevant models proposed by Van Heusen et al. [1] introduce *a priori* information in the model in order to guarantee robustness in case the patient's dynamics significantly differ from the model. The model identification in [1] is conducted *in silico* with 10 representative subjects of the UVA/Padova metabolic simulator with a protocol that cannot be performed in a clinical environment, but with all the important information and without noise information required. In the experiment, the total simulations lasts 72 hours, and three bolus of 1, 2 and 3 units, respectively, is provided to the 10 subjects. The first bolus is given after the subjects reach the fasting blood glucose. The second bolus is delivered after 24 hours and the third bolus after 48 hours. For each subject a transfer function is estimated. The cross-over frequency of the open-loop

systems, frequency at which the phase angle curve crosses zero degrees, is found to be approximately 2×10^{-4} rad/s and, therefore, the closed loop bandwidth is expected to be between 5×10^{-5} rad/s and 4×10^{-4} rad/s [1]. The model input is the insulin delivered by the pump and the output is the blood glucose concentration. In Van Heusen et al. a discrete third-order transfer function model is defined:

$$M_r(z^{-1}) = \frac{G(s)}{I(s)} = \frac{Kz^{-3}}{(1 - 0.98z^{-1})(1 - 0.965z^{-1})^2} \quad (3.1)$$

where

$$K = -2.005 \times 10^{-4} \text{ (mg/dl)/(pmol/min)}$$

The insulin units are (pmol/min) and the glucose units are (mg/dl). The Bode diagram of this model is compared to the ten subjects' Bode diagrams in Figure 3.1. The phase for the model is lower and its gain is overestimated, leading to a more robust and conservative control if the expected closed-loop bandwidth is correct.

Personalized Models

A conservative model fixed gain that may result in poor controller performance when a significant patient-model mismatch occurs. This problem can be minimized by replacing the fixed model gain with a gain that is personalized for each subject using *a priori* information. The dynamics of the personalized model are fixed, but, the gain is adjusted on the basis of subject's sensitivity to insulin. The model with the personalized gain is in the form:

$$M_i(z^{-1}) = \frac{G(s)}{I(s)} = \frac{F_s K_i c z^{-3}}{(1 - 0.98z^{-1})(1 - 0.965z^{-1})^2} \quad (3.2)$$

Where M_i is the model for subject i , F_s is the safety factor, K_i is the individualized gain which is calculated based on the subject's total daily insulin (TDI) with the 2400 rule:

$$K_i = \frac{2400}{TDI} \quad (3.3)$$

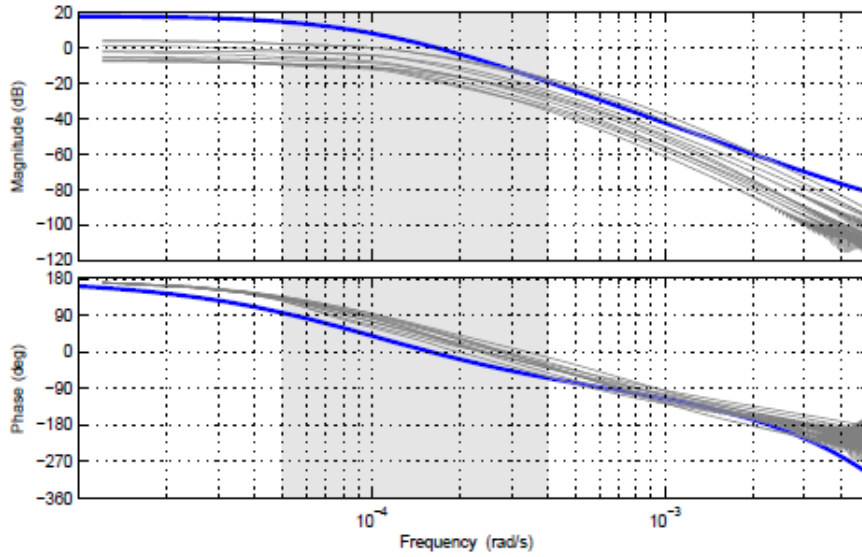


Figure 3.1: Bode diagrams for the model (blue line) and for the ten subjects (gray lines) [1].

and c is a constant determined in part by the units used and in part by a scaling factor. In this research, $c = 1.255 \times 10^{-6}$ (pmol/min/U/h). The safety factor F_s is chosen by the physician. Its value is normally ≤ 1 and guidelines which suggest how to select the safety factor are available in [1]. The aim of the safety factor is to compensate the uncertainty due to the underestimation of the TDI. In this thesis F_s is considered to be equal to 1. The design of any linear model-based controller can be conducted using this personalized model [1].

3.3 Controller Design

The controller design consists of two main steps: (i) find a continuous low-order approximation of the transfer function model in Eq. (3.2) and (ii) use this approximation to implement a PID controller using the IMC design method. In the following two sections, these two steps are described.

3.3.1 Model Approximation

In order to design an IMC controller, the first step is to find the continuous control-relevant model starting from its discrete form.

The bilinear (Tustin) transform approximation is a simple and easy to use method in order to relate the s- and z- domains. It is in the form:

$$z = e^{sT_s} \approx \frac{1 + sT_s/2}{1 - sT_s/2} \quad (3.4)$$

where T_s is the sampling period of the discrete system ($T_s = 5$ min) [27].

After, applying the approximation to the discrete model, the following continuous transfer function model is obtained in the gain time-constant form (in h):

$$M_r(s) = \frac{K(-0.03s + 1)^3 e^{-0.25s}}{(4.12s + 1)(2.33s + 1)^2} \quad (3.5)$$

$$K = -8.184 \text{ (mg/dl)/(pmol/min)}$$

Its Bode digram is shown in Figure 3.2

The expected frequency of interest is between 5×10^{-5} rad/s and 4×10^{-4} rad/s. Since any model which shows the current dynamic behavior for this frequency range would be satisfactory for the controller design, the M_r continuous transfer function is a good approximation.

Next, the model in Eq. (3.6) is reduced to either a second and first-order model plus time-delay (FOPTD or SOPTD) using Skogestad's Half Rule in Chapter 2.

$$M_r(s) = \frac{K e^{-\theta_0 s} (-T_0 s + 1)^3}{(\tau_{10} s + 1)(\tau_{20} s + 1)^2} \quad (3.6)$$

$$K = -8.134 \text{ (mg/dl)/(pmol/min)}$$

$$T_0 = -0.03 \text{ h}$$

$$\tau_{10} = 4.12 \text{ h}$$

$$\tau_{20} = 2.33 \text{ h}$$

$$\theta = 0.25 \text{ h}$$

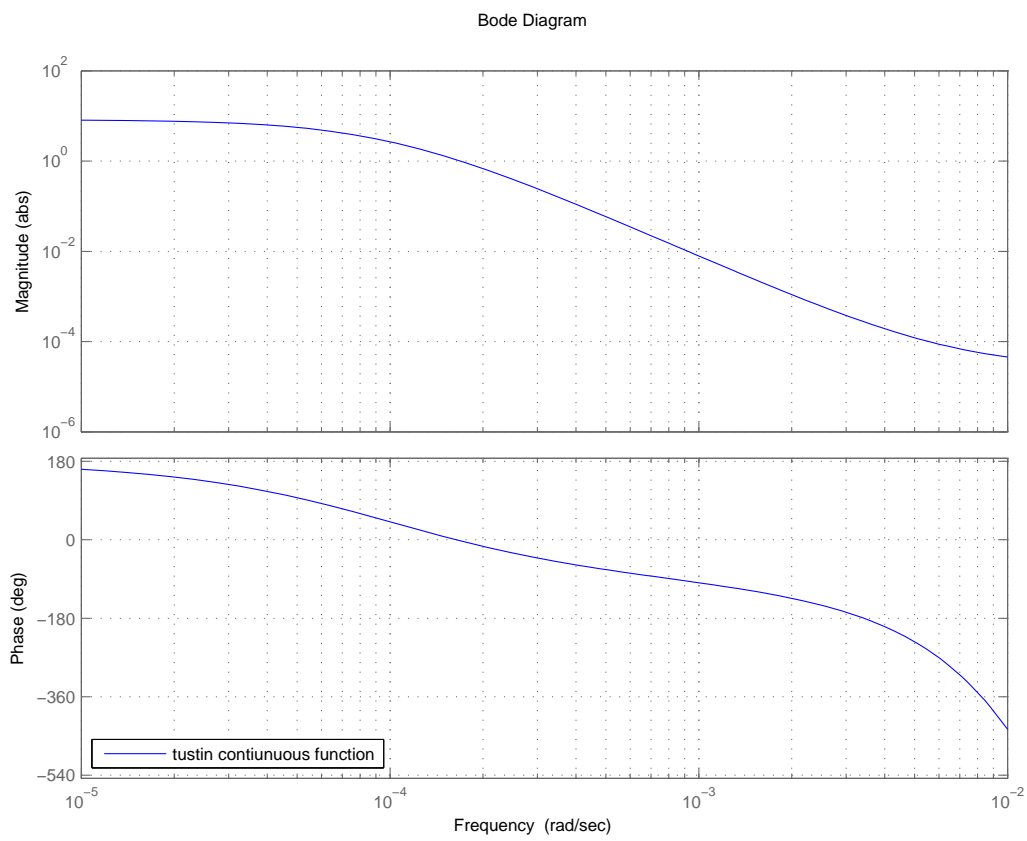


Figure 3.2: Bode diagram of M_r continuous transfer function

Applying Eq. (2.24) and Eq. (2.25) gives:

$$\tau_1 = \tau_{10} + \frac{\tau_{20}}{2} = 5.3 \text{ h} \quad (3.7)$$

$$\theta = \frac{\tau_{20}}{2} + \tau_{20} + \theta_0 + 3T_0 + \frac{h}{2} = 3.9 \text{ h} \quad (3.8)$$

Obtaining the FOPTD model:

$$M'_r(s) = \frac{K e^{-3.9s}}{5.3s + 1} \quad (3.9)$$

And applying Eq. (2.26)-2.28 gives:

$$\tau_1 = \tau_{10} = 4.12 \text{ h} \quad (3.10)$$

$$\tau_2 = \tau_{20} + \frac{\tau_{20}}{2} = 3.49 \text{ h} \quad (3.11)$$

$$\theta = \frac{\tau_{20}}{2} + \theta_0 + 3T_0 + \frac{h}{2} = 1.56 \text{ h} \quad (3.12)$$

And the SOPTD model:

$$M_r(s)'' = \frac{K e^{-1.56s}}{(4.12s + 1)(3.49s + 1)} \quad (3.13)$$

$$K = -8.184 \text{ (mg/dl)/(pmol/min)}$$

From Figures 3.3 and 3.4 a comparison between the discrete model presented by Van Husen et al. [1] and its continuous approximation as either a FOPTD or SOPTD is provided. In Figure 3.3 the Bode diagrams show that the approximations are similar to the discrete model in the frequency range of interest. In Figure 3.4 the step responses of the three models are very similar. Nevertheless, considering both the Bode diagrams and the step responses, the SOPTD model provides the better approximation. For this reason the model chosen for the IMC-PID controller design was the SOPTD model.

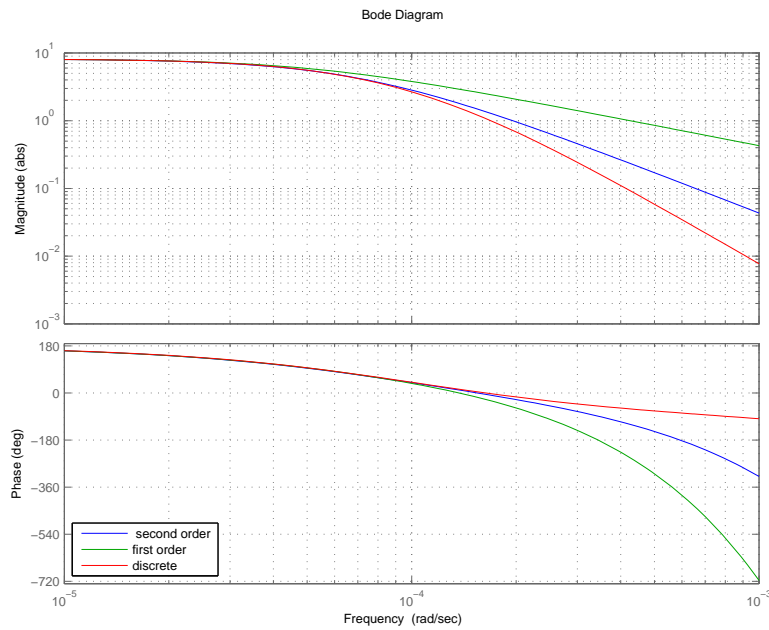


Figure 3.3: Bode diagrams for the FOPTD, SOPTD and discrete models.

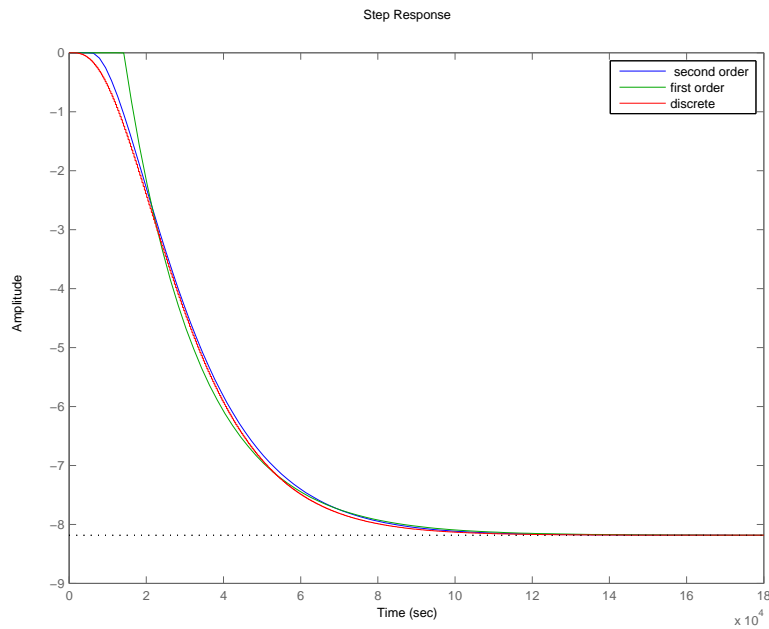


Figure 3.4: Step responses for the FOPTD, SOPTD and discrete models.

3.3.2 PID Controller Tuning

In a SOPTD model, Eqs. 2.40 to 2.42 lead to the following PID controller settings:

$$K_c = \frac{7.61}{K(\tau_c + 1.56)} \quad (3.14)$$

$$\tau_I = 7.61 \text{ h} \quad (3.15)$$

$$\tau_D = 1.89 \text{ h} \quad (3.16)$$

3.4 Simulator PID Implementation

The two main parts of the controller part of the simulator are a setup script and a run-time algorithm. The setup script allows the controller to be tuned for each subject and thus provides the personalized information to the run-time controller. The run-time algorithm applies the tuned control algorithm. The control algorithm is implemented in the form of a *Simulink*[®] block and the input and output of the control block are fixed. In the main panel of the *Simulink*[®] simulator, Figure 3.5 the control law block is the orange block at the bottom.

Within the orange block the controller was implemented. For the first implementation of the controller, the noise introduced by the CGM sensor was not considered, and glucose concentration values are provided to the PID controller from the input 1 (glucose). In the PID block the PID algorithm was implemented.

3.4.1 Discrete PID Control

Since the CGM device provides samples of the subcutaneous glucose amount every five minutes, the digital implementation of the parallel form of the PID controller was considered. The discrete IMC-PID algorithm was implemented with an m -file in the controller block. In order to obtain the discrete form, the integral and derivative terms in Eq. (2.10) were replaced by difference approximations.

$$\int_0^t e(t^*) dt^* \approx \sum_{j=1}^k e_j \Delta t \quad (3.17)$$

$$\frac{de}{dt} \approx \frac{e_k - e_{k-1}}{\Delta t} \quad (3.18)$$

Δt : T_s

e_k : error at the k^{th} sampling instant for $k=1,2..$

With this two approximation, the discrete PID control algorithm becomes:

$$u_k = \bar{u} + K_c \left[e_k + \frac{\Delta t}{\tau_I} \sum_{j=1}^k e_j + \frac{\tau_D}{\Delta t} (e_k - e_{k-1}) \right] \quad (3.19)$$

u_k : is the controller output at the k^{th} sampling instant.

In order to avoid the derivative kick issue, the derivative action is applied only at the measured subcutaneous glucose concentration rather than the error signal as well as in the continuous manner. The resulting digital PID formula will be:

$$u_k = \bar{u} + K_c \left[e_k + \frac{\Delta t}{\tau_I} \sum_{j=1}^k e_j + \frac{\tau_D}{\Delta t} (y_{m,k-1} - y_{m,k}) \right] \quad (3.20)$$

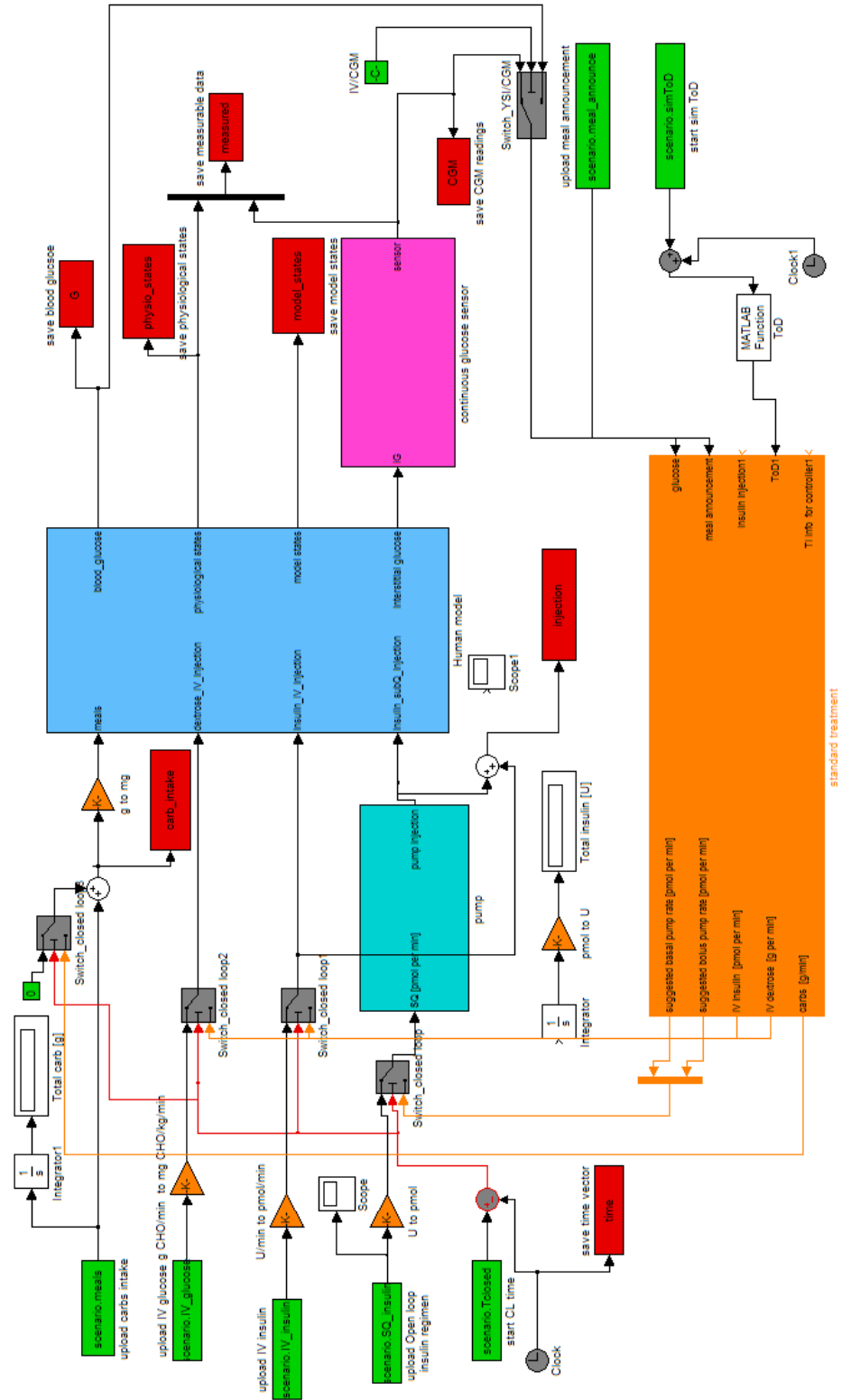


Figure 3.5: The UVA/Padova metabolic simulator. Main panel with the control law block at the bottom(orange).

Chapter 4

Controller With a Non-personalized Controller Gain

In this chapter, first a population of ten representative subjects from the UVA/Padova metabolic simulator is used to investigate the best tuning of the PID controller for a single non-personalized model. Then, a different population of ten subjects is used to validate the selected controller tuning. The main results for all the simulations conducted are reported in this chapter, and in Appendix all the single subject results are reported as well.

4.1 Effect of τ_c

In this section the results of controller tuning are reported. Since the controller gain is not personalized and thus is fixed for each subject, the only tuning parameter is τ_c . A population of ten adult subjects of the UVA/Padova metabolic simulator is used to conduct simulations in order to evaluate the effect of τ_c on the controller performance for post-prandial conditions. The scenario chosen for the on-line tuning is:

- $t=2$ h: controller turned on;
- $t=7$ h: a single meal of 50 g CHO is given to the subject;
- $t=30$ h: simulation ends.

The controller set point is 110 mg/dl for all the subjects. The simulation lasts 30 h in order to observe the entire response and determine whether or not the set point is reached for the critical case of undershoot and hypoglycemia. Based on the FOPTD model in Eq. (3.9), three values of τ_c were considered: $\tau_c=1, 2$ and 5 h.

Table 4.1 shows the PID controller settings for these three values of τ_c . Note that controller aggressiveness decreases as τ_c increases because K_c also decreases (in absolute values).

Table 4.1: PID settings for different values of τ_c

τ_c	K_c	τ_I	τ_D
h	pmol/min mg/dl	h	h
1	-0.37	7.63	1.88
2	-0.26	7.63	1.88
5	-0.14	7.63	1.88

The simulation results for the three different values of τ_c are reported in Figures 4.1- 4.3 and Tables 4.2 and 4.3. Observing the glucose concentration (at the top of each figure) as well as the insulin infusion rate (at the bottom), the effect of τ_c on controller of aggressiveness is quite evident. No hypo- or hyperglycemia events occurred. Furthermore, the blood glucose concentration is never below 80 mg/dl for all the subjects and τ_c values. For $\tau_c = 1$ h, all the subjects except # 6 reach the set point. Moreover, there were only three subjects (# 4, 6 and 7) that show undershoot; however, their minimum glucose values were well above the hypoglycemia threshold of 80 mg/dl. Results for $\tau_c = 1$ h do not differ so much from the $\tau_c = 2$ h case. Responses for $\tau_c = 5$ h reveal a less aggressive controller output, since none of the subjects shows glucose values below 99 mg/dl and most of them do not reach the set point during the simulation time, the lowest glucose value mean is 116 ± 10 mg/dl.

The idea that a more conservative response lead to higher glucose peak is confirmed by comparing the ΔG values in Table 4.3, where the mean of the glucose peak relative to the value at t_{meal} is 69 ± 22 for $\tau_c = 1$ h and 83 ± 24 for

$\tau_c = 5$ h. The glucose concentration remains within the glucose range $80 \div 140$ (normo-glycemia range) for $66(\pm 13)\%$ of the time for $\tau_c = 1$ h, whereas in $\tau_c = 5$ h glucose concentration remains only $55(\pm 15)\%$ of the time in the same range.

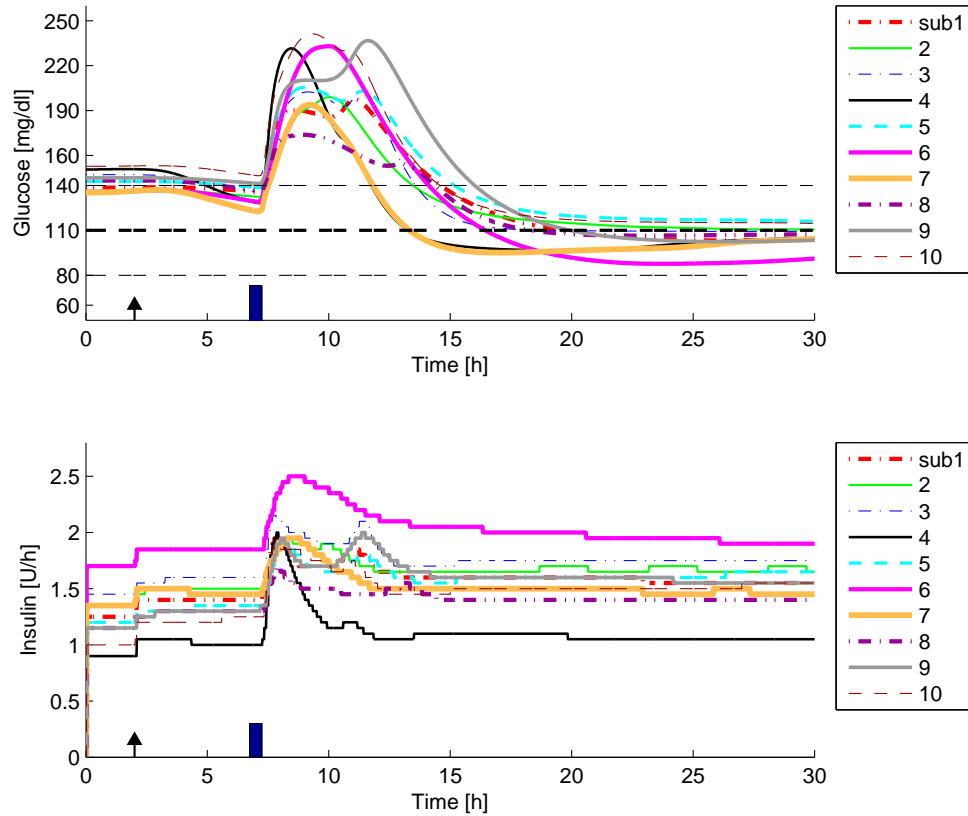


Figure 4.1: Post-prandial responses for $\tau_c = 1$ h. The thick dashed line indicates the set point (110 mg/dl). The two thin dashed lines indicate the normo-glycemia zone (80-140 mg/dl).

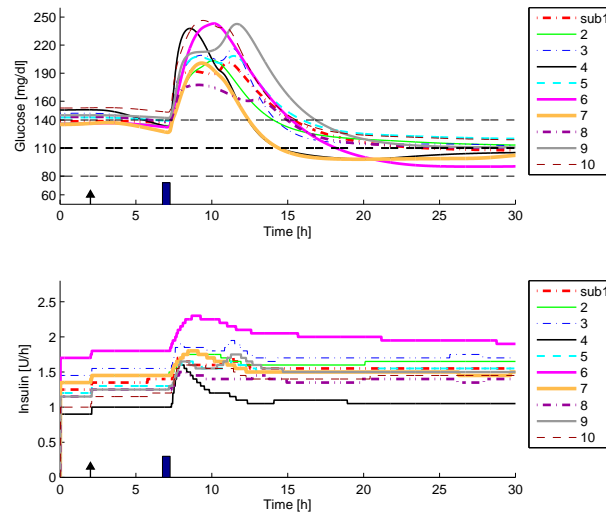


Figure 4.2: Post-prandial responses for $\tau_c = 2$ h. The thick dashed line indicates the set point (110 mg/dl). The two thin dashed lines indicate the normo-glycemia zone (80-140 mg/dl).

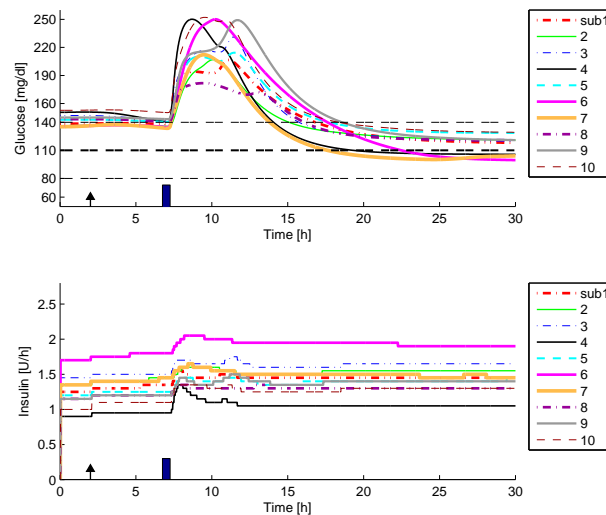


Figure 4.3: Post-prandial responses for $\tau_c = 5$ h. The thick dashed line indicates the set point (110 mg/dl). The two thin dashed lines indicate the normo-glycemia zone (80-140 mg/dl).

Table 4.2: Single meal statistics: percentage of time that glucose concentration (mg/dl) remains within the indicated range. Average values for the ten subjects.

range	$\tau_c = 1$ h	$\tau_c = 2$ h	$\tau_c = 5$ h
$60 < G < 80$	0	0	0
$80 < G < 140$	66 (± 13)	63 (± 13)	55 (± 15)
$70 < G < 180$	88 (± 6)	86 (± 6)	84 (± 5)
$180 < G < 250$	12 (± 6)	14 (± 6)	16 (± 5)

Table 4.3: Single meal metrics: mean and standard deviation for each τ_c value. ΔG is the glucose peak value relative to the value t_{meal} , the meal time: $\Delta G = G_{max} - G_{meal}$. G_{max} is the maximum blood glucose value and G_{min} is the minimum value, during the post-prandial response. t_r is the time to return to the normo-glycemia zone after the meal.

metrics	$\tau_c = 1$ h	$\tau_c = 2$ h	$\tau_c = 5$ h
ΔG (mg/dl)	69 (± 22)	75 (± 22)	83 (± 24)
G_{max} (mg/dl)	212 (± 21)	218 (± 22)	225 (± 23)
G_{min} (mg/dl)	104 (± 9)	108 (± 9)	116 (± 10)
t_r (h)	6.5 (± 2)	7 (± 2)	9 (± 2)

In Figures 4.4 and 4.5 the effect of the three different τ_c values for subject # 5 and 6 is showed. Subject # 6 shows the most undershoot among all the subject, and when $\tau_c = 1$ h the controller performance in term of time required to make the glucose return in the normo-glycemia zone is improved (7.1 h, Table C.5) compared to $\tau_c = 5$ h (10.6 h, Table C.5), subject # 6 shows a longer undershoot for $\tau_c = 1$ h, but still remains in the normo-glycemia range (88 mg/dl is the minimum glucose value). For # 5 the difference in the glucose concentration between the effect of the τ_c is not so marked. However, a better performance for $\tau_c = 1$ can be observed.

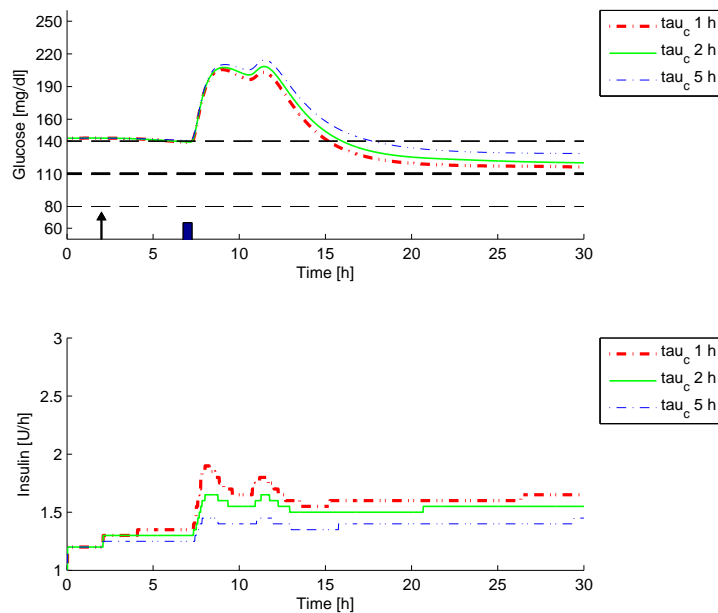


Figure 4.4: Post-prandial responses for subject # 5 and different τ_c value. The thick dashed line indicates the set point (110 mg/dl). The two thin dashed lines indicate the normo-glycemia zone (80-140 mg/dl).

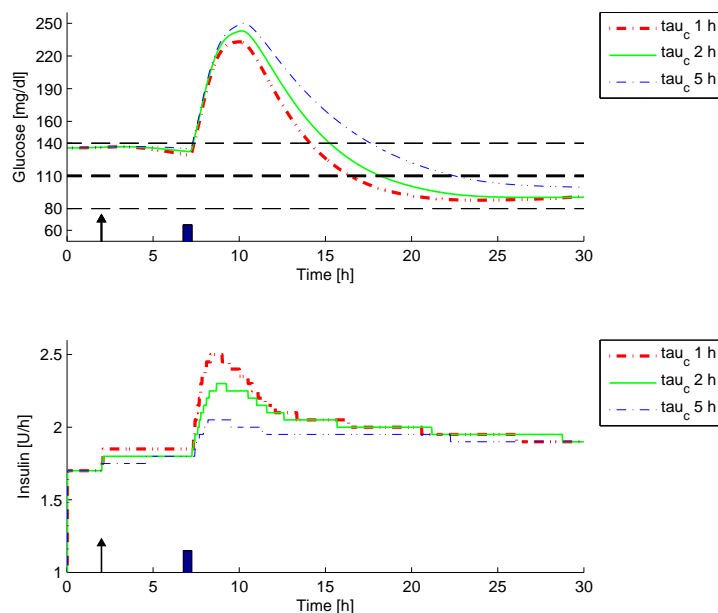


Figure 4.5: Post-prandial responses for subject # 6 and different τ_c value. The thick dashed line indicates the set point (110 mg/dl). The two thin dashed lines indicate the normo-glycemia zone (80-140 mg/dl).

4.1.1 Robustness Test

Although these results show a better performance for $\tau_c = 1$ h for all the subjects, another test should be conducted in order to verify the controller robustness, before establishing the best PID controller tuning settings. The objective of the robustness test was to verify the controller behavior for intra-subject insulin sensitivity changes of $\pm 50\%$. Thus, the controller output was reduced and increased by 50%, to mimic the decrease and increase of the insulin sensitivity for the same scenario. The robustness test results with the controller output $\pm 50\%$ are reported for each τ_c value.

$\tau_c = 1$ h

Robustness results for $\tau_c = 1$ h are reported in Figs. 4.6-4.9. When the controller output is reduced by 50%, the glucose concentration is in general higher compared to the one obtained with the normal controller output, for all the subjects. On the other hand, the undershoot smaller; however, after the meal, all the subjects return around the set point value at the end of the simulation.

With the controller output is increased by 50%, the controller aggressiveness results in lower the glucose concentration peaks and in a pronounced undershoot, but never below the the normo-glycemia lower bound (80 mg/dl).

Subject # 6, as observed also in the previous results, show the most critical case, therefore the three output conditions for this subject are reported. However, for all the three conditions (normal, output controller $\pm 50\%$) the controller performs well, avoiding hypo- hyperglycemia events, even with the subject is more sensitive to the insulin.

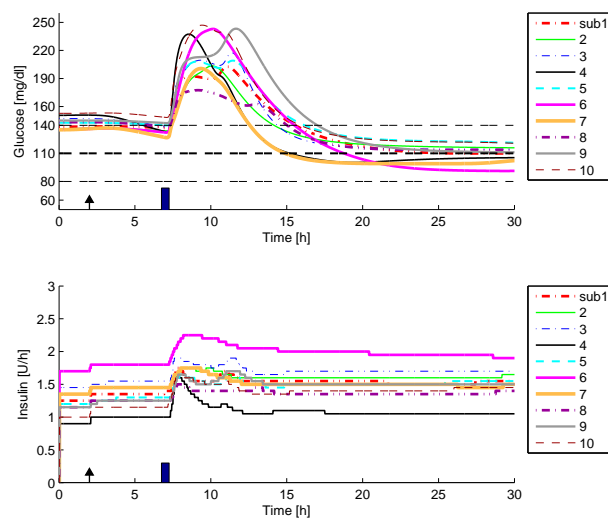


Figure 4.6: Post-prandial responses for $\tau_c = 1$ h. The thick dashed line indicates the set point (110 mg/dl). The two thin dashed lines indicate the normo-glycemia zone (80-140 mg/dl). The controller output is reduced by 50%.

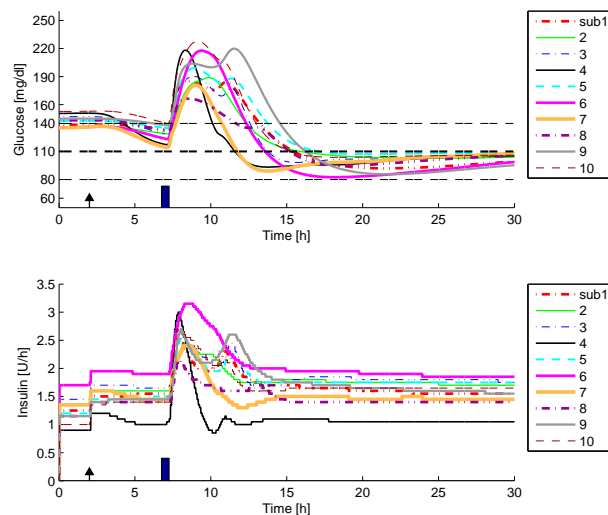


Figure 4.7: Post-prandial responses for $\tau_c = 1$ h. The thick dashed line indicates the set point (110 mg/dl). The two thin dashed lines indicate the normo-glycemia zone (80-140 mg/dl). The controller output is increased by 50%.

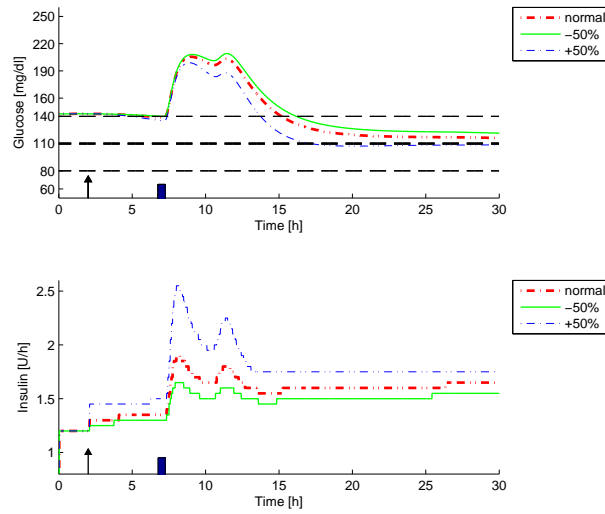


Figure 4.8: Post-prandial responses for subject # 5, $\tau_c = 1$ h and the three controller output conditions (normal, increase by 50% and decrease of the 50%). The thick dashed line indicates the set point (110 mg/dl). The two thin dashed lines indicate the normo-glycemia zone (80-140 mg/dl).

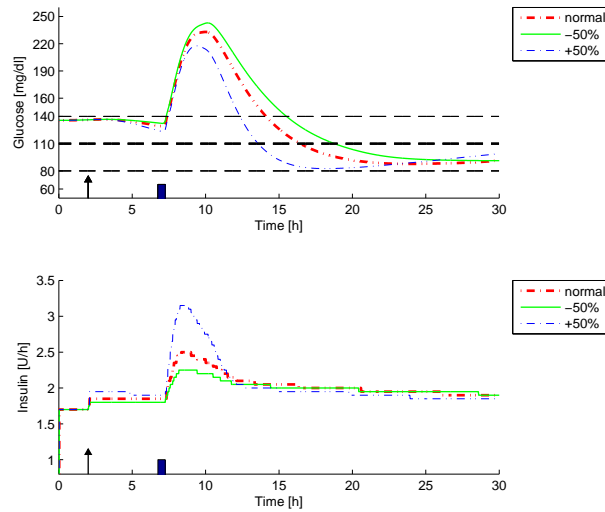


Figure 4.9: Post-prandial responses for subject # 6, $\tau_c = 1$ h and the three controller output conditions (normal, increase by 50% and decrease of the 50%). The thick dashed line indicates the set point (110 mg/dl). The two thin dashed lines indicate the normo-glycemia zone (80-140 mg/dl).

$\tau_c = 2 \text{ h}$

Robustness results for $\tau_c = 2 \text{ h}$ are reported in Figures 4.10-4.13 and they similar to the robustness results for $\tau_c=1 \text{ h}$. Nevertheless, when the controller output is decreased, the controller action results to be less aggressive and some subjects are not longer close to the set point at the end of the simulation.

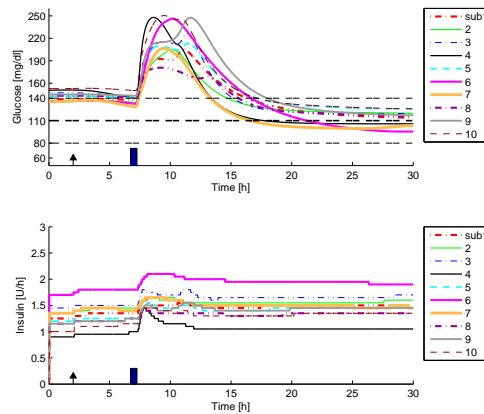


Figure 4.10: Post-prandial responses for $\tau_c = 2 \text{ h}$. The thick dashed line indicates the set point (110 mg/dl). The two thin dashed lines indicate the normo-glycemia zone (80-140 mg/dl). The controller output is reduced by 50%.

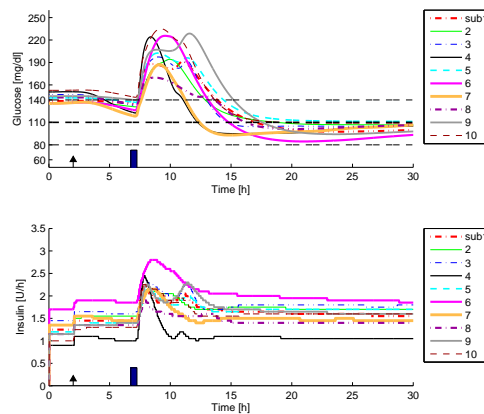


Figure 4.11: Post-prandial responses for $\tau_c = 2 \text{ h}$. The thick dashed line indicates the set point (110 mg/dl). The two thin dashed lines indicate the normo-glycemia zone (80-140 mg/dl). The controller output is increased by 50%

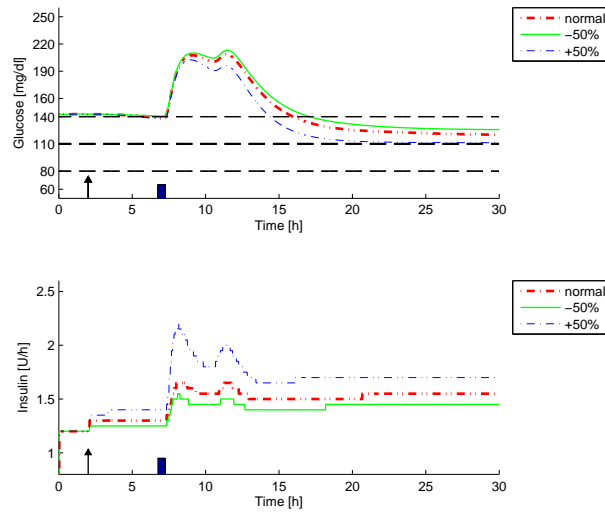


Figure 4.12: Post-prandial responses for subject # 5, $\tau_c = 2$ h and the three controller output conditions (normal, increase by 50% and decrease of the 50%). The thick dashed line indicates the set point (110 mg/dl). The two thin dashed lines indicate the normo-glycemia zone (80-140 mg/dl).

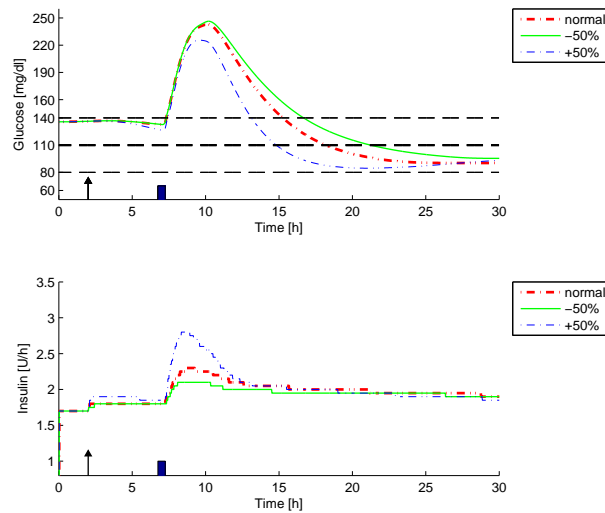


Figure 4.13: Post-prandial responses for subject # 6, $\tau_c = 2$ h and the three controller output conditions (normal, increase by 50% and decrease of the 50%). The thick dashed line indicates the set point (110 mg/dl). The two thin dashed lines indicate the normo-glycemia zone (80-140 mg/dl).

$$\tau_c = 5 \text{ h}$$

Robustness results for $\tau_c=5$ h are reported in Figures 4.15-4.17. When the controller output is reduced by 50%, the controller is less aggressive and is not able to bring the glucose concentration close to the set point for the majority of the subjects, even though there are no cases of undershoot. The insulin delivered by the pump at the bottom of the Figure 4.15 show that the controller is not aggressive enough, since when the meal is detected (blue bar for $t = 7$ h), a really small response is performed by the controller.

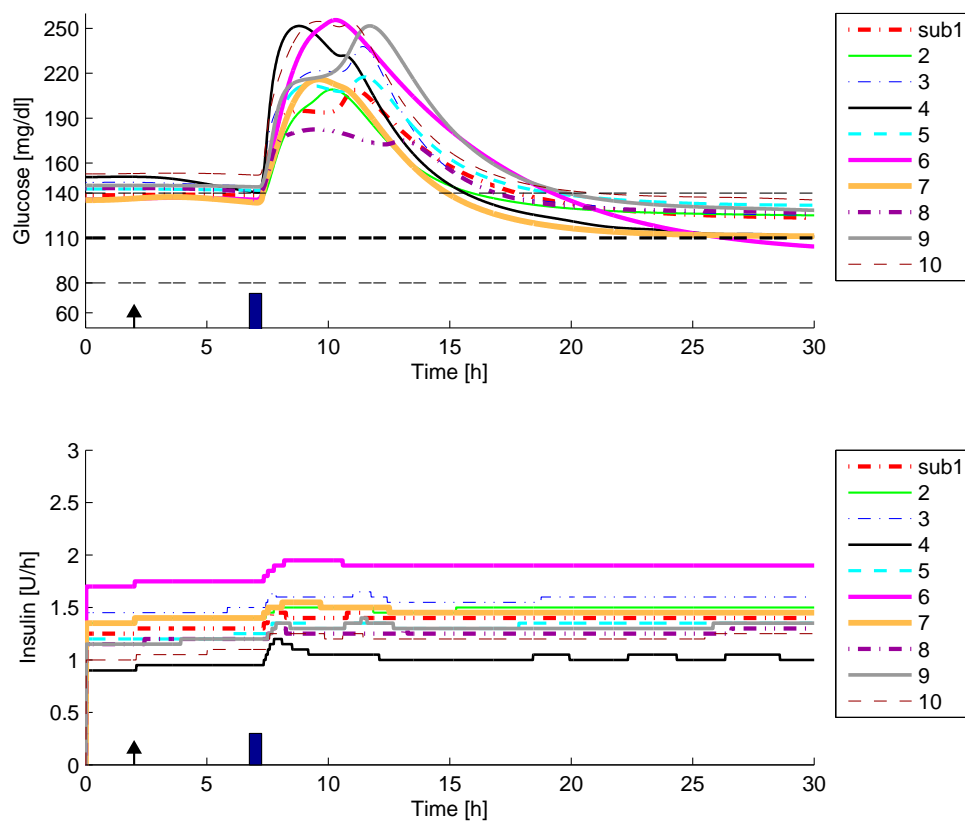


Figure 4.14: Post-prandial responses for $\tau_c = 5$ h. The thick dashed line indicates the set point (110 mg/dl). The two thin dashed lines indicate the normo-glycemia zone (80-140 mg/dl). The controller output is reduced by 50%.

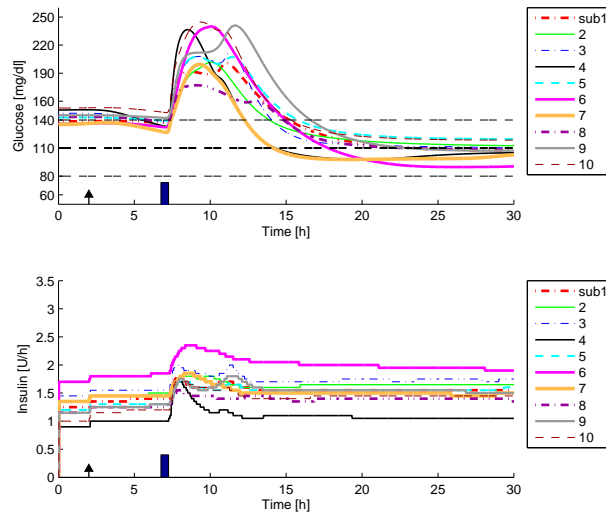


Figure 4.15: Post-prandial responses for $\tau_c = 5$ h. The thick dashed line indicates the set point (110 mg/dl). The two thin dashed lines indicate the normo-glycemia zone (80-140 mg/dl). The controller output is increased by 50%.

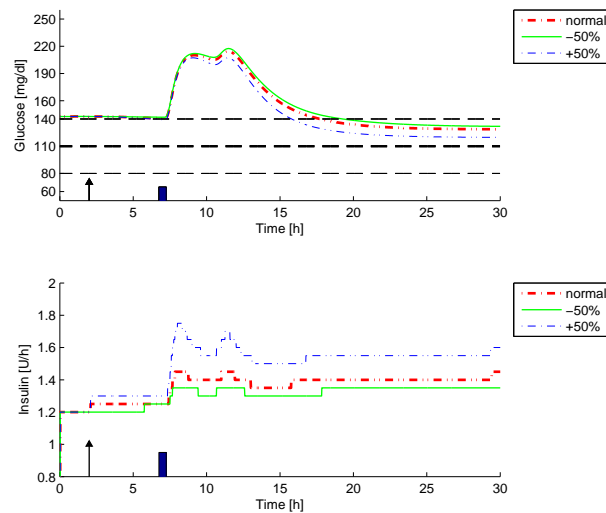


Figure 4.16: Post-prandial responses for subject # 5, $\tau_c = 5$ h and the three controller output conditions (normal, increase by 50% and decrease by 50%). The thick dashed line indicates the set point (110 mg/dl). The two thin dashed lines indicate the normo-glycemia zone (80-140 mg/dl).

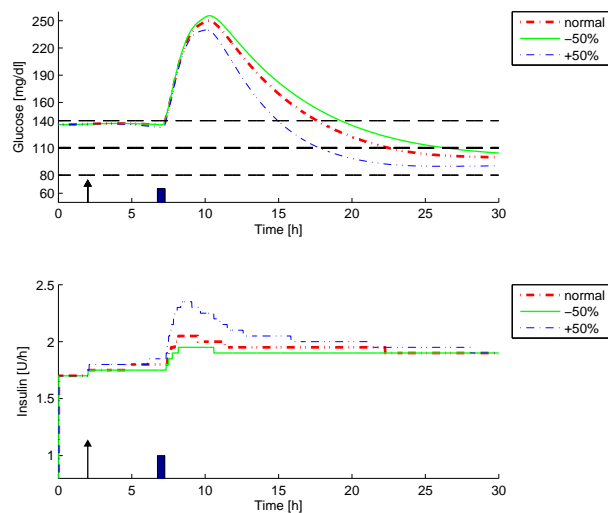


Figure 4.17: Post-prandial responses for subject # 6, $\tau_c = 5$ h and the three controller output conditions (normal, increase by 50% and decrease by 50%). The thick dashed line indicates the set point (110 mg/dl). The two thin dashed lines indicate the normo-glycemia zone (80-140 mg/dl).

In Tables 4.4-4.7 the robustness results for different τ_c values are reported in terms of means and standard deviations. There are no cases of hypoglycemia or hyperglycemia, and none of the subjects shows glucose concentration in the range 60-80 mg/dl. According to the figures and tables, $\tau_c = 1$ h shows the best performance. Indeed, when the controller output is increased by 50%, the glucose concentration remains in the range of normo-glycemia 80-140 for 73 (± 12)% of the time, whereas for $\tau_c = 5$ h only for 63(± 13)% of the time. Percentage of time spent in the range 180-250 changes from 8% (± 5) to 13% (± 6) with $\tau_c = 1$ h and 5 h, respectively. When the controller output is decreased by 50%, the time spent in the range 80-140 is 62(± 14)% for $\tau_c = 1$ h and 51(± 15)%.

Table 4.4: Single meal statistics: percentage of time that glucose concentration (mg/dl) remains within the indicated range. Average values for the ten subjects, when the controller output is increased by 50%.

range	$\tau_c=1$ h	$\tau_c=2$ h	$\tau_c=5$ h
$60 < G < 80$	0	0	0
$80 < G < 140$	73 (± 12)	69 (± 12)	63 (± 13)
$70 < G < 180$	92 (± 5)	89 (± 5)	87 (± 6)
$180 < G < 250$	8 (± 5)	11 (± 6)	13 (± 6)

Table 4.5: Single meal statistics: percentage of time that glucose concentration (mg/dl) remains within the indicated range. Average values for the ten subjects, when the controller output is decreased by 50%.

range	$\tau_c = 1$ h	$\tau_c = 2$ h	$\tau_c = 5$ h
$60 < G < 80$	0	0	0
$80 < G < 140$	62 (± 14)	58 (± 14)	51 (± 15)
$70 < G < 180$	86 (± 6)	85 (± 5)	82 (± 5)
$180 < G < 250$	14 (± 6)	16 (± 5)	17 (± 4)

Table 4.6: Single meal statistics: mean and standard deviation for each τ_c value. ΔG is the glucose peak value relative to the value t_{meal} , the meal time: $\Delta G = G_{max} - G_{meal}$. G_{max} is the maximum glucose concentration value. G_{min} is the minimum value. t_r is the time to return to the normo-glycemia zone after the meal. the controller output is increased by 50%.

metrics	$\tau_c = 1$ h	$\tau_c = 2$ h	$\tau_c = 5$ h
ΔG (mg/dl)	57 (± 20)	63 (± 21)	73 (± 22)
G_{max} (mg/dl)	199 (± 19)	205 (± 20)	216 (± 22)
G_{min} (mg/dl)	95 (± 8)	100 (± 8)	122 (± 10)
t_r (h)	5 (± 2)	6 (± 2)	7 (± 2)

Table 4.7: Single meal metrics: mean and standard deviation for each τ_c value. ΔG is the glucose peak value relative to the value t_{meal} , the meal time: $\Delta G = G_{max} - G_{meal}$. G_{max} is the maximum blood glucose value. G_{min} is the minimum. t_r is the time to return to the normo-glycemia zone after the meal. the controller output is decreased by 50%

metrics	$\tau_c = 1$ h	$\tau_c = 2$ h	$\tau_c = 5$ h
ΔG (mg/dl)	76 (± 23)	80 (± 23)	86 (± 25)
G_{max} (mg/dl)	218 (± 22)	223 (± 23)	228 (± 24)
G_{min} (mg/dl)	110 (± 9)	114 (± 10)	122 (± 10)
t_r (h)	7 (± 2)	8 (± 2)	10 (± 3)

4.1.2 Discussion

Both the results for the effect of the τ_c values and the robustness test show that the best PID tuning results are for $\tau_c = 1$ h. The mean values is of 6.5 h to return in the normo-glycemia zone after the meal intake, the highest glucose concentration value is 247 mg/dl for subject # 10 when controller output decreased by 50%, and the lowest glucose concentration value is 86 mg/dl when the controller output is increased by 50%. These results ensure that for this value of τ_c a safe controller results, avoiding any dangerous cases of hypo- or hyperglycemia.

4.2 Validation Test: Post-prandial Results

Once the effect of τ_c values has been analyzed and has been observed that the best controller performance is achieved for $\tau_c = 1$ h, a validation test is conducted. A population of new 10 subjects (different from the previous 10 subjects population) from the UVA/Padova metabolic simulator is used to investigate the controller performance when three meals (dinner, breakfast and lunch) are provided. The validation test scenario is:

- $t=0$ h (1 pm): simulation starts
- $t=2$ h (3 pm): controller turned on;
- $t=5$ h (8 pm): a meal of 50 g CHO (dinner) is given;
- $t=16$ h (7 am): meal of 40 g CHO (breakfast) is given;
- $t=21$ h (12 pm): meal of 50 g CHO (lunch) is given t;
- $t=30$ h (9 pm): simulation ends.

Figure 4.18 and Tables 4.8-4.11 show the validation test results. The first important result is that none of the subjects had hypoglycemic events. Moreover, only 1.6% ($\pm 2.7\%$) of the time the glucose concentration remains within the range 60-80 in average (values of 7,3, and 6 % for subjects # 6, 9, and 10 respectively). The minimum glucose value is 70 mg/dl for subject # 6 and, from

Figure 4.18, it occurs around 9 pm, when another meal is given. In particular, the controller action for subject # 3 and 9 is good, since they remain in the range 70-180 for all the simulation. Only subjects # 1, 6, and 10 show hyperglycemia events; nevertheless the highest glucose values are moderate: 279, 182 and 252 mg/dl respectively. The time to return in the normo-glycemia zone after meal is less than 7.3 h after the first meal; after the second meal some of the subjects do not even reach the normo-glycemia zone (# 5, 7 and 8) before the third meal is provided. After the third meal, the time to reach the normo-glycemia zone is less 6.5 h for all ten subjects. Subjects # 9 and 3 after the first meal return in the normo-glycemia zone for almost all the time.

These results demonstrate that the choice of $\tau_c = 1$ h guarantees a safe controller action with moderate glucose concentration maximum values.

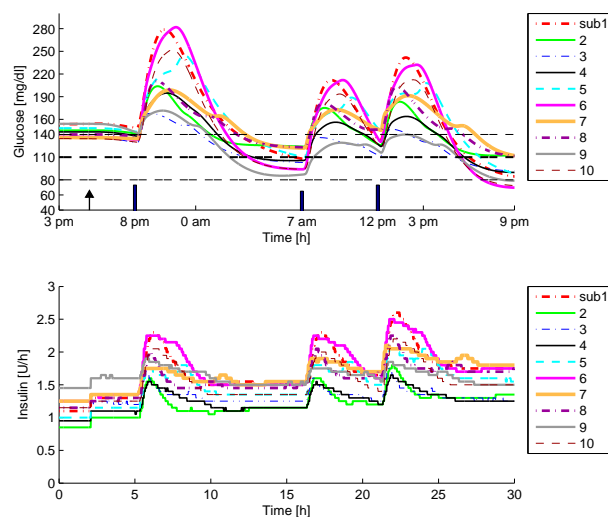


Figure 4.18: Post-prandial responses to three meals. The thick dashed line indicates the set point (110 mg/dl). The two thin dashed lines indicate the normo-glycemia zone (80-140 mg/dl).

Table 4.8: Single meal statistics: percentage of time that the glucose concentration remains within the indicated range.

Subject	60<G<80	80<G<140	70<G<180	180<G<250	G>250
1	0	32	68	26	6
2	0	44	91	9	0
3	0	82	100	0	0
4	0	46	92	8	0
5	0	27	70	31	0
6	7	45	65	27	8
7	0	40	84	17	0
8	0	45	84	16	0
9	3	65	100	0	0
10	6	51	74	25	2
mean(\pm std)	1.6(\pm 2.7)	48 (\pm 15)	83(\pm 12)	16 (\pm 11)	2(\pm 3)

Table 4.9: The glucose (mg/dl) peak value relative to the value at t_{meal} , the meal time: $\Delta G = G_{max} - G_{meal}$.

Subject	dinner	breakfast	lunch
1	130	104	108
2	62	51	56
3	38	33	34
4	56	51	36
5	96	74	56
6	149	118	97
7	64	51	44
8	73	58	57
9	28	42	21
10	123	99	86
mean	82	68	59
\pm std	\pm 39	\pm 28	\pm 27

Table 4.10: Time to return to the normo-glycemia zone after the meal.

Subject	dinner	breakfast	lunch
1	6.8 h	4.7 h	4.7 h
2	5.0	4.0	3.9
3	4.3	0.0	2.0
4	5.4	4.1	4.0
5	7.3	/	5.3
6	6.1	4.9	4.7
7	7.3	/	6.4
8	6.7	/	5.6
9	4.8	0.0	0.0
10	5.7	4.5	4.5

Table 4.11: Blood glucose (mg/dl) maximum (G_{max}) and minimum (G_{min}) glucose values during the post-prandial response.

Subject	G_{min}	G_{max}
1	84	279
2	112	204
3	92	168
4	90	195
5	88	245
6	70	282
7	112	199
8	111	211
9	79	171
10	72	252
mean	91	220
\pm std	± 15	± 39

Chapter 5

Controllers With a Personalized Controller Gain

The structure for this chapter is the same as Chapter 4. The same population of ten subjects from the UVA/Padova metabolic simulator used in Chapter 4 Section 4.1 is used to investigate the best tuning of the PID controller, when the controller gains are personalized. Then, the different population used for the validation test in Chapter 4 is used to validate the selected controller tuning. The mean results for all the simulations conducted are reported in this chapter, and in Appendix all the single subject results are reported as well.

5.1 Effect of τ_c

In this section the results of the controller tuning are reported. The controller gain is now personalized for each subject based on the TDI value. The controller gain K_c in Eq. (3.14) depends either on the process model gain (K) and on the desired speed-of-response time constant τ_c . Table 5.1 reports the process model personalized gains. The model gains can be personalized either using the subjects' TDI, or by determining the process gain for each subject with a step test as explained in Appendix B. However, the use of only TDI information is the better way to personalize the gain, since it is *a priori* information provided by physicians. In Table 5.1, the gain calculated by the step test are reported as well, to provide a

comparison between the two types of gain calculations. Both TDI based gains and step-test gains are between - 4.2 and -0.67 (mg/dl/pmol/min), which are smaller than the fixed gain used by van Hausden [1] -8.13 (mg/dl/pmol/min). Indeed, the fixed gain was chosen to lead to a robust and conservative controller rather than an aggressive one, since the controller output is inversely proportional to the model gain. These relationships can be verified in Table 5.2 where the personalized with TDI information and non personalized controller gains for $\tau_c = 1, 2, 3, 4$ and 5 h are reported.

The same population of Chapter 4 is used to conduct simulations in order to evaluate the effect of τ_c on the controller performance for post-prandial conditions. The scenario chosen for the controller tuning is:

- $t=2$ h: controller turned on;
- $t=7$ h: a single meal of 50 g CHO is given;
- $t=30$ h: simulation ends.

The controller set point is 110 mg/dl for all the subjects. The simulation lasts 30 h in order to observe the entire response and determine whether or not the set point is reached for the critical case of undershoot and hypoglycemia. Based on the FOPTD model in Eq. (3.9) and on the more aggressive model gains, five values of τ_c were considered: $\tau_c = 1, 2, 3, 4$ and 5 h.

The simulation results for the three different values of τ_c are reported in Figures 5.1- 5.5 and Tables 5.3 and 5.4. For $\tau_c = 1$ h the personalized controller is too aggressive, since, on average, $3(\pm 3)\%$ of the time the glucose concentration is within the range 60-80 mg/dl, and all the subjects exhibit undershoot more or less marked (subjects # 6, 7 and 9 show the largest undershoots). However, for none of the τ_c values considered show hypoglycemia or hyperglycemia events. Similar results are obtained for $\tau_c = 2$ h, even though the undershoots are reduced; only subjects # 6 and 9 are below 80 mg/dl, and in particular only subject # 9 is below the normo-glycemia lower bound for a considerable percentage of time (20%). A relevant improvement in the controller performance is achieved for $\tau_c = 3$ h, since only subject # 9 shows a glucose concentration below 80 mg/dl, and for only 8

Table 5.1: Process gains calculations (mg/dl/pmol/min) with step changes calculated in Appendix B and TDI.*

Subject	TDI	Step test
1	-2.38	-1.29
2	-2.07	-1.04
3	-2.13	-1.37
4	-3.55	-3.65
5	-1.76	-0.67
6	-1.95	-2.84
7	-2.86	-4.18
8	-2.81	-1.51
9	-1.79	-1.00
10	-1.86	-0.98

* Van Hausden's gain -8.13

Table 5.2: Personalized controller gains K_c (pmol/min/mg/dl)

Subject	$\tau_c = 1$ h	$\tau_c = 2$ h	$\tau_c = 3$ h	$\tau_c = 4$ h	$\tau_c = 5$ h
1	-1.25	-0.90	-0.70	-0.58	-0.49
2	-1.44	-1.03	-0.81	-0.66	-0.56
3	-1.40	-1.01	-0.79	-0.65	-0.55
4	-0.84	-0.60	-0.47	-0.39	-0.33
5	-1.70	-1.22	-0.95	-0.78	-0.66
6	-1.53	-1.10	-0.86	-0.70	-0.60
7	-1.04	-0.75	-0.59	-0.48	-0.41
8	-1.06	-0.76	-0.60	-0.49	-0.41
9	-1.67	-1.20	-0.94	-0.77	-0.65
10	-1.60	-1.15	-0.90	-0.74	-0.63
Van Hausden	-0.37	-0.26	-0.21	-0.17	-0.14

% of the time. The less aggressive controller action for $\tau_c = 3$ h results in higher values of ΔG , G_{max} , G_{min} and t_r , but still guarantees a good performance. For $\tau_c = 4$ and 5 h, the controller aggressiveness is further reduced, resulting in no subjects with glucose concentration in the range 60-80 mg/dl, but increasing the percentage of time in the range 60-80 mg/dl $11(\pm 5)\%$ for $\tau_c = 5$ h.

In Figures 5.6 and 5.7 the effect of the five τ_c values for subjects $\#$ 5 and 9 is showed. Subject $\#$ 9 shows the most undershoot for all ten subjects. Comparing the controller action for $\tau_c = 1$ h and $\tau_c = 3$ h, it can be observed that the better trade-off between speed of response and undershoot occurs for $\tau_c = 3$ h where the undershoot remains above 80 mg/dl and time to return in the normo-glycemia zone is $5.2 (\pm 5) \%$.

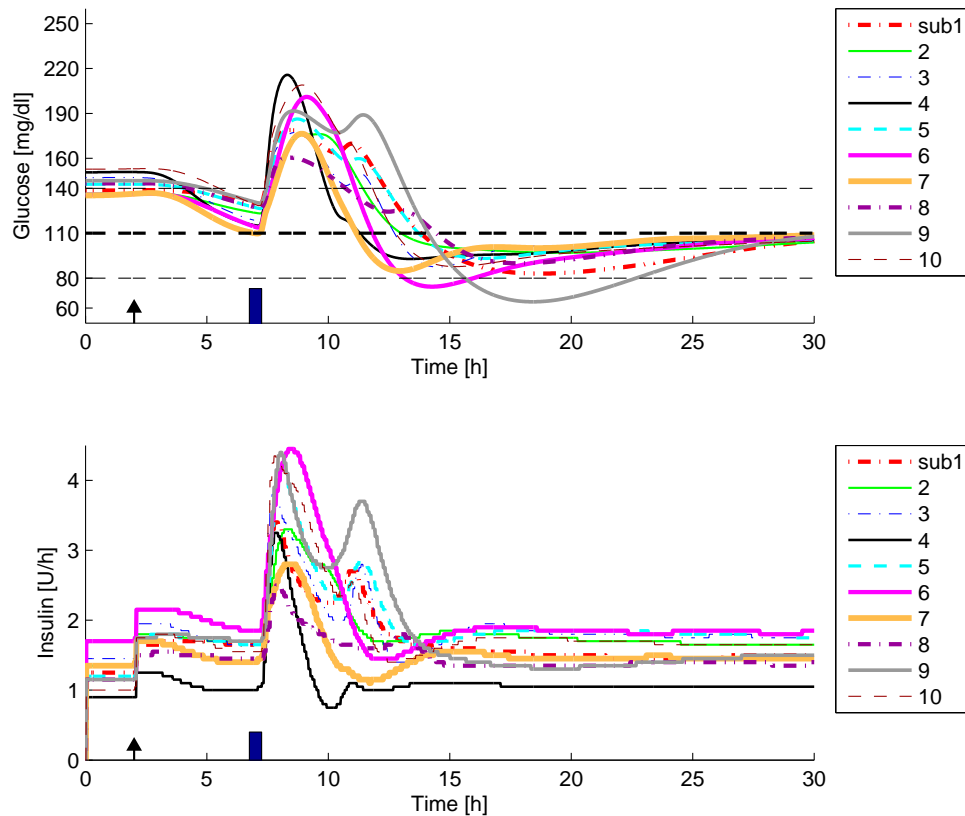


Figure 5.1: Post-prandial responses for $\tau_c = 1$ h. The thick dashed line indicates the set point (110 mg/dl). The two thin dashed lines indicate the normo-glycemia zone (80-140 mg/dl).

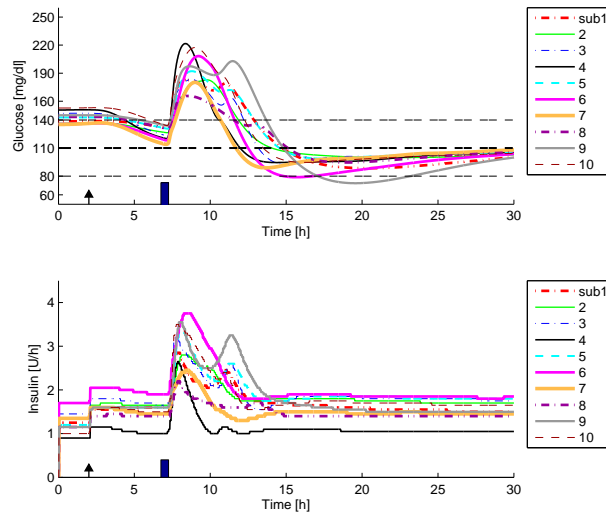


Figure 5.2: Post-prandial responses for $\tau_c = 2$ h. The thick dashed line indicates the set point (110 mg/dl). The two thin dashed lines indicate the normo-glycemia zone (80-140 mg/dl).

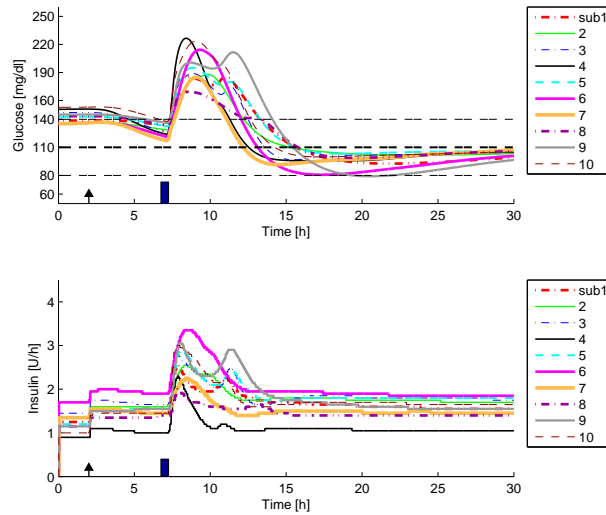


Figure 5.3: Post-prandial responses for $\tau_c = 3$ h. The thick dashed line indicates the set point (110 mg/dl). The two thin dashed lines indicate the normo-glycemia zone (80-140 mg/dl).

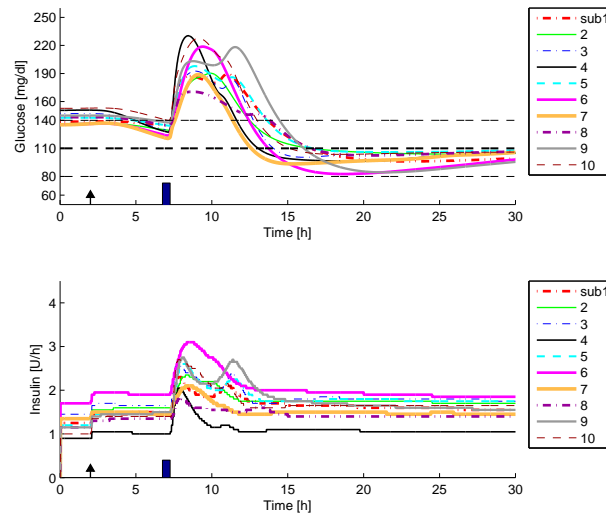


Figure 5.4: Post-prandial responses for $\tau_c = 4$ h. The thick dashed line indicates the set point (110 mg/dl). The two thin dashed lines indicate the normo-glycemia zone (80-140 mg/dl).

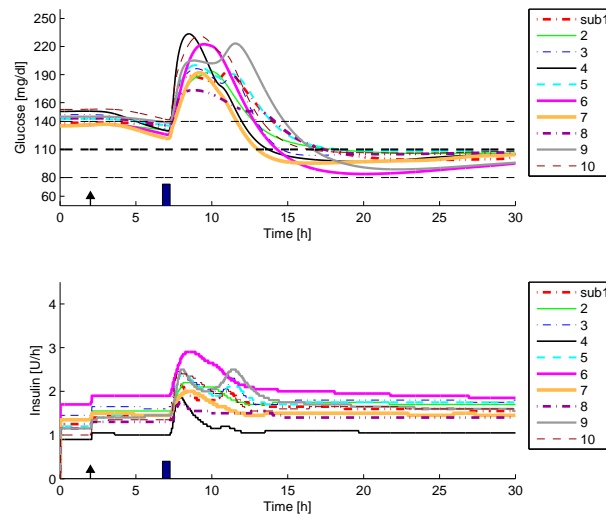


Figure 5.5: Post-prandial responses for $\tau_c = 5$ h. The thick dashed line indicates the set point (110 mg/dl). The two thin dashed lines indicate the normo-glycemia zone (80-140 mg/dl).

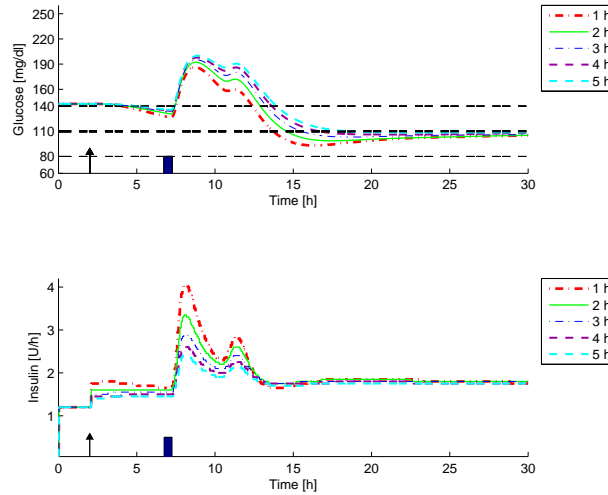


Figure 5.6: Post-prandial responses for subject # 5 and different τ_c . The thick dashed line indicates the set point (110 mg/dl). The two thin dashed lines indicate the normo-glycemia zone (80-140 mg/dl).

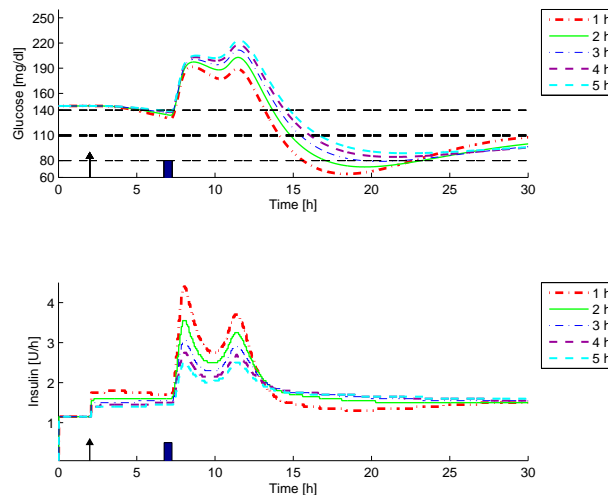


Figure 5.7: Post-prandial responses for subject # 9 and different τ_c . The thick dashed line indicates the set point (110 mg/dl). The two thin dashed lines indicate the normo-glycemia zone (80-140 mg/dl).

Table 5.3: Single meal statistics: percentage of time that the glucose concentration (mg/dl) remains within the indicated range. Average values for the ten subjects.

range	$\tau_c = 1$ h	$\tau_c = 2$ h	$\tau_c = 3$ h	$\tau_c = 4$ h	$\tau_c = 5$ h
$60 < G < 80$	3 (± 7)	3 (± 6)	1 (± 2)	0	0
$80 < G < 140$	75 (± 13)	73 (± 13)	72 (± 12)	71 (± 11)	70 (± 11)
$70 < G < 180$	95 (± 7)	94 (± 4)	93 (± 4)	91 (± 5)	90 (± 5)
$180 < G < 250$	4 (± 4)	6 (± 5)	8 (± 5)	10 (± 5)	11 (± 5)

Table 5.4: Single meal metrics: mean and standard deviation for each τ_c value. ΔG is the glucose peak value relative to the value t_{meal} , the meal time: $\Delta G = G_{max} - G_{meal}$. G_{max} is the maximum blood glucose value and G_{min} is the minimum value, during the post-prandial response. t_r is the time to return to the normoglycemia zone after the meal.

metrics	$\tau_c = 1$ h	$\tau_c = 2$ h	$\tau_c = 3$ h	$\tau_c = 4$ h	$\tau_c = 5$ h
ΔG (mg/dl)	46 (± 16)	52 (± 17)	57 (± 18)	61 (± 19)	64 (± 19)
G_{max} (mg/dl)	187 (± 16)	194 (± 17)	199 (± 18)	202 (± 19)	199 (± 18)
G_{min} (mg/dl)	85 (± 9)	90 (± 8)	94 (± 8)	94 (± 8)	94 (± 8)
t_r (h)	4.2 (± 1.2)	4.7 (± 1.3)	5.2 (± 1.4)	5.5 (± 1.4)	5.8 (± 1.5)

5.1.1 Robustness Test

In order to verify the controller behavior for intra-subject changes of $\pm 50\%$ in the insulin sensitivity, as explained in Chapter 4, the controller output was reduced or increased by 50%. In this case, the robustness test can also give information about the controller performance, when the actual subject's TDI value differs from the TDI estimated by the 2400 rule Eq. (3.3). The robustness test results with the controller output changes by $\pm 50\%$ are reported for each τ_c value investigated, except for $\tau_c = 1$ h, because the performance was already poor for normal conditions.

$\tau_c = 2$ h

Robustness results for $\tau_c = 2$ h are reported in Figures 5.8 - 5.11. When the controller output is increased by 50%, all post-prandial responses result in more oscillatory behavior, with really large undershoots especially for subject $\# 9$.

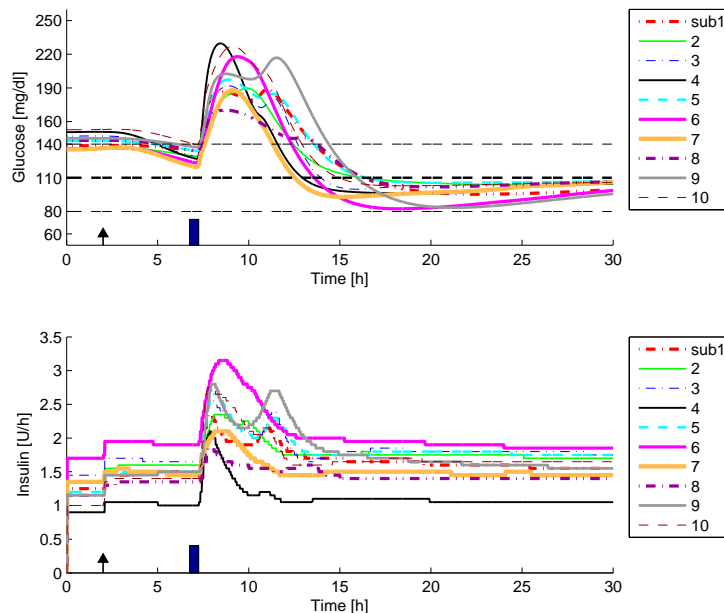


Figure 5.8: Post-prandial responses for $\tau_c = 2$ h. The thick dashed line indicates the set point (110 mg/dl). The two thin dashed lines indicate the normo-glycemia zone (80-140 mg/dl). The controller output is reduced by 50%.

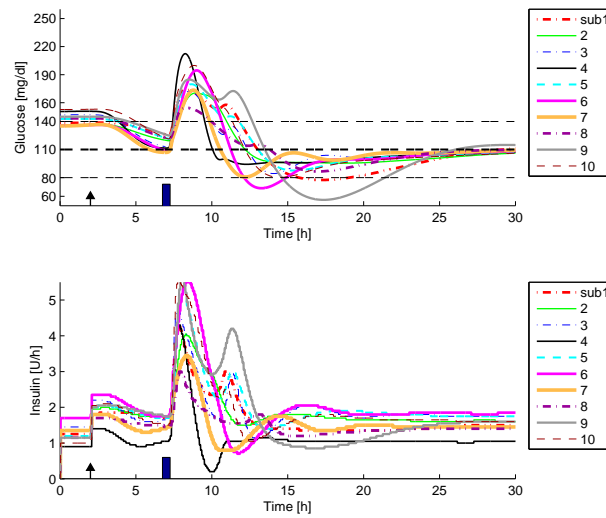


Figure 5.9: Post-prandial responses for $\tau_c = 2$ h. The thick dashed line indicates the set point (110 mg/dl). The two thin dashed lines indicate the normo-glycemia zone (80-140 mg/dl). The controller output is increased by 50%.

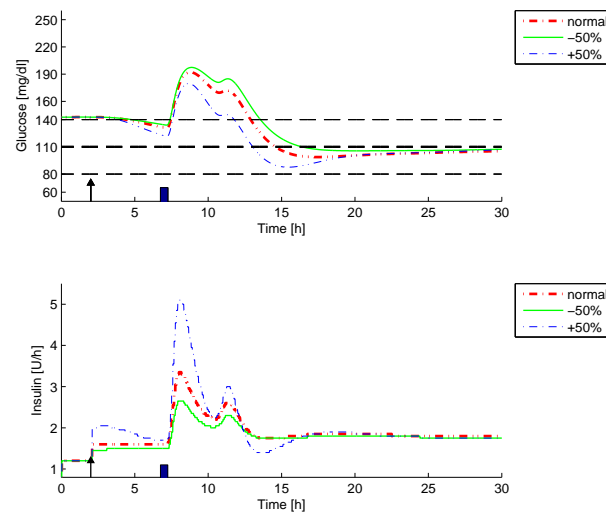


Figure 5.10: Post-prandial responses for subject # 5, $\tau_c = 2$ h and the three controller output conditions (normal, increase by 50% and decrease by 50%). The thick dashed line indicates the set point (110 mg/dl). The two thin dashed lines indicate the normo-glycemia zone (80-140 mg/dl).

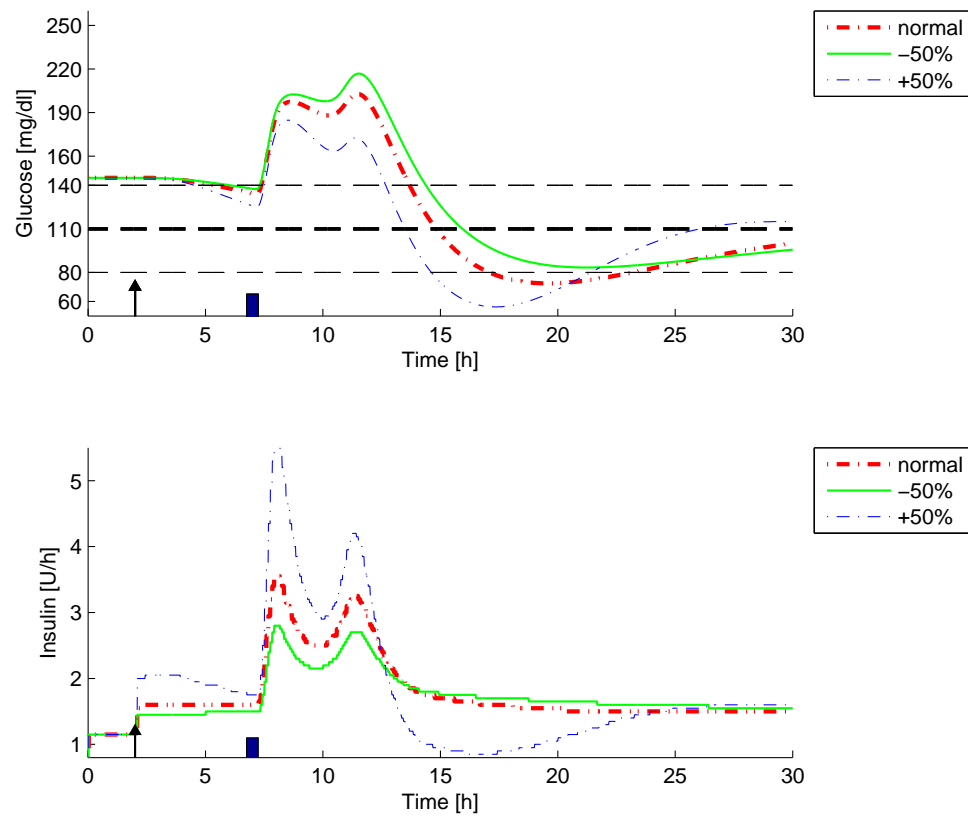


Figure 5.11: Post-prandial responses for subject # 9, $\tau_c = 2$ h and the three controller output conditions (normal, increase by 50% and decrease by 50%). The thick dashed line indicates the set point (110 mg/dl). The two thin dashed lines indicate the normo-glycemia zone (80-140 mg/dl).

$$\tau_c = 3 \text{ h}$$

Robustness results for $\tau_c=3$ h are reported in Figures 5.12 - 5.15. When the controller is increased by 50%, the post-prandial response still show significant undershoots, but no hypoglycemic events occur.

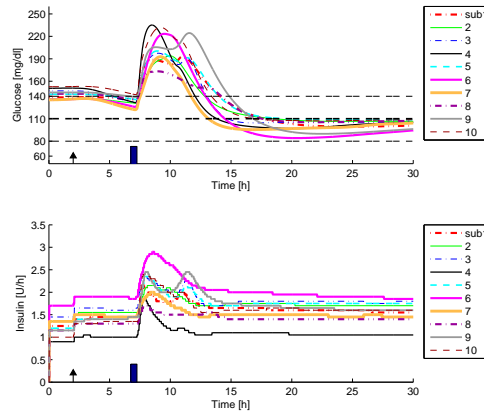


Figure 5.12: Post-prandial responses for $\tau_c = 3$ h. The thick dashed line indicates the set point (110 mg/dl). The two thin dashed lines indicate the normo-glycemia zone (80-140 mg/dl). The controller output is reduced by 50%.

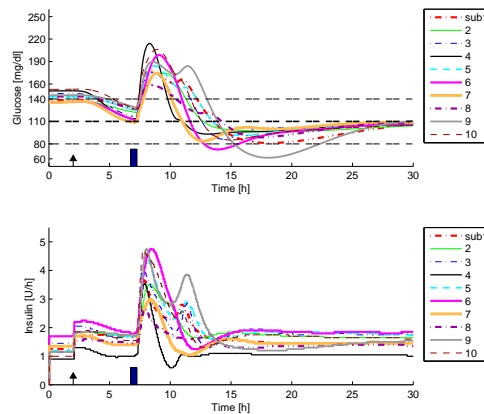


Figure 5.13: Post-prandial responses for $\tau_c = 3$ h. The thick dashed line indicates the set point (110 mg/dl). The two thin dashed lines indicate the normo-glycemia zone (80-140 mg/dl). The controller output is increased by 50%

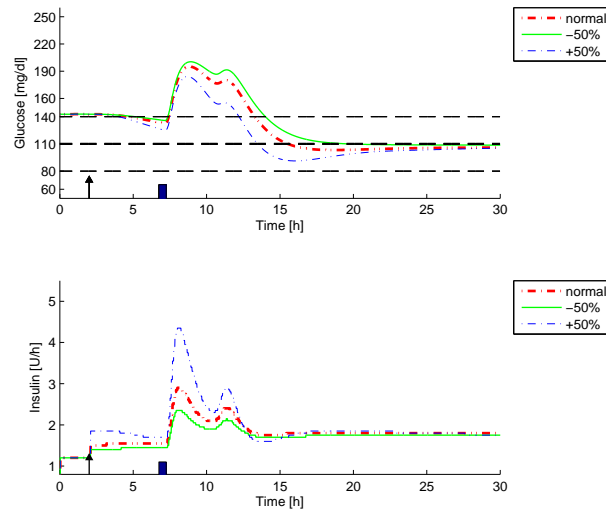


Figure 5.14: Post-prandial responses for subject # 5, $\tau_c = 3$ h and the three controller output conditions (normal, increase by 50% and decrease by 50%). The thick dashed line indicates the set point (110 mg/dl). The two thin dashed lines indicate the normo-glycemia zone (80-140 mg/dl).

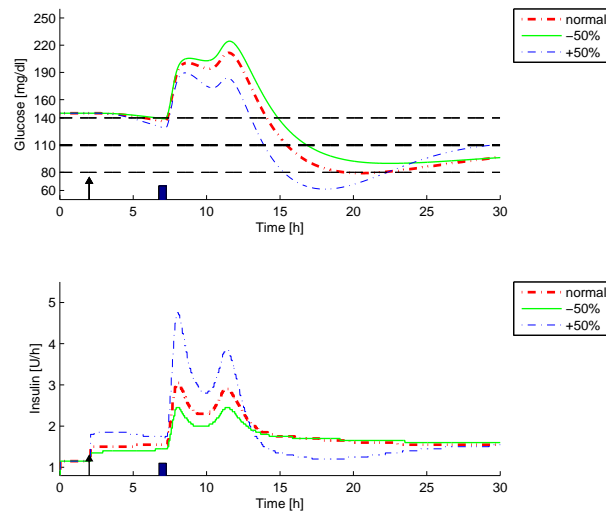


Figure 5.15: Post-prandial responses for subject # 9, $\tau_c = 3$ h and the three controller output conditions (normal, increase by 50% and decrease by 50%). The thick dashed line indicates the set point (110 mg/dl). The two thin dashed lines indicate the normo-glycemia zone (80-140 mg/dl).

$$\tau_c = 4 \text{ h}$$

Robustness results for $\tau_c = 4 \text{ h}$ are reported in Figures 5.16 - 5.19, and the only subject that show a relevant undershoot when the controller output is increased by 50% is $\# 9$, since its response is below the normo-glycemia undershoot.

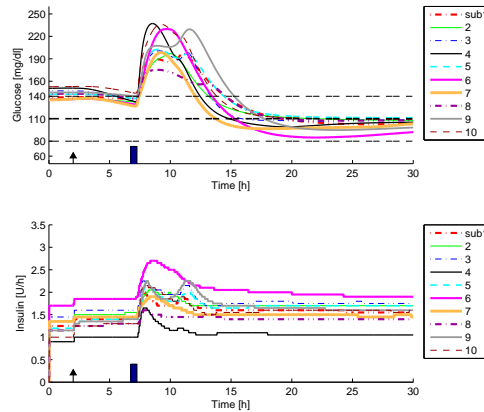


Figure 5.16: Post-prandial responses for $\tau_c = 4 \text{ h}$. The thick dashed line indicates the set point (110 mg/dl). The two thin dashed lines indicate the normo-glycemia zone (80-140 mg/dl). The controller output is reduced by 50%.

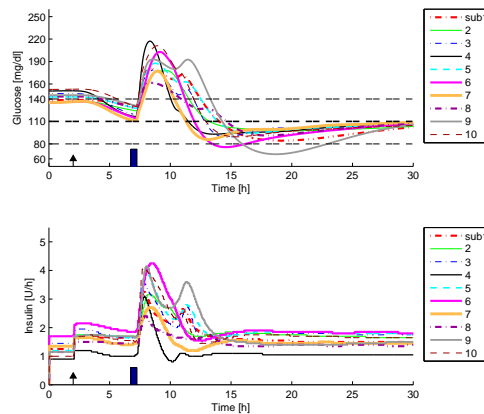


Figure 5.17: Post-prandial responses for $\tau_c = 4 \text{ h}$. The thick dashed line indicates the set point (110 mg/dl). The two thin dashed lines indicate the normo-glycemia zone (80-140 mg/dl). The controller output is increased by 50%

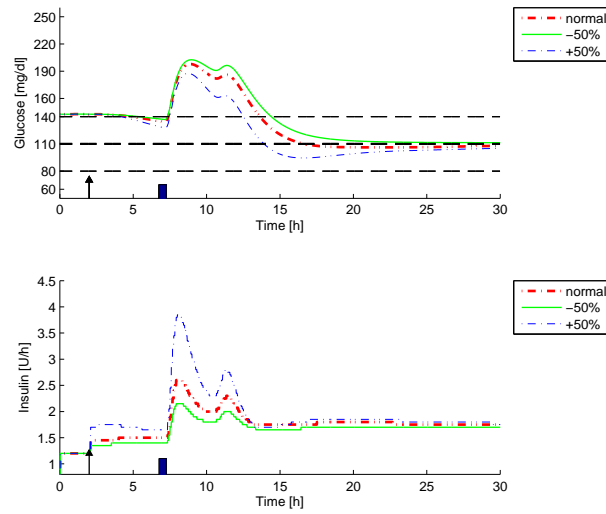


Figure 5.18: Post-prandial responses for subject # 5, $\tau_c = 4$ h and the three controller output conditions (normal, increase by 50% and decrease by 50%). The thick dashed line indicates the set point (110 mg/dl). The two thin dashed lines indicate the normo-glycemia zone (80-140 mg/dl).

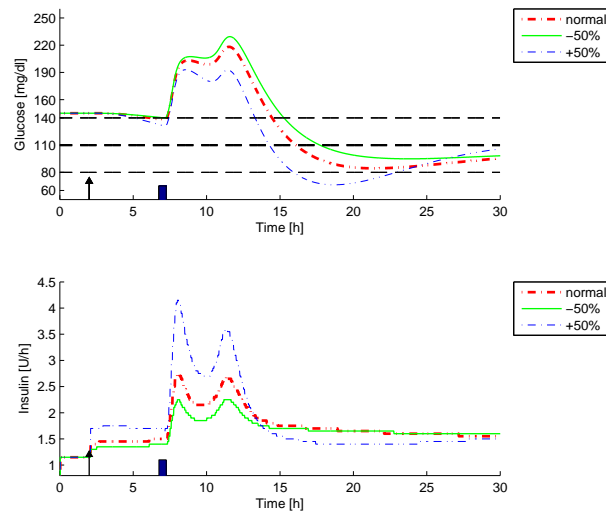


Figure 5.19: Post-prandial responses for subject # 9, $\tau_c = 4$ h and the three controller output conditions (normal, increase by 50% and decrease by 50%). The thick dashed line indicates the set point (110 mg/dl). The two thin dashed lines indicate the normo-glycemia zone (80-140 mg/dl).

$$\tau_c = 5 \text{ h}$$

Robustness results for $\tau_c=5$ h are reported in Figures 5.20 - 5.23, the controller performance is similar to the one for $\tau_c=4$ h

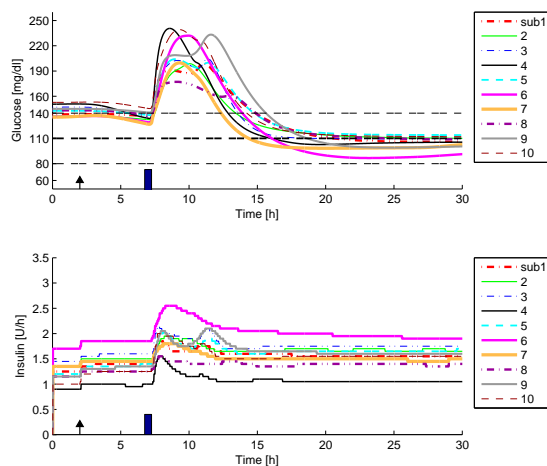


Figure 5.20: Post-prandial responses for $\tau_c = 5$ h. The thick dashed line indicates the set point (110 mg/dl). The two thin dashed lines indicate the normo-glycemia zone (80-140 mg/dl). The controller output is reduced by 50%.

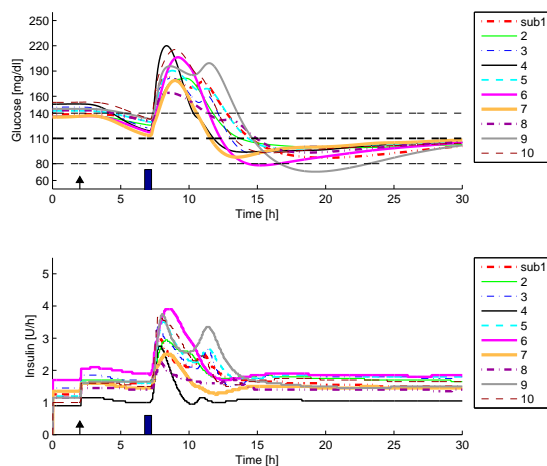


Figure 5.21: Post-prandial responses for $\tau_c = 5$ h. The thick dashed line indicates the set point (110 mg/dl). The two thin dashed lines indicate the normo-glycemia zone (80-140 mg/dl). The controller output is increased by 50%

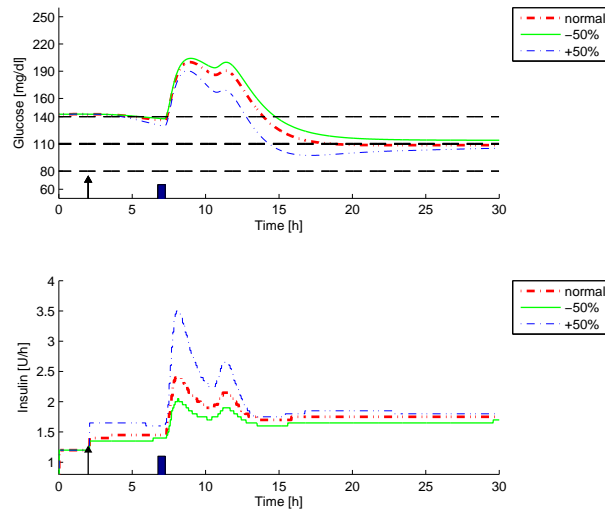


Figure 5.22: Post-prandial responses for subject # 5, $\tau_c = 5$ h and the three controller output conditions (normal, increase by 50% and decrease by 50%). The thick dashed line indicates the set point (110 mg/dl). The two thin dashed lines indicate the normo-glycemia zone (80-140 mg/dl).

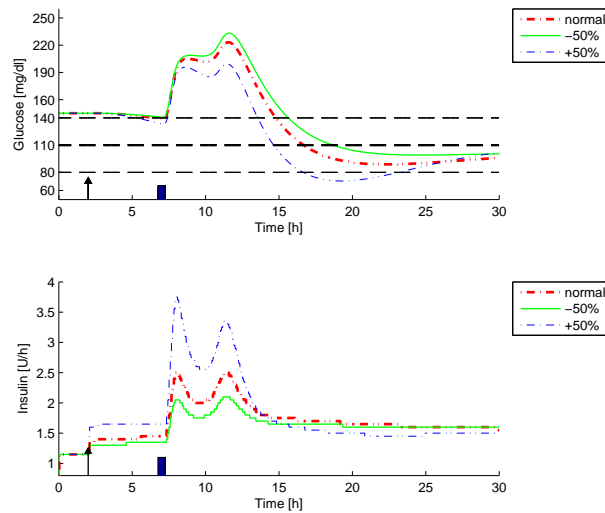


Figure 5.23: Post-prandial responses for subject # 9, $\tau_c = 5$ h and the three controller output conditions (normal, increase by 50% and decrease by 50%). The thick dashed line indicates the set point (110 mg/dl). The two thin dashed lines indicate the normo-glycemia zone (80-140 mg/dl).

In Tables 5.5-5.8 the robustness results for different τ_c values are reported in terms of means and standard deviations. When the controller output is increased by 50%, for $\tau_c = 2$ h, the glucose concentration remains in the hypoglycemia zone $0.9(\pm 2.7)\%$ of the time, demonstrating that the controller is robust. For $\tau_c = 3, 4$ and 5 h, there are no cases of hypoglycemia, even when the controller output is increased by 50%. The percentage of time in the other ranges are similar for $\tau_c = 3, 4$ and 5 h, but for $\tau_c = 3$, $3(\pm 3)\%$ of the time, glucose concentration is in the range 180-250, whereas for $\tau_c = 5$ h the time in the same range is $5(\pm 5)\%$ of the time. In general $\tau_c = 3$ h performed the best compared to the other τ_c values, e.g. t_r is equal to $3.9(\pm 1.2)$ instead of $4.6(\pm 1.3)$ for $\tau_c = 5$ h, still avoiding the risk of hypoglycemia.

When the controller output is reduced by 50%, the percentage of time in the range 180-250 is increased, and for $\tau_c = 5$ h it reaches the average of $13(\pm 5)\%$. For $\tau_c = 3$ h the percentage of time in the same glucose zone is reduced and at the same time, good performance is guaranteed even with the more conservative controller, since the highest glucose value is $207 (\pm 19)$.

Table 5.5: Single meal statistics: percentage of time that glucose concentration (mg/dl) remains within the indicated range. Average values for the ten subjects, when the controller output is increased by 50%.

range	$\tau_c = 2$ h	$\tau_c = 3$ h	$\tau_c = 4$ h	$\tau_c = 5$ h
$G < 60$	$0.9 (\pm 2.7)$	0	0	0
$60 < G < 80$	$3 (\pm 5)$	$3 (\pm 7)$	$3 (\pm 7)$	$3 (\pm 7)$
$80 < G < 140$	$76 (\pm 12)$	$76 (\pm 13)$	$74 (\pm 14)$	$73 (\pm 14)$
$70 < G < 180$	$96 (\pm 6)$	$96 (\pm 7)$	$95 (\pm 7)$	$95 (\pm 5)$
$180 < G < 250$	$2 (\pm 2)$	$3 (\pm 3)$	$4 (\pm 5)$	$5 (\pm 5)$

Table 5.6: Single meal metrics: mean and standard deviation for each τ_c value. ΔG is the glucose peak value relative to the value t_{meal} , the meal time: $\Delta G = G_{max} - G_{meal}$. G_{max} is the highest blood glucose value and G_{min} is the lowest value, during the post-prandial response. t_r is the time to return to the normo-glycemia zone after the meal. The controller output is increased by 50%

metrics	$\tau_c = 2$ h	$\tau_c = 3$ h	$\tau_c = 4$ h	$\tau_c = 5$ h
ΔG (mg/dl)	40 (± 16)	43 (± 16)	46 (± 16)	50 (± 17)
G_{max} (mg/dl)	182 (± 16)	185 (± 16)	189 (± 16)	192 (± 17)
G_{min} (mg/dl)	81 (± 11)	84 (± 10)	87 (± 9)	89 (± 8)
t_r (h)	3.6 (± 1.2)	3.9 (± 1.2)	4.3 (± 1.2)	4.6 (± 1.3)

Table 5.7: Single meal statistics: percentage of time that glucose concentration (mg/dl) remains within the indicated range. Average values for the ten subjects, when the controller output is decreased by 50%

range	$\tau_c = 2$ h	$\tau_c = 3$ h	$\tau_c = 4$ h	$\tau_c = 5$ h
60 < G < 80	0	0	0	0
80 < G < 140	71 (± 11)	69 (± 12)	67 (± 12)	65 (± 12)
70 < G < 180	91 (± 5)	89 (± 5)	88 (± 5)	88 (± 5)
180 < G < 250	9 (± 5)	11 (± 5)	12 (± 5)	13 (± 5)

Table 5.8: Single meal statistics: mean and standard deviation for each τ_c value. ΔG is the glucose peak value relative to the value t_{meal} , the meal time: $\Delta G = G_{max} - G_{meal}$. G_{max} is the maximum blood glucose value. G_{min} is the minimum value. t_r is the time to return to the normo-glycemia zone after the meal. the controller output is decreased by 50%.

metrics	$\tau_c = 2$ h	$\tau_c = 3$ h	$\tau_c = 4$ h	$\tau_c = 5$ h
ΔG (mg/dl)	60 (± 19)	64 (± 20)	68 (± 20)	71 (± 21)
G_{max} (mg/dl)	202 (± 19)	207 (± 19)	210 (± 20)	213 (± 21)
G_{min} (mg/dl)	96 (± 8)	100 (± 8)	102 (± 8)	105 (± 20)
t_r (h)	5.5 (± 1.4)	5.9 (± 1.5)	6.3 (± 1.6)	6.6 (± 1.6)

5.1.2 Discussion

Both the results of the effect of the τ_c values and the robustness test show the best PID tuning settings results when $\tau_c = 3$ h. Indeed, no cases of hypo- or hyperglycemia occurred for the three controller conditions (normal, $\pm 50\%$). Moreover 96(± 7)% of the time the glucose concentration remains within the range 70-180; in particular subjects # 1, 2, 3, 7, and 8 remain in that range for 100 % of the time. The highest glucose concentration value, among all the subjects, is 235 mg/dl for subject # 4 when the controller output is decreased by 50%; the lowest glucose concentration value is 61 mg/dl when the controller output is increased by 50%.

5.2 Validation Test: Post-prandial Results

After analyzing the effect of τ_c and concluding that the best controller performance is achieved for $\tau_c = 3$ h, a validation test is conducted, as in Chapter 4. The same population from the UVA/Padova metabolic simulator that was used for the validation test of the non-personalized gain is used here. Again a three meal challenge (dinner, breakfast and lunch) is evaluated. The validation test scenario is:

- $t=0$ h (1 pm): simulation starts
- $t=2$ h (3 pm): controller turned on;
- $t=5$ h (8 pm): a meal of 50 g CHO (dinner) is given;
- $t=16$ h (7 am): meal of 40 g CHO (breakfast) is given;
- $t=21$ h (12 pm): meal of 50 g CHO (lunch) is given;
- $t=30$ h (9 pm): simulation ends.

Figure 5.24 and Tables 5.9-5.12 show the validation test results. The first important result is that none of the subjects exhibited cases of hypoglycemia. Nevertheless, the lowest value of the glucose concentration detected is 60 mg/dl for subject # 6 , extremely close to the hypoglycemia zone; however, this low

glucose level occurs around 9 pm, when another meal is supposed to be given. The percentage of time in the range 70-180 is $88(\pm 11)\%$ and in particular it is 100% for subjects $\#$ 3 and 9. After the meal intake, the time to return to the normo-glycemia for all the subjects is below 6.2 h, and the glucose concentration of subject $\#$ 9, after the first meal, remains in the normo-glycemia zone for the entire simulation. The highest glucose concentration excursions, due to the meals, occur after the the first meal (dinner), and The average maximum excursion is of $73(\pm 34)$ mg/dl (the highest value is 130 mg/dl for subject $\#$ 6). After the other meals, it gradually decreases to $60 (\pm 28)$ mg/dl. The maximum value of the glucose concentration is 260 mg/dl for subject $\#$ 6, with an average for the 10 subjects of $208(\pm 34)$ mg/dl. hyperglycemia only for $0.8(\pm 1.7)\%$ of time. These results demonstrate that the choice of $\tau_c = 3$ h guarantees a safe controller action with moderate peak values.

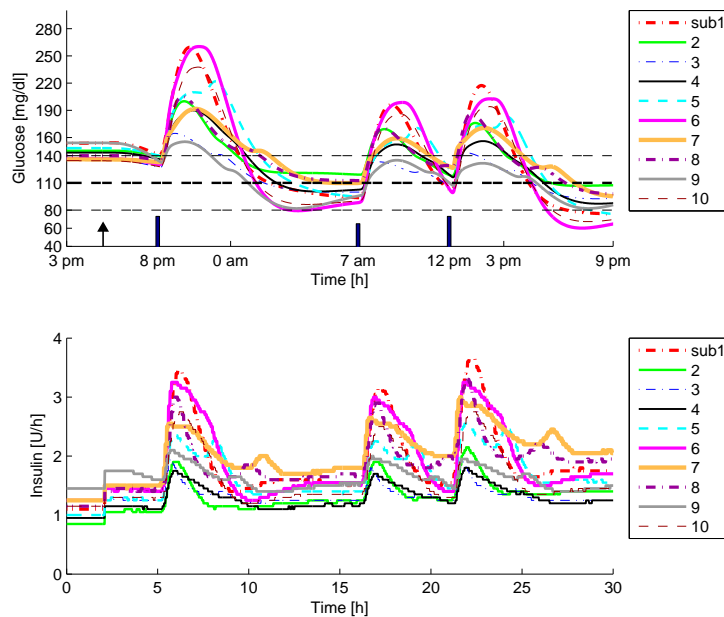


Figure 5.24: Post-prandial responses to three meals. The thick dotted line indicates the set point (110 mg/dl). The two dotted lines indicate the normo-glycemia zone (80-140 mg/dl).

Table 5.9: Single meal statistics: percentage of time that glucose concentration (mg/dl) remains within the indicated range.

Subject	$G < 60$	$60 < G < 80$	$80 < G < 140$	$70 < G < 180$	$180 < G < 250$	$G > 250$
1	0	9	40	79	18	3
2	0	0	53	95	6	0
3	0	0	87	100	0	0
4	0	0	54	94	6	0
5	0	4	36	86	14	0
6	0	16	47	64	21	5
7	0	0	58	94	6	0
8	0	0	65	92	8	0
9	0	0	77	100	0	0
10	0	11	55	73	19	0
mean	0	4 (± 6)	57(± 15)	88(± 11)	10(± 7)	1(± 2)

Table 5.10: The glucose (mg/dl) peak value relative to the value at t_{meal} , the meal time: $\Delta G = G_{max} - G_{meal}$.

Subject	dinner	breakfast	lunch
1	118	102	114
2	60	50	57
3	37	33	35
4	53	50	37
5	79	73	55
6	130	111	99
7	59	49	42
8	70	58	57
9	20	39	21
10	109	96	88
mean	73	66	60
std	± 34	± 26	± 29

Table 5.11: Time to return to the normo-glycemia zone after the meal.

Subject	dinner	breakfast	lunch
1	4.5 h	3.6 h	3.6 h
2	4.3	3.1	3.1
3	3.6	/	1.6
4	4.9	3.5	3.3
5	5.6	4.5	4.5
6	4.7	4.1	4.0
7	6.2	3.9	4.1
8	5.6	3.3	3.2
9	2.9	/	/
10	4.6	3.9	3.8

Table 5.12: Maximum (G_{max}) and minimum (G_{min}) glucose concentration (mg/dl) values during the post-prandial response.

Subject	G_{min}	G_{max}
1	76	259
2	107	200
3	92	164
4	87	190
5	76	222
6	60	260
7	95	192
8	98	205
9	82	155
10	67	238
mean	84	208
std	± 14	± 34

Chapter 6

Comparison of The Controllers Performance

In this chapter a direct comparison between the results obtained with the non-personalized controller and the personalized controller are presented. In particular, figures and tables of the single meal post-prandial responses for both the final controllers with the selected settings are reported along with the robustness test when the insulin sensitivity is increased by 50%. The validation test results for the three meal, 30 hours scenario are also included.

6.1 Normal output

Figures 6.1-6.6 and Tables 6.1 and 6.2 show the results for the personalized and non-personalized controllers with the selected settings, for the post-prandial response simulations in Chapter 4 and Chapter 5 and a single meal of 50 g of CHO. With a personalization of the controller the percentage of time in the range 70-180 results is considerably improved compared to the non-personalized controller, increasing from $88 (\pm 6)\%$ to $93 (\pm 4)\%$. Also the time in the normo-glycemia range improves from $66(\pm 13)\%$ for the non-personalized controller to $72 (\pm 13)\%$ after introducing the personalization. The personalized controllers reduce the highest peak from $212 (\pm 21)$ mg/dl to $199 (\pm 18)$ mg/dl, as well as the time to return in the normo-glycemia zone after the meal (from $6.5 (\pm 1.8)$ h to $5.2(\pm 1.2)$ h). The

single subject figures show that the personalized controller is in general more aggressive than the non-personalized, but the aggressiveness results in glucose concentration values that are lower and a faster response leading to a better performance, e.g. subject # 5; on the other hand, the controller personalization often increases the undershoots, but never below the normo-glycemia zone (subject # 6,9 and 10).

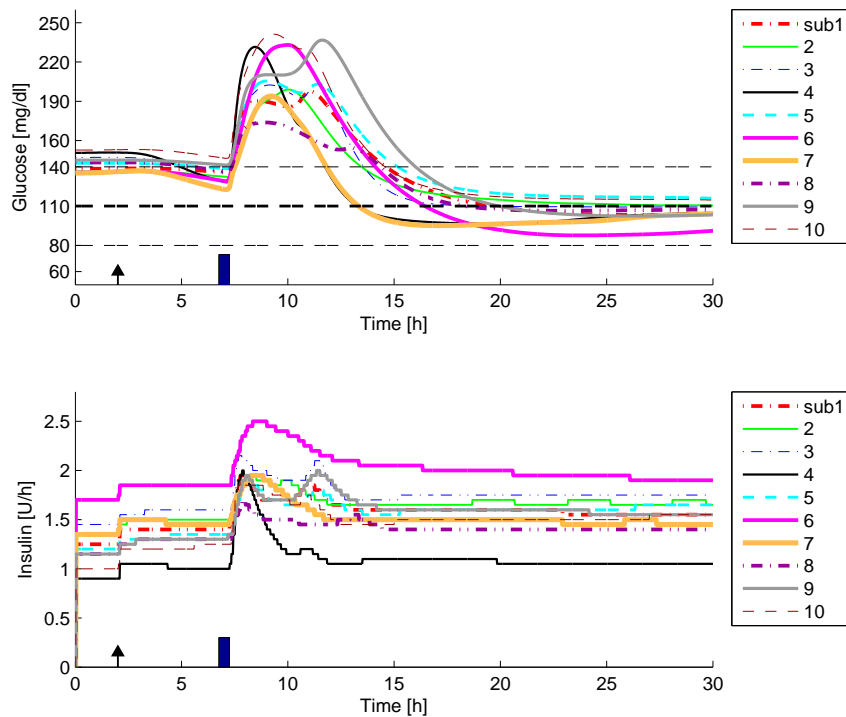


Figure 6.1: Post-prandial responses with a non-personalized controller. The thick dashed line indicates the set point (110 mg/dl). The two thin dashed lines indicate the normo-glycemia zone (80-140 mg/dl).

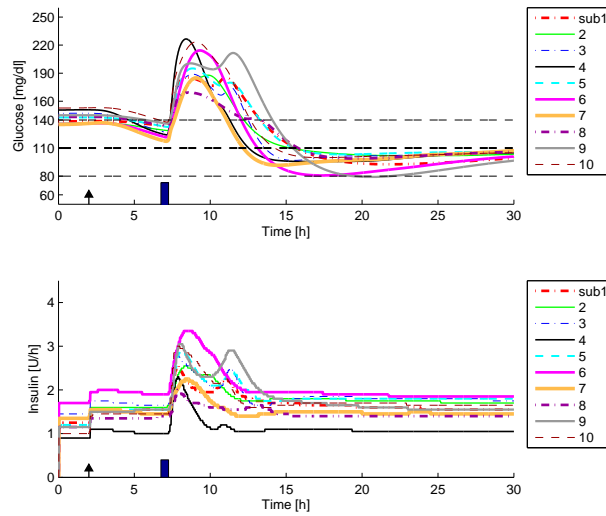


Figure 6.2: Post-prandial responses with a personalized controller. The thick dashed line indicates the set point (110 mg/dl). The two thin dashed lines indicate the normo-glyciemia zone (80-140 mg/dl).

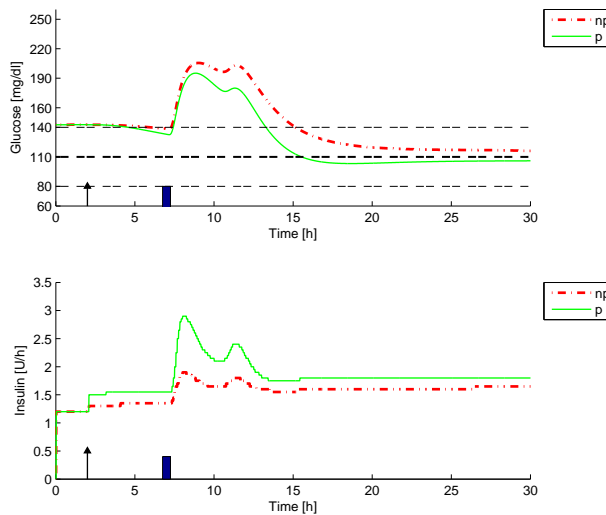


Figure 6.3: Post-prandial responses comparison for personalized (p) and non-personalized controllers (np) for subject # 5. The thick dashed line indicates the set point (110 mg/dl). The two thin dashed lines indicate the normo-glyciemia zone (80-140 mg/dl).

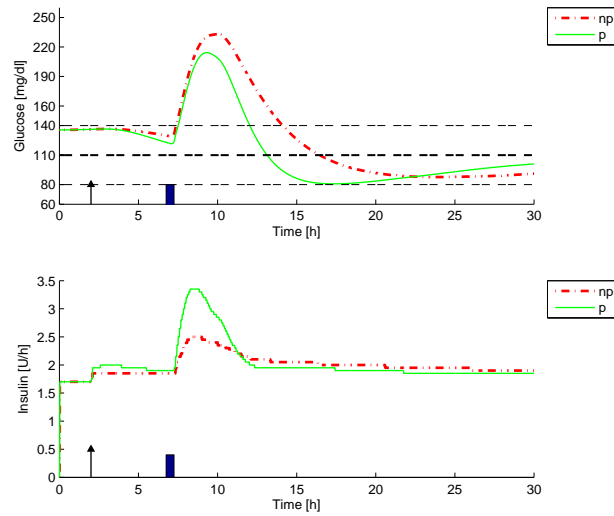


Figure 6.4: Post-prandial responses comparison for personalized (p) and non-personalized controllers (np) for subject # 6. The thick dashed line indicates the set point (110 mg/dl). The two thin dashed lines indicate the normo-glyciemia zone (80-140 mg/dl).

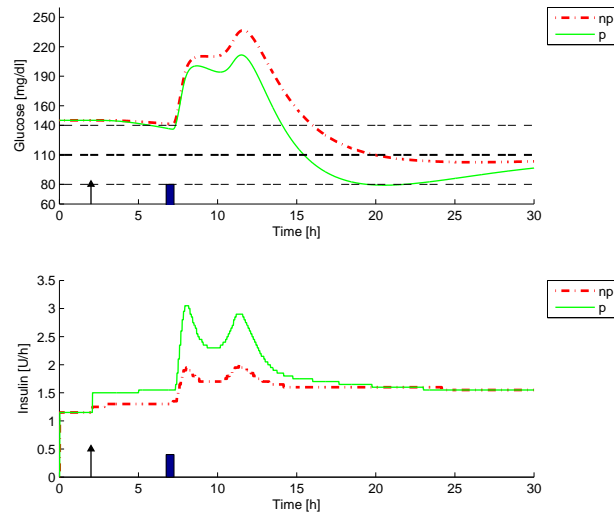


Figure 6.5: Post-prandial responses comparison for personalized (p) and non-personalized controllers (np) for subject # 9. The thick dashed line indicates the set point (110 mg/dl). The two thin dashed lines indicate the normo-glyciemia zone (80-140 mg/dl).

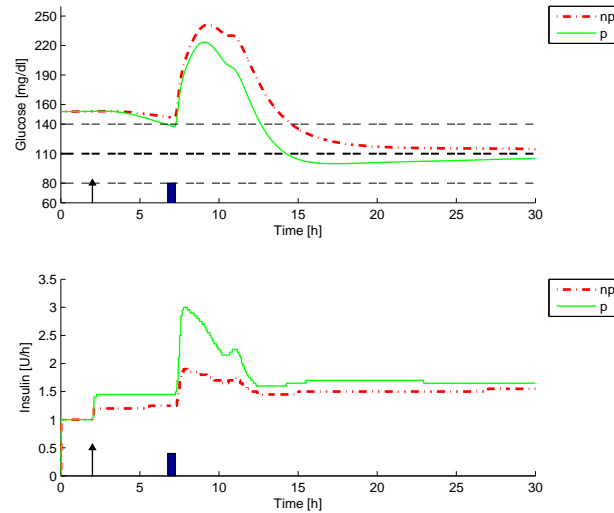


Figure 6.6: Post-prandial responses comparison for personalized (p) and non-personalized controllers (np) for subject # 10. The thick dashed line indicates the set point (110 mg/dl). The two thin dashed lines indicate the normo-glycemia zone (80-140 mg/dl).

Table 6.1: Single meal statistics: percentage of time that glucose concentration (mg/dl) remains within the indicated range. Average values for the ten subjects. np=non-personalized gain, p=personalized gains

range	np	p
$60 < G < 80$	0 (± 5)	1 (± 2)
$80 < G < 140$	66 (± 13)	72 (± 13)
$70 < G < 180$	88 (± 6)	93 (± 4)
$180 < G < 250$	12 (± 6)	8 (± 5)

Table 6.2: Single meal metrics: mean and standard deviation for each τ_c value. ΔG is the glucose peak value relative to the value t_{meal} , the meal time: $\Delta G = G_{max} - G_{meal}$. G_{max} is the highest blood glucose value and G_{min} is the lowest value, during the post-prandial response. t_r is the time to return to the normo-glycemia zone after the meal. np=non-personalized gain, p=personalized gains

metrics	np	p
ΔG (mg/dl)	69 (± 22)	57 (± 18)
G_{max} (mg/dl)	212 (± 21)	199 (± 18)
G_{min} (mg/dl)	104 (± 9)	94 (± 18)
t_r (h)	6.5 (± 1.8)	5.2 (± 1.2)

6.2 Controller output increased of the 50%

In Figures 6.7-6.10 the comparison between personalized and non-personalized controllers performances for some subjects is reported, when the insulin sensitivity is increased by 50%. When the insulin sensitivity increases, the personalized controller provides a more oscillatory post-prandial response, but only for subject # 9 the performance of the personalized controller is much worse than the non-personalized, since the undershoot is quite close to 60 mg/dl. But on the other hand the higher glucose concentration values are considerably reduced.

Tables 6.3 and 6.4 compare personalized and non-personalized controller performances. For the non-personalized controller, none of the subjects spend time in the range 60-80 mg/dl when the insulin sensitivity is 50% higher, but for 3(± 7)% of the time the glucose concentration is in that range for the personalized controller. However, all the other metrics provide better results when a controller personalization is performed.

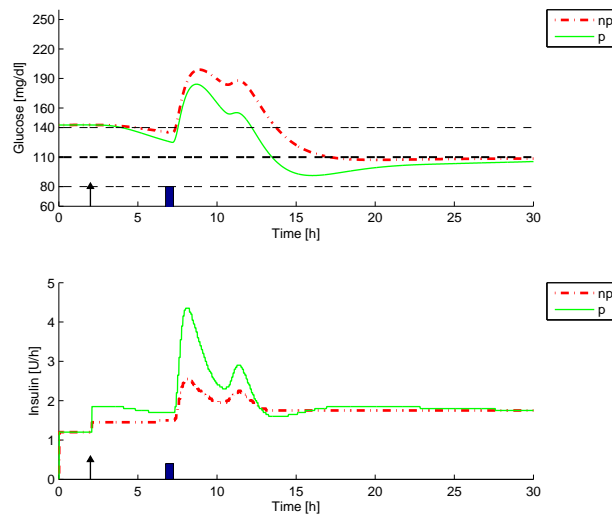


Figure 6.7: Post-prandial responses comparison for personalized (p) and non-personalized controllers (np) for subject # 5. The thick dashed line indicates the set point (110 mg/dl). The two thin dashed lines indicate the normo-glycemia zone (80-140 mg/dl). The controller output is increased by 50%.

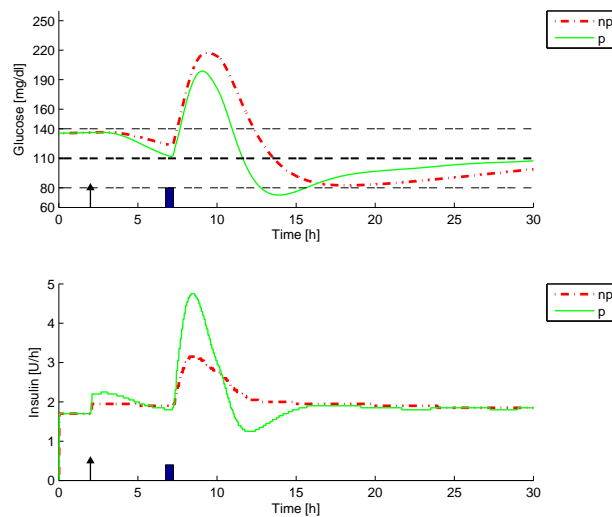


Figure 6.8: Post-prandial responses comparison for personalized (p) and non-personalized controllers (np) for subject # 6. The thick dashed line indicates the set point (110 mg/dl). The two thin dashed lines indicate the normo-glycemia zone (80-140 mg/dl). The controller output is increased by 50%.

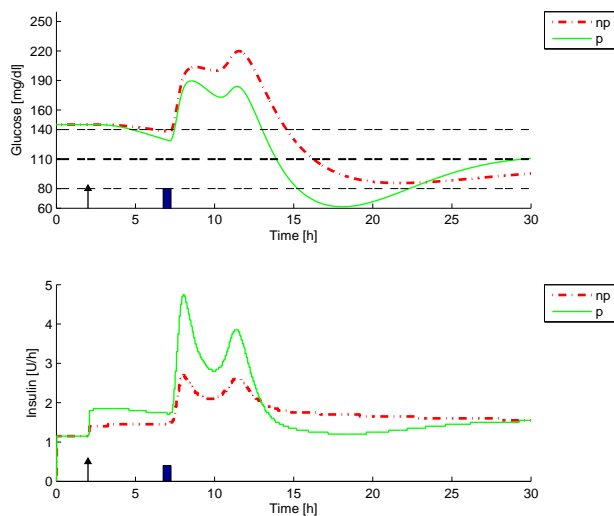


Figure 6.9: Post-prandial responses comparison for personalized (p) and non-personalized controllers (np) for subject # 9. The thick dashed line indicates the set point (110 mg/dl). The two thin dashed lines indicate the normo-glycemia zone (80-140 mg/dl). The controller output is increased by 50%.

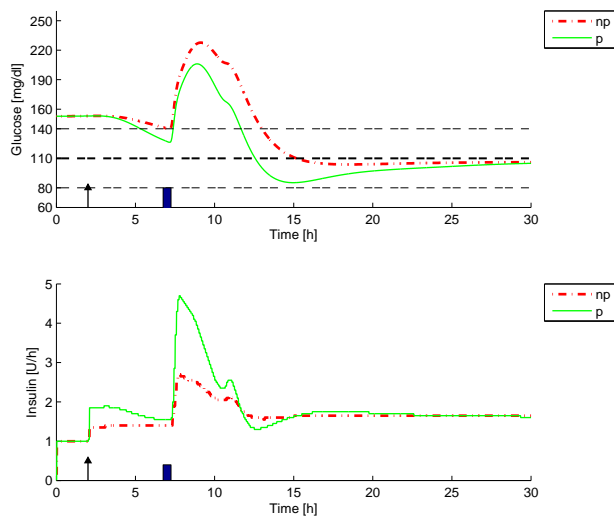


Figure 6.10: Post-prandial responses comparison for personalized (p) and non-personalized controllers (np) for subject # 10. The thick dashed line indicates the set point (110 mg/dl). The two thin dashed lines indicate the normo-glycemia zone (80-140 mg/dl). The controller output is increased by 50%.

Table 6.3: Single meal statistics: percentage of time that glucose concentration (mg/dl) remains within the indicated range. Average values for the ten subjects. np=non-personalized gain, p=personalized gains

range	np	p
60<G<80	0 (± 5)	3 (± 7)
80<G<140	73 (± 12)	76 (± 13)
70<G<180	92 (± 5)	96 (± 7)
180<G<250	8 (± 5)	3 (± 3)

Table 6.4: Single meal metrics: mean and standard deviation for each τ_c value. ΔG is the glucose peak value relative to the value t_{meal} , the meal time: $\Delta G = G_{max} - G_{meal}$. G_{max} is the highest blood glucose value and G_{min} is the lowest value, during the post-prandial response. t_r is the time to return to the normo-glycemia zone after the meal. np=non-personalized gain, p=personalized gains.

metrics	np	p
ΔG (mg/dl)	57 (± 20)	43 (± 16)
G_{max} (mg/dl)	199 (± 19)	185 (± 16)
G_{min} (mg/dl)	95 (± 8)	84 (± 10)
t_r (h)	5.1 (± 1.5)	3.9 (± 1.2)

6.3 Validation test

Figures 6.11 and 6.12 show the non-personalized and personalized controllers performances, respectively, in the validation test presented in Chapters 4 and 5. Figures 6.13-6.16 show the comparison between the personalized and non-personalized controllers for the three meal test, whereas Tables 6.5 and 6.6 compare the numerical results. For both the personalized and non-personalized controllers, there are no cases of hypoglycemia, but the personalized controller is able to maintain the subjects in the normo-glycemia zone for $57(\pm 15)\%$ and for $88(\pm)\%$ in the range 70-180 mg/dl, while for the non-personalized controller the percentage of time in the normo-glycemia zone is $48(\pm 15)\%$ and $83(\pm 12)\%$ in the range 70-180 mg/dl. All the other metrics show that the best performance is achieved with the personalized controller, since the post-prandial glucose concentration peak after the meal intake is reduced for all the subjects and never results in hypoglycemia.

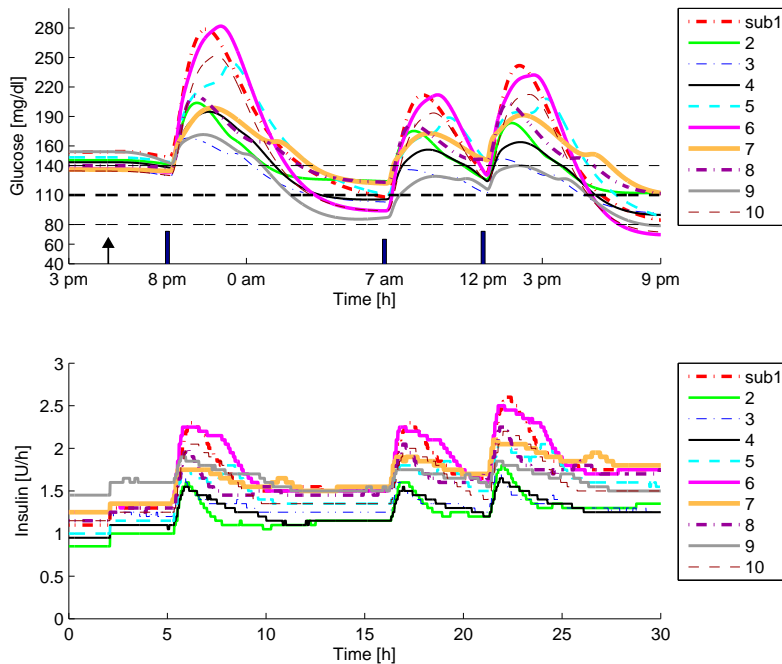


Figure 6.11: Post-prandial responses to three meals with a non-personalized controller. The thick dashed line indicates the set point (110 mg/dl). The two thin dashed lines indicate the normo-glycemia zone (80-140 mg/dl).

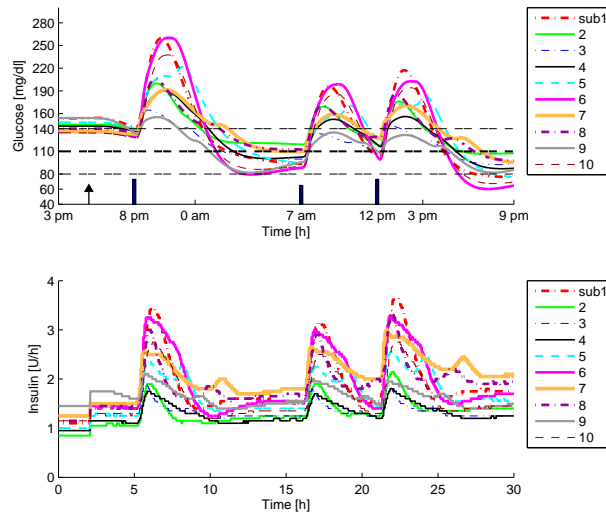


Figure 6.12: Post-prandial responses to three meals with a personalized controller. The thick dashed line indicates the set point (110 mg/dl). The two thin dashed lines indicate the normo-glyciemia zone (80-140 mg/dl).

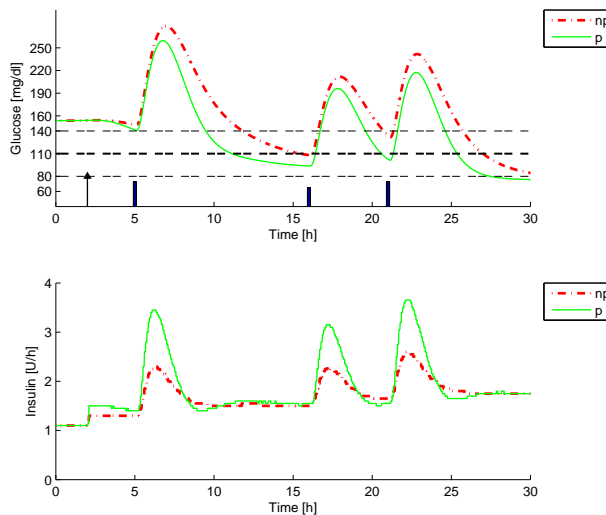


Figure 6.13: Post-prandial responses comparison for personalized (p) and non-personalized controllers (np) for subject #1. The thick dashed line indicates the set point (110 mg/dl). The two thin dashed lines indicate the normo-glyciemia zone (80-140 mg/dl).

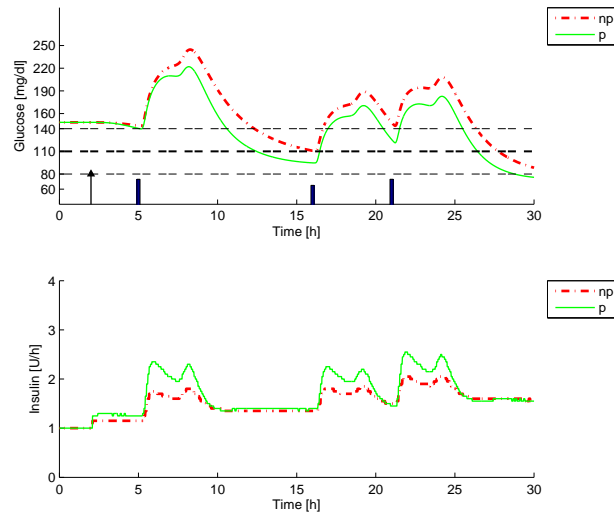


Figure 6.14: Post-prandial responses comparison for personalized (p) and non-personalized controllers (np) for subject # 5. The thick dashed line indicates the set point (110 mg/dl). The two thin dashed lines indicate the normo-glycemia zone (80-140 mg/dl).

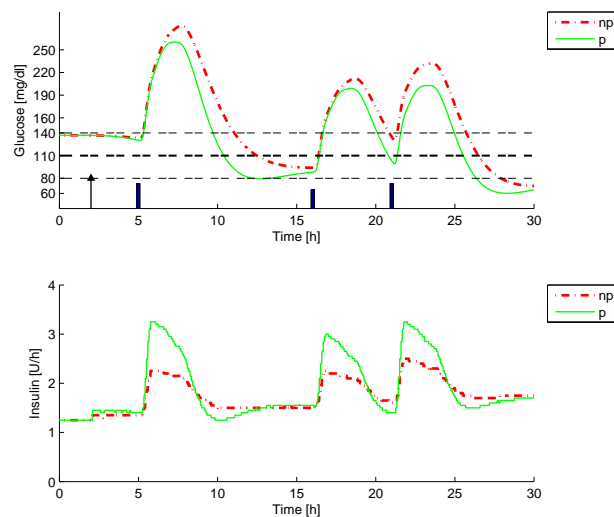


Figure 6.15: Post-prandial responses comparison for personalized (p) and non-personalized controllers (np) for subject # 6. The thick dashed line indicates the set point (110 mg/dl). The two thin dashed lines indicate the normo-glycemia zone (80-140 mg/dl).

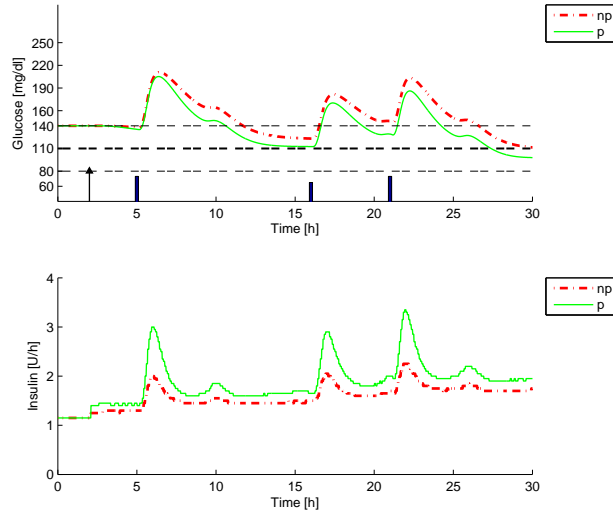


Figure 6.16: Post-prandial responses comparison for personalized (p) and non-personalized controllers (np) for subject # 8. The thick dashed line indicates the set point (110 mg/dl). The two thin dashed lines indicate the normo-glycemia zone (80-140 mg/dl).

Table 6.5: One day statistics: percentage of time that glucose concentration (mg/dl) remains within the indicated range. Average values for the ten subjects. np=non-personalized gain, p=personalized gains

range	np	p
$G < 60$	0	0
$60 < G < 80$	2 (± 5)	4 (± 6)
$80 < G < 140$	48 (± 15)	57 (± 15)
$70 < G < 180$	83 (± 12)	88 (± 11)
$180 < G < 250$	16 (± 11)	10 (± 7)
$G > 250$	2 (± 3)	1 (± 2)

Table 6.6: Single meal metrics: mean and standard deviation for each τ_c value. ΔG_{max} is the maximum glucose peak value relative to the value t_{meal} , the meal time: $\Delta G = G_{max} - G_{meal}$. G_{max} is the maximum blood glucose value and G_{min} is the minimum value, during the post-prandial response. np=non-personalized gain, p=personalized gains.

metrics	np	p
ΔG_{max} (mg/dl)	82(\pm 39)	73 (\pm 40)
G_{max} (mg/dl)	220 (\pm 39)	208 (\pm 34)
G_{min} (mg/dl)	91 (\pm 15)	84 (\pm 14)

Conclusion

The aim of this work was to develop a novel and robust PID control algorithm to control the glucose concentration in people with type 1 diabetes mellitus. A discrete third-order control-relevant model (van Hausden et al. [1]) was approximated to a continuous, second-order plus time delay model. The model gain can be either personalized with the subject TDI or be fixed. Then, this continuous model was used for the PID algorithm designed based on the IMC approach. With this approach the three PID tuning settings were calculated on the basis of the process dynamics and the model gain and they were reduced to a single adjustable parameter (τ_c).

Two types of controllers were implemented: (i) a non-personalized controller (with a fixed model gain) and (ii) a personalized controller (with a model gain based on the subject TDI). The investigation of the best τ_c value for both the controllers was conducted *in silico* with a population of ten subjects of the UVA/Padova metabolic simulator. The ten simulated subjects were used to determine a conservative value τ_c . This value provided good post-prandial responses and a reasonable degree of robustness for changes of +/- 50% in the insulin sensitivity. Then ten additional subjects were simulated in a validation study that included three meals (50, 40 and 50 g CHO) during a 30 hour period. For the validation study, the average amount of time that the glucose concentration was in the desired range (70-180 mg/dl) was 88% for the personalized controller and 83% for the non-personalized. Similarly, the average values for the 180-250 mg/dl range were 10% and 16% for the personalized and fixed controllers, respectively. Neither design method resulted in hypoglycemia (<60 mg/dl).

These results show that the controllers designed are both robust, but that

the personalized controllers performance is superior to the non-personalized controllers. Therefore, in the future only the personalized controller should be considered. Moreover, further tests should be performed, e.g. robustness test for three unannounced meals and more days of simulations (3-4 days) in order to see the controller behavior for a longer period. Simulations with the controller and insulin bolus should be conducted to see the controller responses for the bolus, as well. A risk of the both implemented PID controllers is the long undershoot that can occur after the meal. The undershoot is mostly due to the integral action of the controller. Thus, an improvement in the controller can be obtained by limiting the integral action with upper and lower constraints.

Appendix A

The UVA/Padova Metabolic Simulator

In January 2008 the UVA/Padova Metabolic simulator was accepted by the Food and Drug Administration (FDA) to replace the classic preclinical procedure of animal trials in order to test closed-loop control strategies. The main motivation is that the results obtained by the modeling are as credible as the results obtained in the clinical trials, and at the same time much faster [28]. However, a control algorithm tested *in silico* can perform in a different way *in vivo*, for this reason a simulation only is considered as a preliminary step to test extreme situations and the general performance of the algorithm. The schematic overview of the UVA/Padova metabolic simulator in Figure A.1 and consists of three main parts: *in silico* subject, *in silico* sensor and *in silico* pump [28].

A.1 Model Development

In silico Subject

The *in silico* subject is modeled with different subsystems. The glucose subsystem is a two-compartment model of the glucose kinetics: the first compartment models the insulin-independent utilization (plasma and fast equilibrating tissues), the second compartment models the insulin-dependent utilization (peripheral tissues). The insulin subsystem is also composed of two compartments: the first

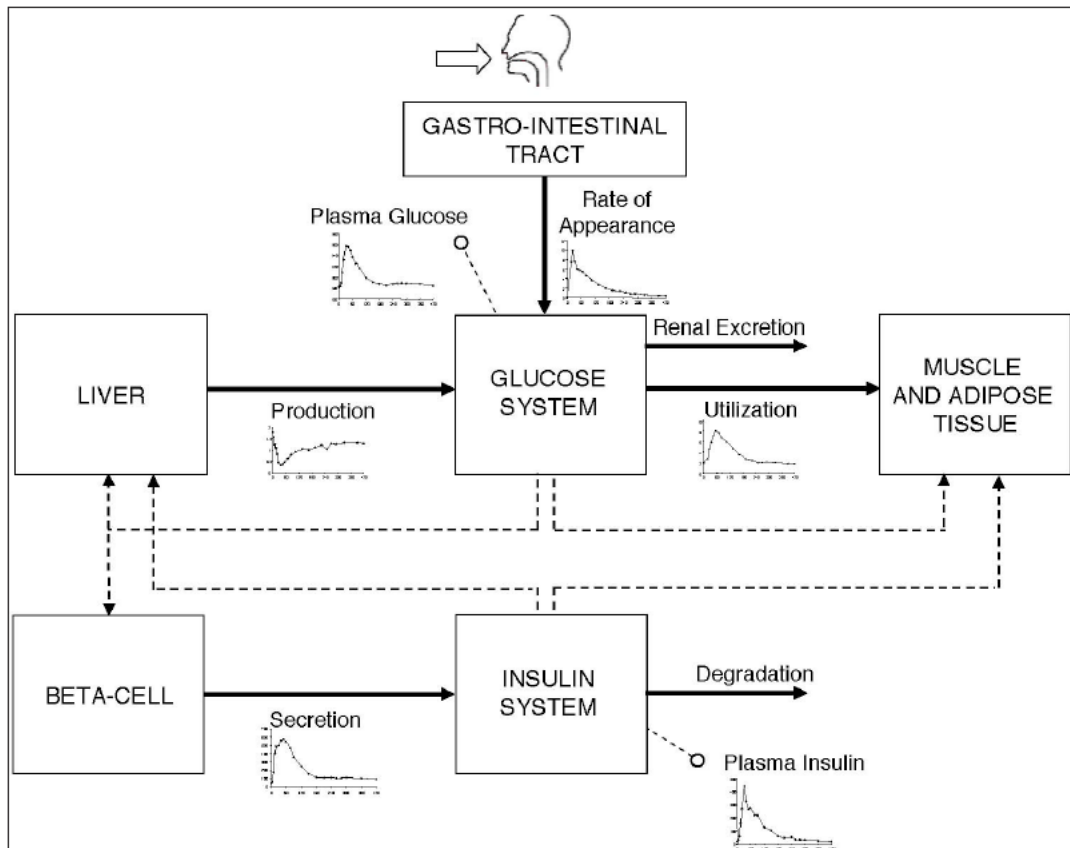


Figure A.1: Scheme of the glucose-insulin control system. the dashed line stands for control signals and continuous lines represents fluxes of materials [29].

models the liver and the second the plasma [28, 29, 30].

The processed unit of glucose and insulin subsystems are endogenous glucose production, glucose rate of appearance, glucose utilization and insulin secretion. Their models were identified using a forcing function strategy. The interruption of the endogenous glucose production is assumed to be linearly dependent on plasma glucose concentration, portal insulin concentration and delayed insulin signal. Glucose rate of appearance is obtained by a physiological model of glucose intestinal absorption. The glucose transit through the stomach and intestine is modeled by two compartments for the stomach (one for the solid phase and one for the triturated phase) and one compartment for the gut. Glucose utilization is assumed to consist of two compartments: one for the insulin-independent (brain and erythrocytes) and it is constant, the second for the insulin-dependent utiliza-

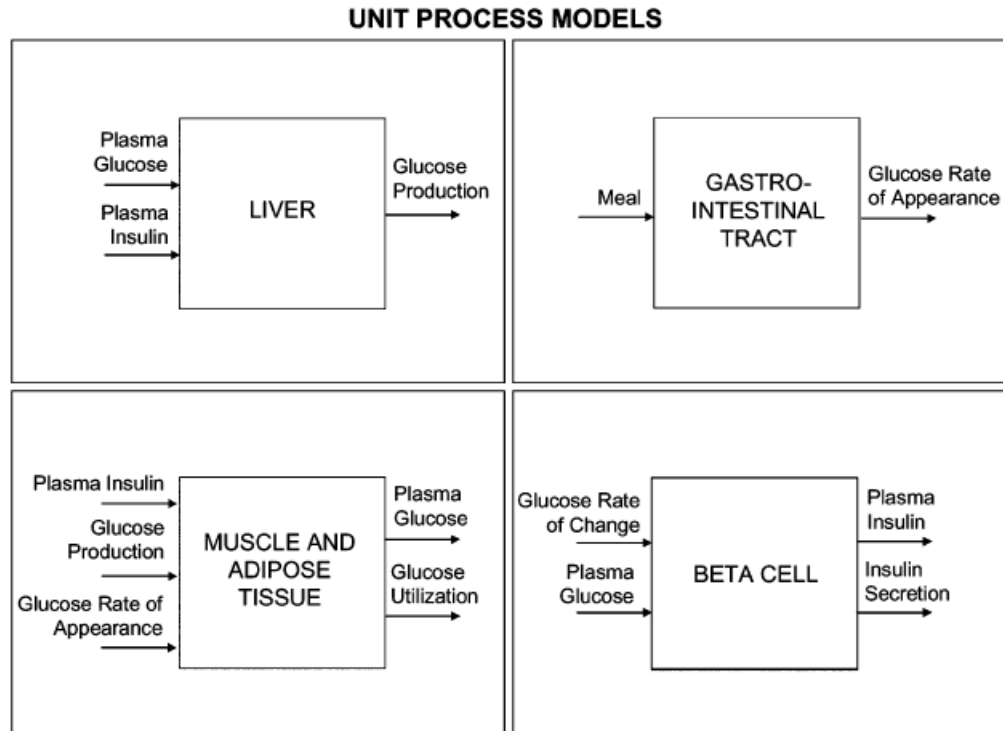


Figure A.2: Unit process models [30]. The entering arrows represents forcing function variables and the outgoing arrows are model output.

tion and is nonlinearly dependent from glucose in the tissues and it occurs in a remote compartment [28, 29, 30].

In order to simulate type 1 diabetic subject the insulin secretion module is substituted by a subcutaneous insulin module. The model has 26 free parameters and the most important are hepatic and peripheral insulin sensitivity.

***In silico* Sensor**

The *in silico* sensors are based on the analysis of sensor errors. CGM technology unfortunately has still to improve in terms of sensitivity, stability, calibration and the physiological time lag between blood and interstitial glucose concentration. The sensor errors is decomposed into errors due to calibration, blood-to-interstitial glucose transfer and random noise. The sensor simulation model provides the worst-case scenario sensor errors and they are described by Breton and Kovatchev [31].

***In silico* Insulin Pump**

The *in silico* insulin pump approximates the subcutaneous insulin delivery, mimicking time and dynamics of insulin transport from subcutaneous tissues into blood. Furthermore, the insulin is delivered by a stepwise basal pump rate and insulin boluses, providing discrete insulin infusion [28].

A.2 Software

The models described above are implemented into a computerized platform using *Simulink*[®] (part of the scientific software *Matlab*[®]). The user can run the simulations by an user interface window of the software. Figure A.3 shows the user interface in which it is possible to choose the scenario, the subjects, where also subgroups can be selected, and some outcome metrics [28].

During the simulation it is possible to have access to some patients characteristics, since these characteristics can be obtained by a screening visit of the patient. This information is:

- a) name;
- b) weight, in Kg;
- c) the patient fasting blood glucose concentration in mg/dl;
- d) the insulin rate in U/h;
- e) the optimum bolus in U/g of carbohydrates;
- f) the maximum drop in mg/dl per Units of insulin;
- g) the average total daily insulin regimen in Units of insulin.

user_interface

Load Scenario

Enter scenario ASCII file (.scn)

Common Scenario

Simulation Parameters

Open loop basal [U/hr] End of commutation / start of regulation [min]

start of closed loop [min] length of simulation [min]

Single Meal

enter amount of carbohydrates [g] timing [min]

enter amount of insulin bolus [U] duration [min]

Note: Meal boluses will only be delivered during open loop control

Multiple Meals

	breakfast (7am)	lunch (noon)	snack (4pm)	dinner (6pm)	snack (11pm)	
carbs [g]	<input type="text" value="45"/>	<input type="text" value="70"/>	<input type="text" value="5"/>	<input type="text" value="80"/>	<input type="text" value="5"/>	<input type="button" value="create 1 day"/>
bolus [U]	<input type="text" value="3"/>	<input type="text" value="4.7"/>	<input type="text" value="0"/>	<input type="text" value="5.3"/>	<input type="text" value="0"/>	<input type="button" value="create 1 week"/>

Note: Meal boluses will only be delivered during open loop control

Select Subject

<ul style="list-style-type: none"> adolescent#001 adolescent#002 adolescent#003 adolescent#004 adolescent#005 adolescent#006 adolescent#007 adolescent#008 adolescent#009 adolescent#010 adolescent#011 adolescent#012 adolescent#013 	<input type="button" value="Add >>"/> <input type="button" value="<< Remove"/>	<ul style="list-style-type: none"> adolescent#001
<input type="button" value="Add all"/> <input type="button" value="Remove all"/>		
<input type="radio"/> Children <input type="radio"/> Adolescents		
<input type="radio"/> Adults <input checked="" type="radio"/> All		

repeat test times

enter random seed:

scenario selected

subject(s) selected

Figure A.3: Simulator user interface [30].

Appendix B

Step Response Test

For each subject of the simulator it is possible calculate the process gain by fitting the glucose responses to a first-order-plus-time delay (FOPTD) model. Indeed, the process gain K of the FOPTD model for each subject in the simulator can be obtained by calculating the slope of the line which approximates two or more points (a regression line) obtained by the basal insulin values changes and the corresponding steady-state glucose changes [19].

For each subject three open-loop simulations were conducted, Figure B.1. One simulation was conducted with the normal basal insulin, the second with a decrease in the basal insulin of 0.1 U/h, and the third with an increase in the basal insulin of 0.1 U/h. For each kind of basal insulin input (normal, low and high) the three correspondent glucose steady-state conditions were measured. In table Table B.1 the three inputs for each subject are reported and in Table B.2 the corresponding outputs.

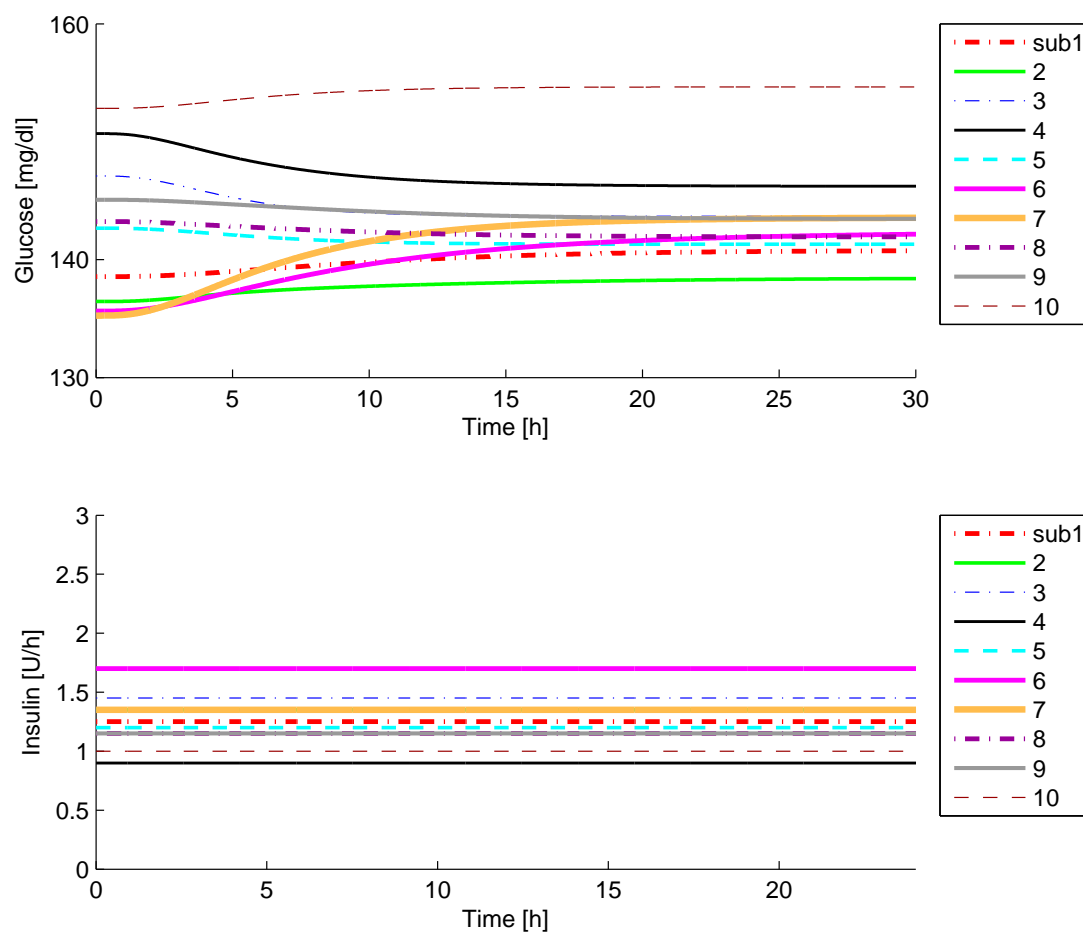


Figure B.1: Open-loop responses to the normal basal insulin for ten subjects of the UVA/Padova simulator

Table B.1: Three different basal insulin conditions (pmol/min).

Subject	Regular	Low	High
1	127	117	137
2	137	127	147
3	143	133	153
4	89	79	99
5	118	108	128
6	172	162	182
7	137	127	147
8	114	104	124
9	113	103	123
10	102	92	112

Table B.2: Steady-state glucose values (mg/dl) corresponding to the three conditions of basal insulin

Subject	Regular	Low	High
1	141	154	128
2	138	149	128
3	144	158	131
4	146	189	117
5	141	148	135
6	142	174	117
7	144	194	111
8	142	158	127
9	143	154	134
10	154	165	145

The three input/output conditions for each subject i (x_{il}, y_{il}) for $l=1,2$ and 3 were used to calculate the regression line for each subject [32]:

$$y_i = mx_i + q \quad (\text{B.1})$$

y_i is the glucose values at the steady state (mg/d) for subject i
 x_i is the basal insulin (pmol/min) for subject i .

Minimizing the residual sum of squares for each subject [32] gives:

$$S(m, q) = \sum_{l=1}^n (mx_l + q - y_l)^2 \quad (\text{B.2})$$

$$(\text{B.3})$$

$$m = \frac{\sum_{l=1}^n x_l y_l - n \bar{x} \bar{y}}{\sum_{l=1}^n x_l^2 - n \bar{x}^2} \quad (\text{B.4})$$

The slope of each regression line m (mg/dl/pmol/min) provides the gain of each subject which are reported in Table B.3.

Table B.3: Gain (mg/dl/pmol/min)

Subject	Gain
1	-1.29
2	-1.04
3	-1.37
4	-3.65
5	-0.67
6	-2.84
7	-4.18
8	-1.51
9	-1.00
10	-0.98
mean	-1.85

Appendix C

Non-personalized Model Gain Results

The results for all the subjects with the non-personalized controller are reported in this chapter along with the robustness results.

Table C.1: Single meal statistics: percentage of time that the glucose concentration remains within the indicated range for $\tau_c = 1$ h.

Subject	60<G<80	80<G<140	70<G<180	180<G<250
1	0	76	86	15
2	0	80	91	10
3	0	60	85	15
4	0	69	91	9
5	0	54	84	16
6	0	78	86	15
7	0	86	94	6
8	0	59	100	0
9	0	47	79	21
10	0	52	83	17
mean (\pm std)	0	66 (\pm 13)	88 (\pm 6)	12 (\pm 6)

Table C.2: Single meal statistics: percentage of time that glucose concentration remains within the indicated range for $\tau_c = 2$ h.

Subject	$60 < G < 80$	$80 < G < 140$	$70 < G < 180$	$180 < G < 250$
1	0	73	85	16
2	0	78	89	11
3	0	57	84	17
4	0	65	88	12
5	0	50	83	17
6	0	74	83	17
7	0	84	91	9
8	0	55	100	0
9	0	44	78	22
10	0	48	82	18
mean (\pm std)	0	63 (± 13)	86 (± 6)	14 (± 6)

Table C.3: Single meal statistics: percentage of time that glucose concentration remains within the indicated range for $\tau_c = 5$ h.

Subject	$60 < G < 80$	$80 < G < 140$	$70 < G < 180$	$180 < G < 250$
1	0	68	83	17
2	0	75	88	12
3	0	48	81	19
4	0	53	85	15
5	0	41	81	19
6	0	66	79	21
7	0	79	88	12
8	0	47	95	5
9	0	38	76	24
10	0	39	79	18
mean (\pm std)	0	55 (± 15)	84 (± 5)	16 (± 5)

Table C.4: The glucose (mg/dl) peak value relative to the value at t_{meal} , the meal time: $\Delta G = G_{max} - G_{meal}$.

Subject	$\tau_c = 1$ h	$\tau_c = 2$ h	$\tau_c = 5$ h
1	62	66	71
2	62	67	70
3	57	69	84
4	81	87	99
5	63	66	72
6	97	107	114
7	58	65	77
8	23	27	31
9	101	107	113
10	88	93	99
mean (\pm std)	69 (\pm 22)	75 (\pm 23)	83 (\pm 24)

Table C.5: Time to return to the normo-glycemia zone after the meal.

Subject	$\tau_c = 1$ h	$\tau_c = 2$ h	$\tau_c = 5$ h
1	7.6 h	8.4 h	9.8 h
2	6.5	7.1	8.1
3	6.6	7.2	8.8
4	4.8	5.4	7.1
5	8.2	9.0	10.7
6	7.1	8.3	10.6
7	4.8	5.4	6.8
8	7.4	8.0	9.1
9	9.0	9.8	11.6
10	7.6	8.6	11.4
mean (\pm std)	6.5 (\pm 1.8)	7.2 (\pm 1.9)	8.7 (\pm 2.3)

Table C.6: Blood Glucose (mg/dl) maximum (G_{max}) and minimum (G_{min}) values.

Subject	G_{max}			G_{min}		
	$\tau_c = 1$ h	$\tau_c = 2$ h	$\tau_c = 5$ h	$\tau_c = 1$ h	$\tau_c = 2$ h	$\tau_c = 5$ h
1	197	202	207	103	108	118
2	199	203	207	110	113	121
3	204	216	231	109	112	120
4	231	238	250	96	98	106
5	205	208	214	116	120	129
6	233	243	250	88	90	100
7	194	201	212	95	98	100
8	174	177	182	106	110	121
9	237	243	249	102	111	121
10	241	246	252	115	119	129
mean	212	218	225	104	108	116
\pm std	± 21	± 22	± 23	± 9	± 9	± 10

C.1 Robustness Test Single results

$\tau_c = 1$ h

Table C.7: Single meal statistics: percentage of time in which the glucose values (mg/dl) remain within the indicated ranges. $\tau_c = 1$ h. The controller output is increased of the 50%

Subject	60<G<80	80<G<140	70<G<180	180<G<250
1	0	81	93	8
2	0	84	93	7
3	0	67	94	6
4	0	77	94	6
5	0	63	87	14
6	0	84	90	10
7	0	90	99	1
8	0	71	100	0
9	0	55	82	18
10	0	57	86	14
mean (\pm std)	0	73 (\pm 12)	92 (\pm 5)	8 (\pm 5)

Table C.8: Single meal statistics: percentage of time that the glucose concentration (mg/dl) remains within the indicated ranges. $\tau_c = 1$ h. The controller output is reduced of the 50%

Subject	60<G<80	80<G<140	70<G<180	180<G<250
1	0	73	84	16
2	0	78	89	11
3	0	55	83	17
4	0	64	88	12
5	0	47	83	18
6	0	73	83	18
7	0	83	91	9
8	0	55	100	0
9	0	43	78	22
10	0	47	82	19
mean (\pm std)	0	62 (\pm 14)	86 (\pm 6)	14 (\pm 6)

Table C.9: The glucose (mg/dl) peak value relative to the value at t_{meal} , the meal time: $\Delta G = G_{max} - G_{meal}$. $\tau_c = 1$ h.

Subject	Normal	-50%	+50%
1	62	49	67
2	62	52	67
3	57	43	70
4	80	67	86
5	63	56	66
6	97	82	107
7	58	45	65
8	23	15	27
9	101	84	107
10	88	75	94
mean	69	76	57
\pm std	\pm 22	\pm 23	\pm 20

Table C.10: Time to return to the normo-glycemia zone after the meal for $\tau_c=1$ h.

Subject	Normal	-50%	+50%
1	7.6 h	6.2 h	8.6 h
2	6.5	5.4	7.2
3	6.6	5.6	7.4
4	4.8	3.1	5.6
5	8.2	6.8	9.2
6	7.1	5.3	8.5
7	4.8	3.7	5.6
8	7.4	4.7	8.0
9	9.0	7.6	10.0
10.0	7.6	8.9	6.0
mean	6.5	7.4	5.1
\pm std	± 1.8	± 2.0	± 1.5

Table C.11: Blood Glucose (mg/dl) maximum (G_{max}) and minimum (G_{min}) values with $\tau_c=1$ h.

Subject	highest			lowest		
	Normal	-50%	+50%	Normal	-50%	+50%
1	197	185	203	103	92	110
2	199	189	203	110	103	116
3	204	190	217	109	98	114
4	231	218	237	96	93	100
5	205	199	209	116	107	121
6	233	218	243	88	82	91
7	194	181	201	95	89	99
8	174	166	177	106	95	114
9	237	220	243	102	86	111
10	241	228	247	115	104	121
mean	212	218	199	104	110	95
\pm std	± 21	± 22	± 19	± 9	± 9	± 8

$\tau_c = 2$ h

Table C.12: Single meal statistics: percentage of time that the glucose concentration (mg/dl) remains within the indicated range for $\tau_c = 2$ h. The controller output is increased of the 50%

Subject	60<G<80	80<G<140	70<G<180	180<G<250
1	0	78	87	13
2	0	82	92	8
3	0	65	87	14
4	0	73	93	7
5	0	59	85	15
6	0	81	88	12
7	0	88	96	4
8	0	63	100	0
9	0	50	81	19
10	0	55	85	15
mean (\pm std)	0	69 (\pm 12)	89 (\pm 5)	11 (\pm 6)

Table C.13: Single meal statistics: percentage of time that the glucose concentration (mg/dl) remains within the indicated range for $\tau_c = 2$ h. The controller output is decreased of the 50%

Subject	60<G<80	80<G<140	70<G<180	180<G<250
1	0	70	84	17
2	0	76	89	12
3	0	50	82	18
4	0	55	86	14
5	0	43	82	18
6	0	69	81	20
7	0	81	89	11
8	0	48	97	3
9	0	40	77	23
10	0	43	80	19
mean (\pm std)	0	58 (\pm 14)	85 (\pm 5)	16 (\pm 5)

Table C.14: The glucose (mg/dl) peak value relative to the value at t_{meal} , the meal time: $\Delta G = G_{max} - G_{meal}$. $\tau_c = 2$ h.

Subject	Normal	-50%	+50%
1	65	54	68
2	66	57	68
3	69	50	80
4	87	73	97
5	66	60	70
6	107	90	110
7	65	52	71
8	27	19	30
9	107	93	112
10	93	82	97
mean	75	80	63
\pm std	± 23	± 23	± 21

Table C.15: Time to return to the normo-glycemia zone after the meal with $\tau_c = 2$ h.

Subject	Normal	-50%	+50%
1	8.4 h	6.9 h	9.3 h
2	7.1	5.9	7.7
3	7.2	6.0	8.2
4	5.4	4.1	6.4
5	9.0	7.4	10.1
6	8.3	6.1	9.7
7	5.4	4.3	6.3
8	8.0	6.7	8.6
9	9.8	8.2	11.0
10	8.6	6.7	10.1
mean	7.2	8.1	5.8
\pm std	± 1.9	± 2.2	± 1.6

$\tau_c = 5$ h

Table C.16: Blood Glucose (mg/dl) maximum (G_{max}) and minimum (G_{min}) values for $\tau_c = 2$ h.

Subject	G_{max}			G_{min}		
	Normal	-50%	+50%	Normal	-50%	+50%
1	202	191	205	108	98	114
2	203	194	205	113	107	120
3	216	197	227	112	104	119
4	238	224	248	98	95	106
5	208	202	213	120	111	126
6	243	226	246	90	84	95
7	201	187	206	98	93	99
8	177	170	181	110	101	116
9	243	229	247	111	94	117
10	246	235	250	119	109	126
mean	218	223	206	108	114	100
\pm std	± 22	± 23	± 20	± 9	± 10	± 8

Table C.17: Single meal statistics: percentage of time that the glucose concentration (mg/dl) remains within the indicated range for $\tau_c = 5$ h. The controller output is increased of the 50%

Subject	$60 < G < 80$	$80 < G < 140$	$70 < G < 180$	$180 < G < 250$
1	0	74	85	15
2	0	79	90	11
3	0	57	84	16
4	0	65	89	11
5	0	51	83	17
6	0	75	84	16
7	0	84	92	8
8	0	55	100	0
9	0	45	78	22
10	0	49	82	18
mean (\pm std)	0	63 (± 13)	87 (± 6)	13 (± 6)

Table C.18: Single meal statistics: percentage of time that the glucose concentration (mg/dl) remains within the indicated range for $\tau_c = 5$ h. The controller output is reduced of the 50%

Subject	60<G<80	80<G<140	70<G<180	180<G<250
1	0	65	82	18
2	0	72	87	13
3	0	43	80	20
4	0	48	82	16
5	0	36	80	20
6	0	60	76	20
7	0	75	86	14
8	0	44	94	7
9	0	34	75	23
10	0	30	78	14
mean (\pm std)	0	51 (\pm 15)	82 (\pm 5)	17 (\pm 4)

Table C.19: The glucose (mg/dl) peak value relative to the value at t_{meal} , the meal time: $\Delta G = G_{max} - G_{meal}$. $\tau_c = 5$ h.

Subject	Normal	-50%	+50%
1	68.4	62.3	70.7
2	69.9	64.9	72.2
3	84.0	66.4	90.8
4	99.2	85.7	100.7
5	71.7	64.6	74.8
6	114.2	104.1	119.7
7	76.7	63.9	80.4
8	31.0	26.3	31.7
9	113.5	105.3	116.0
10	99.3	91.8	101.8
mean	82.8	85.9	73.5
\pm std	\pm 23.9	\pm 24.6	\pm 22.5

Table C.20: Time to return to the normo-glycemia zone after the meal for $\tau_c = 5$ h.

Subject	Normal	-50%	+50%
1	9.8 h	8.2 h	10.8 h
2	8.1	6.9	8.9
3	8.8	7.0	10.1
4	7.1	5.3	8.6
5	10.7	8.8	12.3
6	10.6	7.9	12.2
7	6.8	5.3	7.9
8	9.1	7.8	9.9
9	11.6	9.6	12.8
10	11.4	8.3	14.0
mean	8.7	10.0	7.0
\pm std	± 2.3	± 2.7	± 1.9

Table C.21: Blood Glucose (mg/dl) maximum (G_{max}) and minimum (G_{min}) values for $\tau_c = 5$ h.

Subject	highest			lowest		
	Normal	-50%	+50%	Normal	-50%	+50%
1	207	200	209	118	107	124
2	207	202	209	121	112	125
3	231	213	238	120	110	125
4	250	237	252	106	97	111
5	214	207	217	129	120	132
6	250	240	256	100	90	104
7	212	199	216	100	98	111
8	182	177	182	121	108	126
9	249	241	252	121	107	128
mean	225	228	216	116	122	107
\pm std	± 23	± 24	± 22	± 10	± 10	± 9

Appendix D

Personalized Model Gains Single Results

The results for all the subjects with the personalized controller are reported in this chapter along with the robustness results.

Table D.1: Single meal statistics: percentage of time that the glucose concentration (mg/dl) remains within the indicated range for $\tau_c = 1$ h.

Subject	60<G<80	80<G<140	70<G<180	180<G<250
1	0	84	100	0
2	0	88	100	0
3	0	72	100	0
4	0	78	95	5
5	0	70	96	4
6	9	79	94	6
7	0	92	100	0
8	0	75	100	0
9	24	41	76	11
10	0	67	92	9
mean (\pm std)	3 (\pm 7)	75 (\pm 13)	95 (\pm 7)	4 (\pm 4)

Table D.2: Single meal statistics: percentage of time that the glucose concentration (mg/dl) remains within the indicated range for $\tau_c = 2$ h.

Subject	60<G<80	80<G<140	70<G<180	180<G<250
1	0	82	97	4
2	0	86	96	4
3	0	70	97	3
4	0	75	94	6
5	0	68	94	6
6	6	80	92	8
7	0	90	100	1
8	0	71	100	0
9	20	41	85	16
10	0	63	89	12
mean (\pm std)	3 (\pm 6)	73 (\pm 13)	94 (\pm 4)	6 (\pm 5)

Table D.3: Single meal statistics: percentage of time that the glucose concentration (mg/dl) remains within the indicated range for $\tau_c = 3$ h.

Subject	60<G<80	80<G<140	70<G<180	180<G<250
1	0	80	92	9
2	0	85	94	6
3	0	68	95	6
4	0	72	93	8
5	0	65	93	8
6	0	85	91	10
7	0	89	97	3
8	0	64	100	0
9	8	50	84	17
10	0	60	87	13
mean (\pm std)	1 (\pm 2)	72 (\pm 12)	93 (\pm 4)	8 (\pm 5)

Table D.4: Single meal statistics: percentage of time that the glucose concentration (mg/dl) remains within the indicated range for $\tau_c = 4$ h.

Subject	$60 < G < 80$	$80 < G < 140$	$70 < G < 180$	$180 < G < 250$
1	0	79	88	12
2	0	84	93	7
3	0	66	91	9
4	0	69	92	8
5	0	63	87	13
6	0	84	90	11
7	0	88	96	5
8	0	62	100	0
9	0	56	83	18
10	0	57	86	14
mean (\pm std)	0	71 (\pm 11)	91 (\pm 5)	10 (\pm 5)

Table D.5: Single meal statistics: percentage of time that the glucose concentration (mg/dl) remains within the indicated range for $\tau_c = 5$ h.

Subject	$60 < G < 80$	$80 < G < 140$	$70 < G < 180$	$180 < G < 250$
1	0	78	87	14
2	0	83	92	8
3	0	65	87	13
4	0	68	91	10
5	0	62	86	14
6	0	82	89	12
7	0	87	95	6
8	0	60	100	0
9	0	54	82	18
10	0	56	86	15
mean (\pm std)	0	70 (\pm 11)	90 (\pm 5)	11 (\pm 5)

Table D.6: The glucose (mg/dl) peak value relative to the value at t_{meal} , the meal time: $\Delta G = G_{max} - G_{meal}$.

Subject	$\tau_c = 1$ h	$\tau_c = 2$ h	$\tau_c = 3$ h	$\tau_c = 4$ h	$\tau_c = 5$ h
1	50	53	56	50	53
2	40	47	52	40	47
3	30	36	42	30	36
4	65	71	76	65	71
5	44	49	52	44	49
6	65	72	78	65	72
7	41	45	49	41	45
8	10	15	18	10	15
9	56	67	76	56	67
10	56	65	71	56	65
mean	46	52	57	61	64
\pm std	± 16	± 17	± 18	± 19	± 19

Table D.7: Time to return to the normo-glycemia zone after the meal for different τ_c values

Subject	$\tau_c = 1$ h	$\tau_c = 2$ h	$\tau_c = 3$ h	$\tau_c = 4$ h	$\tau_c = 5$ h
1	5.4 h	5.9 h	6.3 h	6.7 h	7.0 h
2	4.4	4.9	5.2	5.5	5.8
3	4.8	5.2	5.5	5.8	6.0
4	2.9	3.6	4.3	4.6	5.0
5	5.4	5.9	6.3	6.6	6.9
6	4.1	4.6	5.1	5.4	5.8
7	3.3	3.7	4.1	4.4	4.7
8	3.7	4.6	6.4	6.8	7.2
9	6.2	6.7	7.1	7.5	7.8
10	4.8	5.3	5.7	6.0	6.3
mean	4.2	4.7	5.2	5.5	5.8
\pm std	± 1.2	± 1.3	± 1.4	± 1.4	± 1.5

Table D.8: Blood Glucose (mg/dl) maximum values.

Subject	$\tau_c = 1$ h	$\tau_c = 2$ h	$\tau_c = 3$ h	$\tau_c = 4$ h	$\tau_c = 5$ h
1	179	183	185	190	193
2	176	183	188	190	193
3	177	183	189	192	196
4	216	222	227	230	233
5	186	192	195	198	200
6	201	208	214	219	222
7	176	180	185	189	192
8	160	166	169	170	173
9	192	203	212	218	223
10	209	217	223	228	231
mean	187	194	199	202	199
\pm std	± 16	± 17	± 18	± 19	± 18

Table D.9: Blood Glucose (mg/dl) maximum values.

Subject	$\tau_c = 1$ h	$\tau_c = 2$ h	$\tau_c = 3$ h	$\tau_c = 4$ h	$\tau_c = 5$ h
1	83	88	93	96	99
2	97	100	112	104	106
3	87	93	97	101	104
4	93	94	96	96	97
5	93	99	103	106	108
6	74	79	81	83	84
7	85	89	91	93	95
8	90	94	99	102	105
9	64	72	79	84	89
10	88	95	100	104	106
mean	85	90	94	94	94
\pm std	± 9	± 8	± 8	± 8	± 8

D.1 Robustness Test Single Results

$$\tau_c = 2 \text{ h}$$

Table D.10: Single meal statistics: percentage of time that the glucose concentration (mg/dl) remains within the indicated range. $\tau_c = 2$ h. The controller output is increased of the 50%

Subject	60<G<80	80<G<140	70<G<180	180<G<250
1	11	74	100	0
2	0	89	100	0
3	0	79	100	0
4	0	80	96	5
5	0	73	100	0
6	9	81	93	5
7	0	93	100	0
8	0	79	100	0
9	14	45	80	3
10	0	70	94	6
mean (\pm std)	3 (\pm 5)	76 (\pm 12)	96 (\pm 6)	2 (\pm 2)

Table D.11: Single meal statistics: percentage of time that the glucose concentration (mg/dl) remains within the indicated range. $\tau_c = 2$ h. The controller output is reduced of the 50%

Subject	60<G<80	80<G<140	70<G<180	180<G<250
1	0	79	89	11
2	0	84	93	7
3	0	67	92	8
4	0	70	92	8
5	0	64	87	13
6	0	84	90	10
7	0	88	96	4
8	0	62	100	0
9	0	57	83	17
10	0	58	87	14
mean (\pm std)	0	71 (\pm 11)	91 (\pm 5)	9 (\pm 5)

Table D.12: The glucose (mg/dl) peak value relative to the value at t_{meal} , the meal time: $\Delta G = G_{max} - G_{meal}$. $\tau_c = 2$ h.

Subject	Normal	-50%	+50%
1	51	42	57
2	46	34	53
3	36	25	45
4	71	61	79
5	49	37	55
6	72	59	82
7	45	38	52
8	15	4	19
9	67	49	81
10	65	47	74
mean	52	60	40
\pm std	\pm 17	\pm 19	\pm 16

Table D.13: Time to return to the normo-glycemia zone after the meal. $\tau_c = 2$ h.

Subject	Normal	-50%	+50%
1	5.9 h	4.9 h	6.6 h
2	4.9	4.0	5.4
3	5.2	3.0	5.7
4	3.6	2.5	4.6
5	5.9	4.8	6.6
6	4.6	3.7	5.3
7	3.7	2.9	4.3
8	4.6	3.0	6.8
9	6.7	5.7	7.4
10	5.3	4.4	5.9
mean	4.7	5.5	3.6
\pm std	± 1.3	± 1.4	± 1.2

Table D.14: Blood Glucose (mg/dl) maximum (G_{max}) and minimum (G_{min}) glucose values during the post-prandial response. $\tau_c = 2$ h.

Subject	highest			lowest		
	Normal	-50%	+50%	Normal	-50%	+50%
1	183	174	189	88	77	95
2	183	170	190	100	95	103
3	183	172	192	93	84	100
4	222	212	230	94	94	96
5	192	180	197	99	87	106
6	208	195	218	79	69	82
7	180	173	188	89	81	93
8	166	155	170	95	87	102
9	203	185	217	72	56	83
10	217	200	227	95	80	103
mean	194	202	182	90	96	81
\pm std	± 17	± 19	± 16	± 8	± 8	± 11

$$\tau_c = 3 \text{ h}$$

Table D.15: Single meal statistics: percentage of time that the glucose concentration (mg/dl) remains within the indicated range. $\tau_c = 3$ h. The controller output is increased of the 50%

Subject	60<G<80	80<G<140	70<G<180	180<G<250
1	0	84	100	0
2	0	88	100	0
3	0	75	100	0
4	0	79	95	5
5	0	71	97	3
6	10	80	94	6
7	0	92	100	0
8	0	77	100	0
9	24	42	77	8
10	0	68	93	8
mean (\pm std)	3 (\pm 7)	76 (\pm 13)	96 (\pm 7)	3 (\pm 3)

Table D.16: Single meal statistics: percentage of time that the glucose concentration (mg/dl) remains within the indicated range. $\tau_c = 3$ h. The controller output is reduced of the 50%

Subject	60<G<80	80<G<140	70<G<180	180<G<250
1	0	78	87	14
2	0	83	92	8
3	0	65	87	14
4	0	67	90	10
5	0	61	86	14
6	0	82	88	12
7	0	86	94	6
8	0	60	100	0
9	0	53	82	19
10	0	55	85	15
mean (\pm std)	0	69 (\pm 12)	89 (\pm 5)	11 (\pm 5)

Table D.17: The glucose (mg/dl) peak value relative to the value at t_{meal} , the meal time: $\Delta G = G_{max} - G_{meal}$. $\tau_c = 3$ h.

Subject	Normal	-50%	+50%
1	52	44	60
2	51	38	57
3	42	28	50
4	76	63	84
5	52	41	58
6	78	63	87
7	49	39	57
8	18	8	22
9	76	54	89
10	71	53	79
mean	57	64	43
\pm std	± 18	± 20	± 16

Table D.18: Time to return to the normo-glycemia zone after the meal. $\tau_c = 3$ h.

Subject	Normal	-50%	+50%
1	6.3 h	5.2 h	7.1 h
2	5.2	4.3	5.8
3	5.5	3.5	6.0
4	4.3	2.8	5.0
5	6.3	5.2	7.0
6	5.1	4.0	5.9
7	4.1	3.1	4.7
8	6.4	3.5	7.2
9	7.1	6.0	7.9
10	5.7	4.7	6.4
mean	5.2	5.9	3.9
\pm std	± 1.4	± 1.5	± 1.2

Table D.19: Blood Glucose (mg/dl) maximum (G_{max}) and minimum (G_{min}) glucose values during the post-prandial response . $\tau_c = 3$ h.

Subject	highest			lowest		
	Normal	-50%	+50%	Normal	-50%	+50%
1	185	177	193	93	81	100
2	188	174	194	102	96	106
3	189	175	197	97	86	104
4	227	214	235	96	93	97
5	195	184	200	103	91	109
6	214	199	223	81	73	84
7	185	175	193	92	84	95
8	169	159	173	99	89	105
9	212	190	224	79	61	90
10	223	206	232	100	85	107
mean	199	207	185	94	100	84
\pm std	± 18	± 19	± 16	± 8	± 8	± 10

$\tau_c=4$ h

Table D.20: Single meal statistics: percentage of time that the glucose concentration (mg/dl) remains within the indicated range for $\tau_c = 4$ h. The controller output is increased of the 50%

Subject	60<G<80	80<G<140	70<G<180	180<G<250
1	0	83	99	1
2	0	87	100	0
3	0	71	100	0
4	0	77	95	6
5	0	70	96	4
6	9	79	93	7
7	0	92	100	0
8	0	75	100	0
9	23	40	75	14
10	0	66	91	9
mean (\pm std)	3 (\pm 7)	74 (\pm 14)	95 (\pm 7)	4 (\pm 5)

Table D.21: Single meal statistics: percentage of time that the glucose concentration (mg/dl) remains within the indicated range. $\tau_c = 4$ h. The controller output is reduced of the 50%

Subject	60<G<80	80<G<140	70<G<180	180<G<250
1	0	76	86	14
2	0	81	91	9
3	0	62	86	14
4	0	64	88	12
5	0	59	85	15
6	0	80	87	13
7	0	85	93	8
8	0	57	100	0
9	0	49	81	19
10	0	54	85	16
mean (\pm std)	0	67 (\pm 12)	88 (\pm 5)	12(\pm 5)

Table D.22: The glucose (mg/dl) peak value relative to the value at t_{meal} , the meal time: $\Delta G = G_{max} - G_{meal}$. $\tau_c = 4$ h.

Subject	Normal	-50%	+50%
1	55	46	62
2	54	41	60
3	45	32	54
4	79	66	86
5	55	45	60
6	83	67	94
7	53	44	63
8	20	11	24
9	82	57	94
10	75	58	83
mean	60	68	46
\pm std	± 19	± 20	± 16

Table D.23: Time to return to the normo-glycemia zone after the meal. $\tau_c = 4$ h.

Subject	Normal	-50%	+50%
1	6.7 h	5.5 h	7.5 h
2	5.5	4.5	6.2
3	5.8	4.9	6.3
4	4.6	3.1	5.5
5	6.6	5.5	7.4
6	5.4	4.2	6.4
7	4.4	3.3	5.0
8	6.8	3.9	7.6
9	7.5	6.3	8.3
10	6.0	4.9	6.8
mean	5.5	6.3	4.3
\pm std	± 1.4	± 1.6	± 1.2

Table D.24: Blood Glucose (mg/dl) maximum (G_{max}) and minimum (G_{min}) glucose values during the post-prandial response. $\tau_c = 4$ h.

Subject	G_{max}			G_{min}		
	Normal	-50%	+50%	Normal	-50%	+50%
1	190	180	197	96	84	102
2	190	178	197	104	97	108
3	192	179	201	101	89	107
4	230	217	237	96	93	99
5	198	188	203	106	94	111
6	219	203	230	83	76	85
7	189	177	198	93	86	97
8	170	162	175	102	91	107
9	218	193	229	84	66	95
10	228	211	236	103	89	109
mean	202	210	189	97	102	87
\pm std	± 19	± 20	± 16	± 8	± 8	± 9

$$\tau_c = 5 \text{ h}$$

Table D.25: Single meal statistics: percentage of time that the glucose concentration (mg/dl) remains within the indicated range. $\tau_c = 5$ h. The controller output is increased of the 50%

Subject	60<G<80	80<G<140	70<G<180	180<G<250
1	0	82	97	3
2	0	87	97	3
3	0	70	98	2
4	0	76	94	6
5	0	68	95	6
6	8	80	93	8
7	0	91	100	0
8	0	73	100	0
9	22	40	85	15
10	0	64	89	11
mean (\pm std)	3 (\pm 7)	73 (\pm 14)	95 (\pm 5)	5 (\pm 5)

Table D.26: Single meal statistics: percentage of time that the glucose concentration (mg/dl) remains within the indicated range. $\tau_c = 5$ h. The controller output is reduced of the 50%

Subject	60<G<80	80<G<140	70<G<180	180<G<250
1	0	75	85	15
2	0	80	91	10
3	0	60	85	15
4	0	63	87	13
5	0	57	85	16
6	0	78	86	14
7	0	84	92	8
8	0	55	100	0
9	0	48	80	20
10	0	53	84	16
mean (\pm std)	0	65 (\pm 12)	88 (\pm 5)	13 (\pm 5)

Table D.27: The glucose (mg/dl) peak value relative to the value at t_{meal} , the meal time: $\Delta G = G_{max} - G_{meal}$. $\tau_c = 5$ h.

Subject	Normal	-50%	+50%
1	58	47	64
2	57	45	62
3	49	35	58
4	83	69	90
5	57	48	61
6	87	70	96
7	56	43	64
8	22	13	26
9	87	64	97
10	78	62	86
mean	64	71	50
\pm std	± 19	± 21	± 17

Table D.28: Time to return to the normo-glycemia zone after the meal. $\tau_c = 5$ h.

Subject	Normal	-50%	+50%
1	7.0 h	5.8 h	7.9 h
2	5.8	4.8	6.4
3	6.0	5.1	6.6
4	5.0	3.3	5.9
5	6.9	5.8	7.8
6	5.8	4.5	6.9
7	4.7	3.6	5.4
8	7.2	4.3	7.9
9	7.8	6.6	8.6
10	6.3	5.1	7.3
mean	5.8	6.6	4.6
\pm std	± 1.5	± 1.6	± 1.3

Table D.29: Blood Glucose (mg/dl) maximum (G_{max}) and minimum (G_{min}) glucose values during the post-prandial response. $\tau_c = 5$ h.

Subject	G_{max}			G_{min}		
	Normal	-50%	+50%	Normal	-50%	+50%
1	193	182	199	99	87	106
2	193	181	199	106	99	110
3	196	182	205	104	91	109
4	233	220	241	97	94	103
5	200	190	204	108	97	114
6	222	206	232	84	78	87
7	192	179	200	95	88	98
8	173	164	177	105	93	109
9	223	199	233	89	70	99
10	231	216	239	106	93	112
mean	206	213	192	99	105	89
\pm std	± 19	± 21	± 17	± 8	± 8	± 8

Bibliography

- [1] K. V. Heusden, E. Dassau, H. C. Zisser, D. E. Seborg, and F. J. Doyle III, “Control-relevant models for glucose control using a priori patient characteristics,” *IEEE Transactions on Biomedical Engineering*, vol. 59(7), pp. 1839–1849, 2012.
- [2] E. B. Wald, A. S. Fauci, D. L. Kasper, S. L. Hauser, D. L. Longo, and J. L. Jameson, *Principi di Medicina Interna*. Milano: McGraw-Hill, 2002.
- [3] D. Fedele, *Manuale di Diabetologia e Malattie del Metabolismo*. C.P 528-87100 Cosenza: Editoriale Bios, 2003.
- [4] R. Harvey, Y. Wang, B. Grosman, M. W. Percival, W. Bevier, D. A. Finan, H. Zisser, D. E. Seborg, L. Jovanovič, F. J. Doyle III, and E. Dassau, “Quest for the artificial pancreas,” *IEEE Engineering in Medicine and Biology Magazine*, vol. 29(2), pp. 53–62, 2010.
- [5] E. P. Widmaier, H. Raff, and K. T. Strang, *Vander’s Human Physiology*. Boston: McGraw-Hill international edition, 2006.
- [6] R. Kirschstein and L. R. Skirboll, *Stem Cells: Scientific Progress and Future Research Directions*. U.S Department of Health and Human Services, 2001. <http://www.hhs.gov/office/scireport/2001report/>.
- [7] B. Grosmann, E. Dassau, H. C. Zisser, M. D. L. Jovanovič, and F. J. Doyle III, “Zone model predictive control: a strategy to minimize hyper- and hypoglycemia events,” *Journal of Diabetes Science and Technology*, vol. 4, pp. 961–975, 2010.

-
- [8] D. Elleri, D. B. Dunger, and R. Hovorka, "Closed-loop insulin delivery for treatment of type 1 diabetes," *BioMed Central Medicine*, vol. 9, pp. 1–9, 2011.
- [9] R. Hovorka, "Continuous glucose monitoring and closed-loop systems," *Diabetes UK Diabetic Medicine*, vol. 23(1), pp. 1–12, 2006.
- [10] T. Didangelos and F. Iliadis, "Insulin pump therapy in adults," *Diabetes Research and Clinical Practice*, vol. 93, pp. 109–113, 2011.
- [11] B. W. Bequette, "A critical assessment of algorithms and challenges in the development of a closed-loop artificial pancreas," *Diabetes Technology and Therapeutics*, vol. 7(2), pp. 28–47, 2005.
- [12] C. Ellingsten, E. Dassau, H. Zisser, B. Grosman, M. W. Percival, L. Jovanovič, and F. J. Doyle III, "Safety constraints in an artificial pancreatic β cell: an implementation of model predictive control with insulin on board," *Journal of Diabetes Science and Technology*, vol. 3(3), pp. 536–544, 2009.
- [13] <http://www.diabetescaregroup.info/insulin-pump-therapy-the-bad/>.
- [14] C. Cobelli, E. Renard, and B. Kovatchev, "Artificial pancreas: past, present, future," *Diabetes*, vol. 60, pp. 2672–2682, 2011.
- [15] T. M. Gross, B. W. Bode, D. Einhorn, D. M. Kayne, J. Reed, N. H. White, and J. J. Mastrototaro, "Performance evaluation of the MiniMed continuous glucose monitoring system during patient home use," *Diabetes Technology and Therapeutics*, vol. 2(1), pp. 49–56, 2000.
- [16] G. Steil, B. Clark, S. Kanderian, and K. Rebrin, "Modeling insulin action for development of a closed-loop artificial pancreas," *Diabetes Technology and Therapeutics*, vol. 7(1), pp. 94–108, 2005.
- [17] G. Marchetti, M. Barolo, L. Jovanovič, H. Zisser, and D. E. Seborg, "An improved pid switching control strategy for type 1 diabetes," *IEEE Transaction on Biomedical Engineering*, vol. 55(3), pp. 857–865, 2008.

- [18] A. E. Pantaleon, M. Loutseiko, G. M. Steil, and K. Rebrin, "Evaluation of the effect of gain on the meal response of an automated closed-loop insulin delivery system," *Diabetes*, vol. 55(7), pp. 1995–2000, 2006.
- [19] D. E. Seborg, T. F. Edgar, D. A. Mellichamp, and F. J. Doyle III, *Process Dynamics and Control 3ed.* New York: John Wiley and Sons., 2010.
- [20] C. Cobelli, C. Dalla Man, G. Sparacino, L. Magni, G. De Nicolao, and B. P. Kovatchev, "Diabetes: models, signals and control," *IEEE Review Biomedical Engineering*, vol. 1(2), pp. 54–96, 2009.
- [21] G. M. Steil, K. Rebrin, C. Darwin, F. Hariri, and M. F. Saad, "Feasibility of automating insulin delivery for the treatment of type 1 diabetes," *Diabetes*, vol. 55(12), pp. 3344–3350, 2006.
- [22] S. Skogestad, "Simple analytic rules for model reduction and PID controller tuning," *Journal of Process Control*, vol. 13(4), pp. 291–309, 2003.
- [23] R. N. Bergman, Y. Z. Yder, C. R. Bowden, and C. Cobelli, "Quantitative estimation of insulin sensitivity," *American Journal of Physiology*, vol. 236(6), pp. 667–677, 1979.
- [24] R. S. Parker and F. J. Doyle III, "Control-relevant modeling in drug delivery," *Advanced Drug Delivery Reviews*, vol. 48(2-3), pp. 211–228, 2000.
- [25] F. Ståhl and R. Johansson, "Diabetes mellitus modeling and short-term prediction based on blood glucose measurements," *Mathematical Biosciences*, vol. 217(2), pp. 101–117, 2009.
- [26] R. S. Parker, *Model-based analysis and control for biosystems.* Delaware: University of Delaware, 1999.
- [27] H. Sheng, Y. Chen, and T. Qiu, *Fractional Processes and Fractional-Order Signal Processing: Techniques and Applications.* New York Dordrecht Heidelberg London: Springer publishing company, 2011.

-
- [28] B. P. Kovatchev, M. Breton, C. Dalla Man, and C. Cobelli, “*In silico* pre-clinical trials: a proof of concept in closed-loop control of type 1 diabetes,” *Journal of Diabetes Science and Technology*, vol. 3(1), pp. 44–55, 2009.
- [29] C. Dalla Man, D. M. Raimondo, R. A. Rizza, and C. Cobelli, “GIM, simulation software of meal glucose-insulin model,” *Journal of Diabetes Science and Technology*, vol. 1(13), pp. 323–330, 2007.
- [30] C. Dalla Man, R. A. Rizza, and C. Cobelli, “Meal simulation model of the glucose-insulin system,” *IEEE Transactions on Biomedical Engineering*, vol. 54(10), pp. 1740–1749, 2007.
- [31] M. Breton and B. P. Kovatchev, “Analysis, modeling and simulation of the accuracy of continuous glucose sensors,” *Journal of Diabetes Science and Technology*, vol. 2(5), pp. 853–862, 2008.
- [32] J. F. Kenney and E. S. Keeping, *Linear Regression and Correlation*. NJ: Van Nostrand: Princestone, 1962.